On the Manufacture of Very Thin Elastomeric Films by Spin-Coating

by

Sriram Krishnan

B. Tech., Mechanical Engineering,
Indian Institute of Technology Madras, India, 1999
S. M., Mechanical Engineering,
Massachusetts Institute of Technology, Cambridge, MA, 2002

Submitted to the Department of Mechanical Engineering
in partial fulfillment of the requirements for the degree of

Doctor of Philosophy in Mechanical Engineering

at the

MASSACHUSETTS INSTITUTE OF TECHNOLOGY
[September 2007]
June 2007

Author .....
Department of Mechanical Engineering
June 15, 2007

Certified by .....
Sanjay E. Sarma
Associate Professor
Thesis Supervisor

Accepted by .....
Lallit Anand
Chairman, Department Committee on Graduate Students

On the Manufacture of Very Thin Elastomeric Films by Spin-Coating

by

Sriram Krishnan

Submitted to the Department of Mechanical Engineering
on June 15, 2007, in partial fulfillment of the
requirements for the degree of
Doctor of Philosophy in Mechanical Engineering

Abstract

I present a process for manufacturing poly-dimethylsiloxane (PDMS) films of thicknesses down to 50 microns. PDMS films are currently fabricated by spin-coating the polymer on a wafer and then manually peeling the film after curing. This is labor-intensive and suffers from low yield, dimensional inaccuracies, tearing and wrinkling. I apply manufacturing principles to the preparation of PDMS to enable more accurate, efficient, and reliable manufacturing.

Difficulties in the preparation of PDMS films occur for two reasons: a) the material properties of PDMS are hard to characterize and b) process steps are hard to characterize. In analyzing the functional steps in PDMS manufacture, I first examine the spin-coating process. There has been surprisingly little work on thickness control, and I show how unlike with photoresist, the thickness of the coat can be controlled quite robustly by a judicious choice of process parameters. I also show how second-order variations can be controlled by using an inexpensive interferometric technique developed by our collaborators. I then analyze the physics of peeling and show why initiation, beading and tearing are difficult issues. Furthermore the line of separation of between the film and the wafer is difficult to advance without dynamic effects and micro-slippage. In order to prevent these problems, I introduce two new process concepts. First, I introduce a thin 'scaffold', incorporated in situ between the PDMS film and the substrate during spin-coating, which can start the peel front, eliminate the bead, as well as support the film as it is peeled. I then introduce the use of an adhesive roller actuator with a compressive pre-load which helps peel the film while controlling the peel-front. I show how, by using a ferro-magnetic material, the scaffold can be separated and handled by magnetic attachment. I show how the scaffolding can also incorporate a kinematic coupling for subsequent registration in layering. Finally, I will present experimental results showing thickness metrology, model verification and peeling success.

Thesis Supervisor: Sanjay E. Sarma
Title: Associate Professor

Acknowledgments

My research and my stay at MIT has truly been a defining experience. There has been many an individual that has crossed paths with me and changed me for the better. I acknowledge the most noteworthy here.

My research advisor, Prof. Sanjay Sarma, took me under his wing for my entire graduate study and allowed me tremendous freedom to learn and grow. His perfectionism, contagious enthusiasm and a carefree attitude made for a fantastic preparation towards my future career. My thesis committee members, Prof. Doug Hart and Prof. Samir Nayfeh, have been very supportive and through their incisive and deep critique have helped shape this dissertation. In particular, Samir taught me motion systems, mechanics and survival skills in research.

At my research home, the Rapid Autonomous Machining Lab (RAMLAB), I have had the pleasure of working with Dr. Mahadevan Balasubramaniam, Dr. Seung-kil Son, Dr. Elmer Lee, Dr. Stephen Ho and Dr. Kashif Khan that, over the years, has left a lasting impression on me. I cherish the collaboration with Dr. Taejung Kim and Chetak Reshamwalla that sowed the seeds for this thesis research. Dr. Joseph Foley shared his thesis stylefiles and saved me from a lot of hassles while writing the dissertation. Joe contributed to my research during our many brainstorming sessions, at times with really crazy ideas. Ajay Deshpande has been a patient, thoughtful sounding board whenever needed.

The Laboratory for Manufacturing and Productivity (LMP), the larger division that our lab has been part of, introduced me to Prof. David Trumper. Dr. Nannaji Saka and Prof. Alex Slocum with whom I have had insightful discussions. The technical instructors at the LMP machine shop Gerry Wentworth, Pat McAutamey and David Dow have been exceptionally patient and helpful over the years during my many attempts at machining. I thank our lab administrators David Rodriguera and Rachel Russell for their kind help in procuring the parts and supplies. Our department head, Prof. Rohan Abeyaratne, and our graduate administrator, Leslie

Regan, have encouraged me in many of my pursuits and I appreciate their guidance.

As part of my research, I collaborated with Kevin Lee and Dr. Harry Lee from the Physical Optics and Electronics group at the MIT Research Lab for Electronics on spin-coating metrology. I greatly appreciate their contributions and assistance in setting up the experiments. I thank Prof. Todd Thorsen's research group, particularly J. P. Urbanski and Hyesung Park, for use of their PDMS preparation equipment. At the MIT Microsystems Technology Laboratories, I thank Kurt Broderick for his patience and kind assistance during the preparation of my experiment samples.

Dr. Brenda Long, Vijay Shilpiekandula and Marketa Valterova proofread this dissertation and I am grateful for their time and efforts.

During my time at MIT, I have had the wonderful privilege of working with fantastic individuals in many different organizations. At Sidney-Pacific, I truly found a home away from home and cherished working with a highly energetic and creative group of friends. At the Graduate Student Council, I learnt the inner workings of an effective student organization and of our University. Working with the faculty, I enjoyed the true spirit of enterprise at MIT. My friends Waleed Farahat, Ola Ayaso, Nici Ames, Vaibhaw Vishal, Olga Heidarsdottir, Lucka Pakostova, Sanith Wijesinghe, Ronak Bhatt, Ryan Tam, Margret Bjarnadottir and Dilan Seneviratne, have egged me on during my entire graduate career and have helped me overcome many an obstacle, academic and otherwise. My squash buddies Amos Winter, Dr. John Hart and Prof. Roberto Fernandez helped turn me into a health nut.

My family – Appa, Amma, Suji and Sriram – have patiently enthused me all along and have always believed in me even when I myself didn't. Their prayers and their personal sacrifices have made my graduate study possible. Dr. Shridar Ganesan has been a friend and a mentor all along and has been my local guardian.

Finally, I fondly remember two exemplary individuals that left their indelible mark on me – Bhuwan Singh and Prof. Vernon Ingram.

This thesis is dedicated in fond memory of my physics teacher,

Prof. S. Balasubramaniam.

THIS PAGE INTENTIONALLY LEFT BLANK

Contents

List of Figures

List of Tables

THIS PAGE INTENTIONALLY LEFT BLANK

Chapter 1

Introduction

In this thesis, I study the manufacture of thin polydimethylsiloxane (PDMS) films by spin-coating on silicon and glass substrates and subsequently peeling. Thin polydimethylsiloxane (PDMS) films of $100\mu m$ or less in thickness have a wide array of applications, many of them novel and recent. I begin by discussing some of the applications and the design metrics they require of PDMS films. I evaluate the current approach for preparing PDMS films and highlight the need for improving the reliability, efficiency and yield of the process. The chapter concludes with a summary of the key contributions herein and an outline of the rest of this thesis.

1.1 Applications for Very Thin PDMS Films

PDMS is finding increasing use in laboratories around the world in a variety of applications. Four main applications exist in the field of soft lithography :

- Multi-layer microfluidic devices: Micro-fluidic logic systems are assembled by stacking many thin layers of patterned PDMS films. The thinner the individual layers, the smaller the logic circuit can be [TMQ02]. Micro-fluidic valves constructed out of multiple layers of thin PDMS films are necessary for applications such as cell-sorting and droplet generation.

- Stencils: Very thin PDMS films can be used as stencils with patterns, either cut out or coated on the film using surface chemistry. The films then provide templates for patterning cells or biomolecules on surfaces [JW03], [VFB+02].
- Membranes and Gaskets: Experiments in electrokinesis and dielectrophoresis require thin, custom-shaped films as gaskets to ensure precise separation between surfaces. Experiments in bio-reactors at the small scale involve use of very thin PDMS membranes for controlled transport of oxygen and biomolecules.
- Curved stamps for micro-contact printing: The use of micro-contact printing stamps can be expanded if they can be fabricated out of very thin PDMS films, enabling them to conformally coat curved surfaces easily.

Very thin polymer films can also be used as scaffolds for tissue engineering and artificial skin [KLBV06].

1.2 Requirements of a PDMS Film Manufacturing Process

The use of thin PDMS films in research applications has seen tremendous growth in recent years. In the future, we expect this trend to continue. As the demand for thin PDMS films grows, there is a clear need to make PDMS films production-ready and to develop a robust manufacturing process. Today, the preparation of thin PDMS films involves a user carrying out a prescribed sequence of tasks for their spin-coating and subsequent peeling. The user spin-coats the PDMS film under conditions identified by previously calibrated experiments to achieve an estimated thickness. Such 'recipes' for PDMS spin-coating do not capture the sensitivity to processing conditions and often lead to large variations in thickness (30% variations are reported in [MFR05]). The current peeling approach is time-consuming and labor-intensive. Despite the time and effort invested, the yield of the process is often low and damage by tearing

is common. Even if, with considerable effort, the user can peel the thin film from the substrate, there still remain questions of how the film will be stored for further use, without wrinkling or contamination.

In this thesis, I analyze the preparation of thin PDMS films and apply manufacturing principles of robustness, repeatibility and efficiency to each aspect of the film preparation.

1.2.1 What is a Robust Manufacturing Process?

A manufacturing process can be defined by the following factors:

1. Accuracy

   The product of a manufacturing process must meet the design specifications and be within tolerance limits. If the product of a manufacturing process does not meet the acceptable quality or design specification, then it is rejected.

2. Yield

   A manufacturing process over several production runs must result in a high percentage of end products of specified quality. The repeatability of a manufacturing process is measured in terms of *yield* – the fraction of the total number of products that meet the specifications.

3. Throughput

   A manufacturing process must produce end products rapidly enough to be economic. Increase in throughput of a manufacturing process can be achieved by increasing production rates. This in many cases involves automation of operations where humans are either slow, expensive or error-prone.

To give a more intuitive idea of these manufacturing principles, allow me to discuss two common examples – 1) Cake baking and 2) Paper spooling in printers.

In order to bake a cake, a consumer must first prepare the cake batter based on a recipe of ingredients. She then bakes the mix in an oven at a prescribed temperature, for a defined period of time. If the manufacturer provides a recipe such that the quality is good only for a very narrow range of temperature and baking time, the consumer may not be able to hit the 'sweet-spot' of the baking process. There will be wastage due to the exacting processing conditions. If we plot the quality of the end product, the cake, as a function of the two parameters (oven temperature and baking time), we obtain a graph such as the one shown in Figure 1-1. In order to provide more tolerance to the consumer's skills, the manufacturer must achieve a good quality cake over a broader range of baking temperatures and times. In effect, the manufacturer strives to increase the yield of the baking mix under different baking conditions. When we view the baking process now as a function of the two or more process parameters, we can prepare a 'process window' (Figure 1-1). A process window identifies the range of process parameters over which we achieve our quality objectives in a manufacturing process . If good quality cake is achieved only within a very narrow range of temperature or time, the process window in the temperature-time space is very small. Our objective with any manufacturing process is to make process windows as large as possible. A process with a large process window is called a robust process, and has a high yield. Because the process window is large, the process is robust to unexpected variations.

The paper-feeding mechanism in printers is an example where the objective is throughput. While the individual components that achieve this task may differ from one printer manufacturer to another, the success of the paper-feeding mechanisms relies on achieving large process windows for various paper thicknesses and alignment errors. Automation of the paper-feeding process improves efficiency and has contributed to the widespread adoption and usage of printers.

In summary, a robust manufacturing process is one where we control the parameters we can control with a high degree of precision, and we render the process

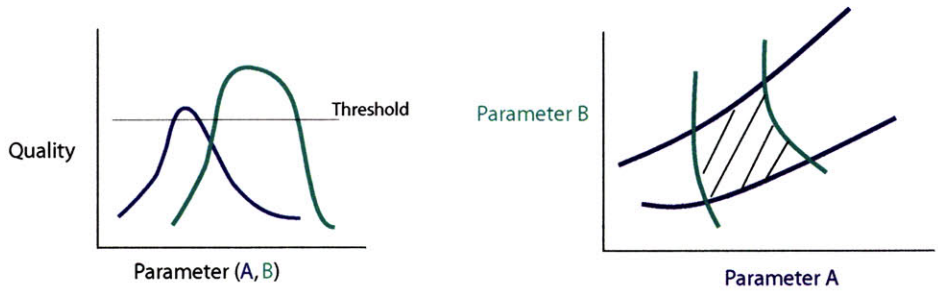

Figure 1-1: The parameter values that yield a product meeting the design objectives defines the 'process window'. The design objective of a manufacturing process is to expand its process windows and increase robustness

insensitive to those parameters which we cannot control. With a good manufacturing process, desired objectives of accuracy and repeatability can be achieved even in the presence of process variations and disturbances.

1.2.2 Need for Thickness Accuracy

When thin PDMS films are prepared for soft-lithographic processes, precise thickness and uniform coating of the film are highly desired. In applications such as multi-layer microfluidic devices, it has been shown that a change in the film thickness from 15 microns to 20 microns can change the actuation pressure from 18 kPa to 30 kPa [SHP+04]. When thin membranes are used in bioreactors, they make use of the oxygen permeability of PDMS [LBRS06]. Since the diffusivity of oxygen through the PDMS films is dependent on its thickness, local variations in thickness of a thin PDMS film could hamper device performance.

In Chapter 3, I will show why current spin-coating of PDMS films leads to large variations. Using a well-known model for axisymmetric viscous flow, I will highlight the sensitivity of PDMS spin-coating to process parameters. I will then propose a robust approach to thickness control in PDMS spin-coating and introduce an inex-

pensive metrology setup.

1.2.3 Need for High Yield

As I stated before, one of the key performance metrics of any manufacturing process is its yield. In the case of PDMS film manufacturing, yield can be defined by the percentage of films that are damage-free and within an acceptable tolerance range for thickness. The process objective for PDMS film manufacturing is therefore one of preparing films without damage, doing so repeatably and thus, maximizing yield.

Today, thin PDMS film preparation involves a great deal of manual intervention, most unavoidably in the separation of the thin films from substrates, *i.e.*, peeling. Several researchers report peeling PDMS films by using carefully learned manual skills; the success thus depends on the dexterity and physical skill of the operator. Beyond an emphasis on operator skills, we have not come across any treatment in the literature for a deterministic and controlled approach for PDMS peeling. The yield of peeling processes has not been measured, but anecdotal evidence shows that even with careful effort, it is still only about 40% [Des] . With the rapidly expanding role of PDMS films in both experimental applications and as a potential mass manufacturing technique, peeling becomes an important bottleneck for scalability.

In Chapters 4, 5 and 6, I present a PDMS film manufacturing process that provides a repeatable means for spin-coating thin PDMS films and for peeling the PDMS films while avoiding risk of damage by tearing.

1.2.4 Storage and Handling of Thin PDMS Films

In current applications, PDMS films are made 'on demand' during the prototyping of a device. Operators often prepare and assemble the thin PDMS film (or parts of it) immediately on the device. Holding the film without wrinkling and registration when assembling it on the device is a major challenge. So far, handling and storage of thin PDMS films has not been studied in a systematic manner. As the use and

adoption of PDMS as a research tool increases, we foresee the need for pre-fabricated thin PDMS films available ready-to-use for new applications.

In Chapter 4, I present a new component that can be used as a scaffold for holding the film and in Chapter 6, I discuss techniques for handling of the PDMS films during and after peeling. I also outline strategies for storing the PDMS films without contamination.

1.2.5 Need for Automation

In the above sections, I have outlined the key needs of a manufacturing process for PDMS films – accuracy, high yield and film handling strategies. Unfortunately, many of these needs are unattainable today due to the dependence on manual procedures and the associated lack of repeatability. To address these issues, I analyzed the physics of the individual steps of PDMS film manufacturing. Once I attained a understanding of PDMS as a material and the manufacturing process for thin PDMS films, I was able to propose automation solutions and design a prototype machine.

1.3 Thesis Contributions

In this thesis, I identify the challenges in current PDMS film preparation, analyze the associated physics and, drawing insights from the physics, I propose new machine elements and an automated approach to PDMS film manufacture. My specific contributions are to:

- outline the specific process steps for the manufacture of thin PDMS films ,
- demonstrate the variability in spin-coating thickness, explain a mechanics model for height variation and improve the robustness of the spin-coating process using the mechanics model,

- describe the challenges in PDMS film manufacturing due to its material property variation,
- analyze the problem of low yield in manual peeling, due to tearing and beading,
- explain the physics of initiation and introduce concepts for peel initiation based on the physics,
- explain the risk of instability in the peeling process and show how such instability could cause damage to the film,
- demonstrate the application of a roller with pre-load for controlling peel-front advance,
- introduce a new component – ' an *in-situ* Scaffold', for repeatable initiation of a peel, for attaching to the film during peeling, for use as scaffolding to avoid wrinkling of peeled film and for registration and alignment,
- introduce the use of an adhesive roller actuator with compressive pre-load for peeling films with a peel initiator,
- implement these components and prototype an automated process for peeling PDMS films down to 50 microns in thickness.

1.4 Roadmap of Thesis

The thesis organization is as follows. In Chapter 2, I present a brief background about the PDMS material, analyze the current approach for PDMS film preparation and outline the inherent key process challenges. I analyze the PDMS spin-coating process and propose a more robust approach for PDMS film thickness control in Chapter 3. In Chapter 4, I analyze the process of peel initiation and propose a new component for peeling PDMS films in a deterministic manner. In Chapters 5 and 6, I study

continuous peeling and the handling of PDMS films upon manufacture. I discuss the physics of each of these stages, discuss a few concepts and describe components that were developed drawing insights from the physics and concept tests. Combining these discussions, in Chapter 7, I present a prototype peeling machine and experimental results for thickness metrology, robust spincoating model and peeling process success. I conclude with process windows for PDMS film manufacture and future directions of this work. Instead of a single consolidated literature review, I review the physics and related work for the individual process steps presented in each chapter.

THIS PAGE INTENTIONALLY LEFT BLANK

Chapter 2

A Review and Analysis of PDMS Film Preparation

Poly-dimethylsiloxane (PDMS) has been developed and used in the recent few decades in applications such as medical devices (catheter tubes, drainage pipes), industrial components (adhesives, insulation), and as a platform for research in soft-lithography techniques such as micro-contact printing and polymer microfabrication. PDMS is biocompatible, oxygen permeable, inert and hydrophobic and thus a good candidate for medical and biological applications. It is a transparent elastomer formed by cross-linking long-chain siloxane monomers. For many applications, one can attach ligands and side-chain molecules to PDMS to modify its surface chemistry.

In this chapter, I briefly discuss the material properties of PDMS that are relevant for understanding its manufacture. Based on some recently reported studies that discuss material property variations in PDMS, I argue that PDMS is not yet well understood. I then describe the current approaches in preparing PDMS films, involving spin-coating the viscous pre-polymer on wafer substrates, curing the polymer into a solid elastomeric film and subsequently peeling the elastomeric film off of these substrates. The spin-coating of PDMS has historically borrowed techniques from the microelectronics industry where photoresist is spin-coated on wafers. I show

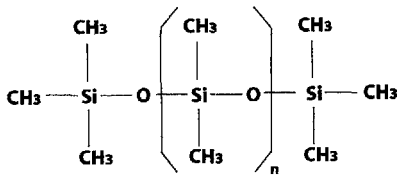

Figure 2-1: Chemical formula of PDMS

how the PDMS film thickness achieved in an open-loop manner leads to inaccuracy. I go on to present the process steps that a user typically follows after spin-coating and curing, in order to separate a cured PDMS film from a substrate. Building on these process level outlines, I highlight the challenges in the current approach of PDMS film preparation – both due to intrinsic physics and due to practical process considerations – which could contribute to thickness variation and low yield. Finally, I discuss a few examples of machines that have been designed for attaching, peeling and handling of thin films of different materials.

2.1 A Primer on Poly-dimethylsiloxane (PDMS)

Polydimethylsiloxane is prepared from a long-chain monomer composed of a siloxane and a cross-linking molecule to form an elastomeric network (schematic shown in Figure 2-1). The backbone of the polymer has several sites that are candidates for attaching ligands. An example is shown in Figure 2-2 where plasma oxidation can be used to change the surface wettability of PDMS. In this section I discuss the preparation of PDMS and how its material properties depend on its preparation.

2.1.1 Raw Material for PDMS Preparation

Historically, PDMS preparation has involved different chemistries and preparation approaches [CW87]. Recently, researchers have begun to use a commercially available

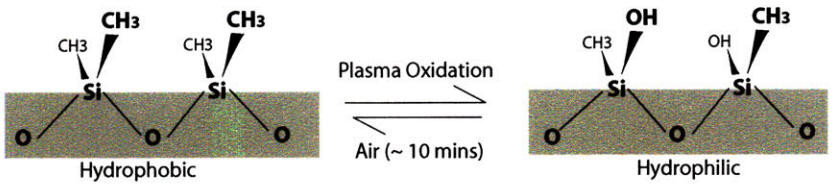

Figure 2-2: Surface modification of PDMS using plasma oxidation

product called Sylgard-184, manufactured by Dow Corning and Company, with a manufacturer recommended protocol for the monomer-crosslinker ratio, as well as specific temperature and time conditions for curing (refer Figures A-1 and A-2 in Appendix A). Even though the discussion in many recent works on PDMS properties is based on the protocol for the Sylgard-184 product, the arguments about sensitivity to processing conditions are applicable to other similar products like GE RTV Silicone.

2.1.2 Mechanical Properties of PDMS

The mechanical properties of PDMS pertinent for thin film manufacture are the dynamic viscosity (μ), modulus of elasticity (E), Poisson's ratio (ν), tensile strength (σ_u) and adhesion energy (γ_{PDMS}). Once the monomer and cross-linker are mixed, the dynamic viscosity of the sample increases over time due to the gelation mechanism [CW87]. In Figure 2-3, I show a sample measurement of PDMS viscosity indicating differences between the measurement and the property values prescribed by the manufacturer. The density of the mixture does not change appreciably during cross-linking because the monomer is non-volatile. The shrinkage in PDMS films during curing has been reported to be about 1% [ACJ+00]. Furthermore, the pot-life of the mixture is about two hours (Figure A-2) and the mixture begins to solidify at longer time durations. The cross-linking mechanism gives elastic stiffness to the PDMS film and the modulus of PDMS will increase with increasing mass fraction of cross-linker to monomer. Conditions that favor the cross-linking reaction will also cause an increase in stiffness.

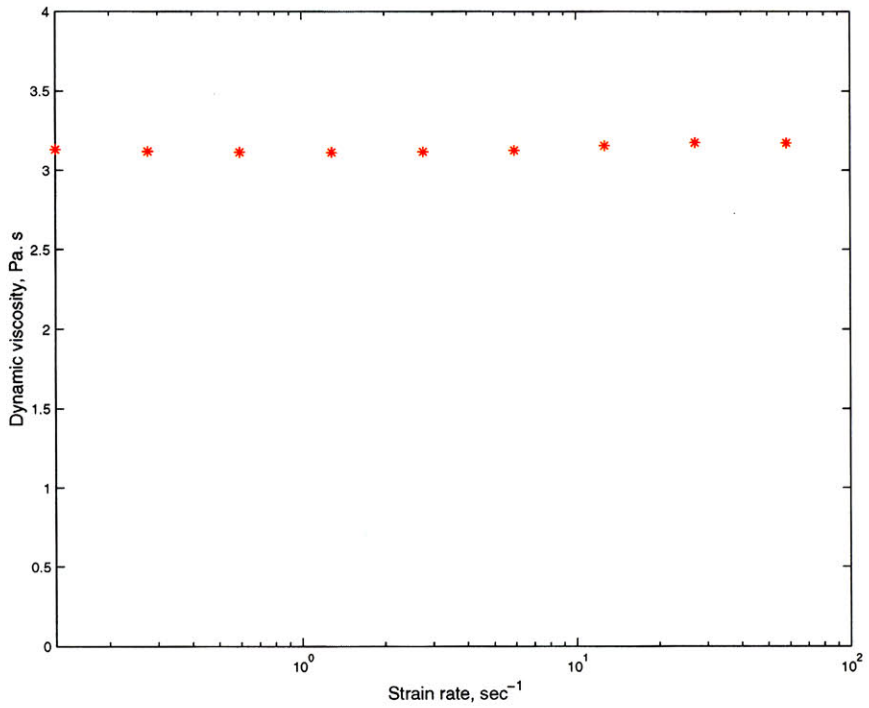

Figure 2-3: Experimental measurement of PDMS viscosity at 10:1 weight ratio of PDMS prepolymer to cross-linker. The measured viscosity of 3.2 Pa-s differs from the manufacturer's quoted viscosity of 3.9 Pa-s. Additionally, we found that the viscosity is nearly constant for strain rates varying over several orders of magnitude. Measurements were obtained on a controlled stress rheometer, using a 6mm 2^o cone with a temperature controlled Peltier plate, at the Hatsopoulos Microfluids Laboratory, MIT.

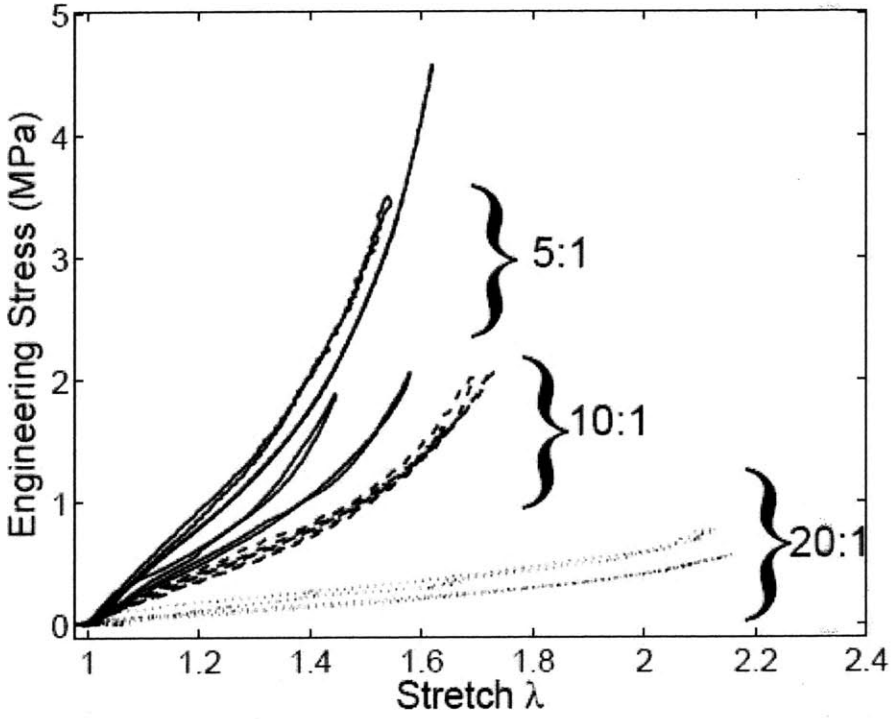

Figure 2-4: Hyperelastic constitutive model for PDMS [HLA04]. Figure included with author's permission [Ana].

The solid PDMS film is hyperelastic and a recent constitutive model has been proposed by Huang and others [HLA04]. This model is shown in Figure 2-4 and shows that as the cross-linking ratio changes, the stiffness curve also shifts dramatically. As the cross-linking ratio decreases, the stiffness decreases, giving the film a much greater stretch. Even for the same cross-linking ratio, stiffness curves are different indicating a lack of repeatability.

While the hyperelastic constitutive model is the most accurate, some studies report the Young's modulus based on a compression test of PDMS [SHB+04] [ECB03]. In [ECB03], we find further evidence that increasing the weight ratio of pre-polymer to cross-linker reduces PDMS modulus. Figure 2-5 shows that PDMS modulus is sensitive to the temperature and duration of curing. In Figure 2-6, we can see that the strength of PDMS material also depends greatly on the cross-linker ratio.

Finally, in [Cha05], we find that the adhesion energy of PDMS depends on the molecular weight of the polymer – a direct consequence of the cross-linker ratio. Instead of a direct estimation of adhesion energy, experiments using the Johnson-Kendall-Roberts (JKR) theory analyze the increase of the normalized Hertzian contact patch size under an applied load [FZCS05].

In summary, we have found the following from our review of current literature on PDMS material properties:

- PDMS is not yet well understood and constitutive laws characterizing its behavior are still under development;
- PDMS properties are not repeatable even for the manufacturer prescribed recipe;
- PDMS is highly sensitive to its preparation conditions and minor variations in the 'recipe' cause significant variations in its properties;
- PDMS density is *not* affected by processing conditions;
- PDMS viscosity is dependent on the 'gelation' reaction with the cross-linker

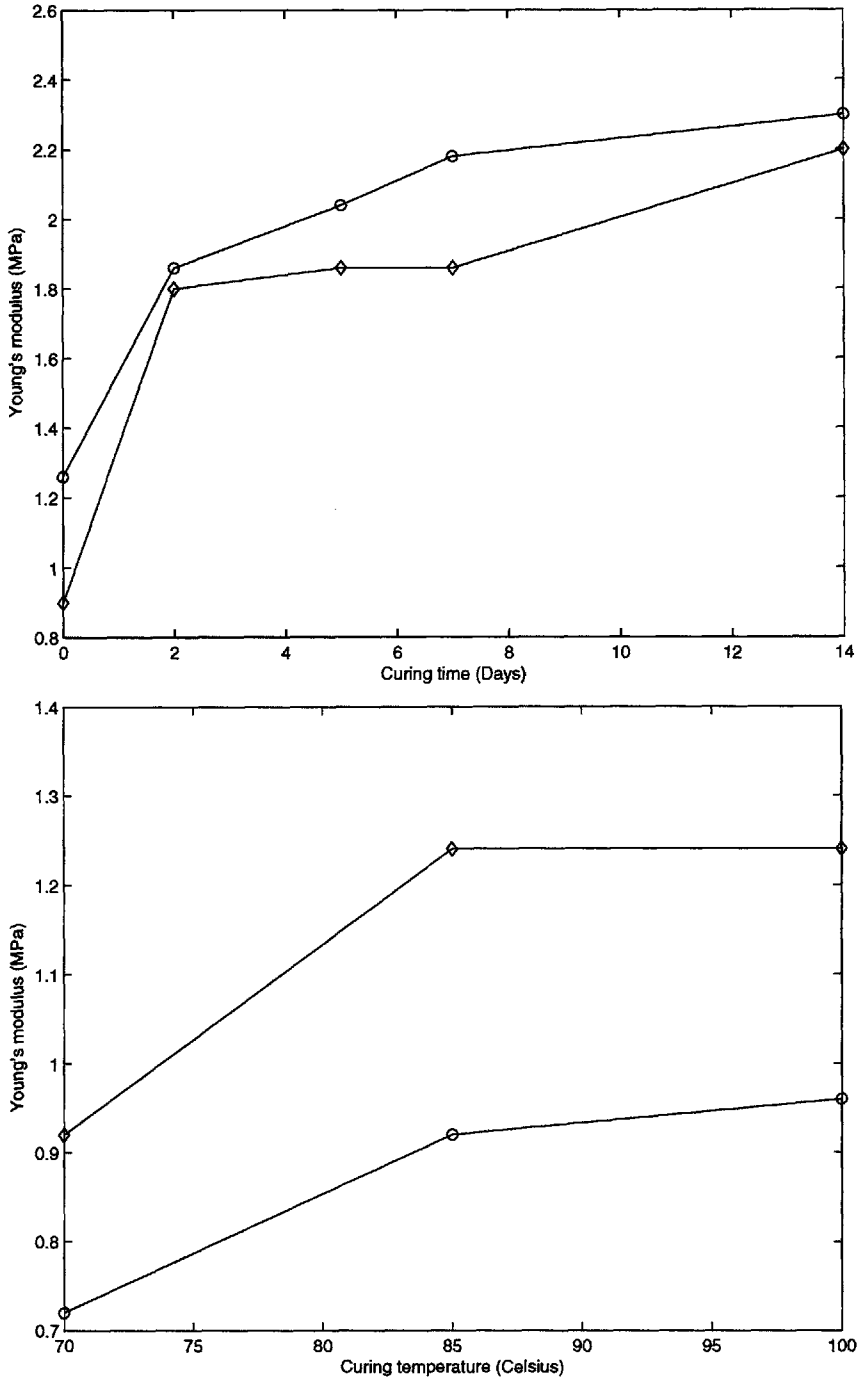

Figure 2-5: Young's modulus variation in PDMS samples for the same curing ratio but for different curing conditions, *i.e.*, time and curing temperature. In each figure, the curve at the top shows property variation for a crosslinker ratio of 10:1 and the curve at the bottom shows property variation for a crosslinker ratio of 11:1. Adapted, with author's permission from [ECB03].

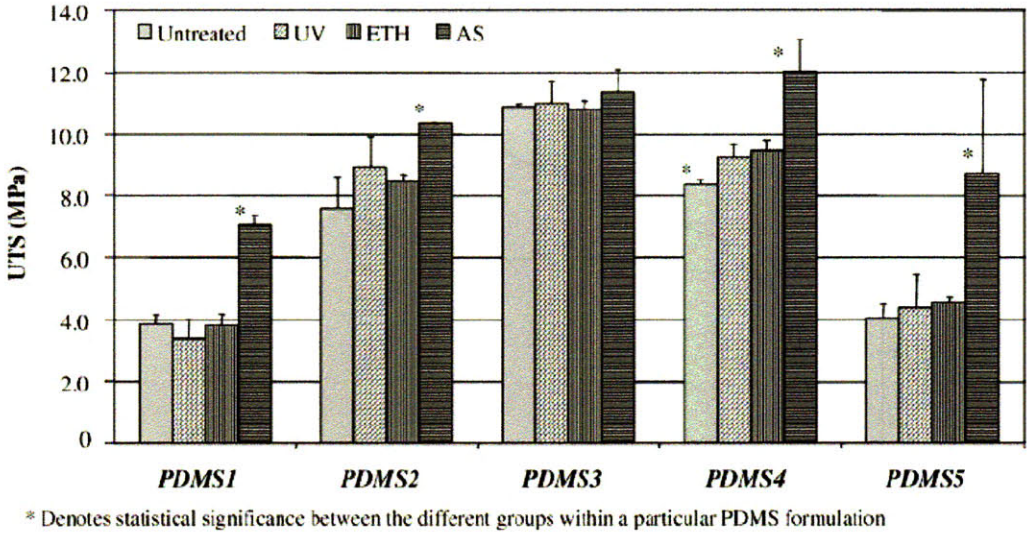

Figure 2-6: Ultimate tensile strength of PDMS as a function of cross-linker ratio of 6, 10, 14, 21 and 43 weight % [MFR05]. Included with permission from the publisher. ©Springer.

and is a function of the cross-linker ratio and the lapsed time since cross-linking started [MFR05];

- Viscosity of PDMS is nearly constant under an applied strain and does not change over the course of the spin-coating process.

2.2 The Current PDMS Film Fabrication Process

2.2.1 Current Spin-Coating of PDMS Films

Spin-coating is the most widely used fabrication method for preparing thin PDMS films of different thickness values. An alternate approach, which employs a knife edge for coating, can be used to manufacture films down to 250 microns thick [Cor], but no thinner. Further, these films only serve the need for unpatterned and smooth films. Spin-coating on silicon substrates is necessary in order to transfer substrate

topography onto the PDMS film.

The spin-coating process begins with cleaning the substrate to remove organic contaminants. It is then dried using nitrogen and coated with a monolayer of silane to reduce the adhesion between PDMS and the silicon dioxide (SiO_2) surface. The most common pre-polymer to cross-linker ratio is 10:1 (refer Appendix A). The mixture of pre-polymer and cross-linker is centrifuged, degassed and spin-coated on the substrate. During spin-coating, a small volume of PDMS is poured near the center of a horizontal substrate (silicon wafer or quartz disk). The substrate is then spun about a vertical axis. During spinning, the PDMS liquid is subject to centrifugal forces causing the liquid to spread on the substrate and progressively thin. The viscous and surface tension forces oppose the spreading due to centrifugal forces. However, the surface tension forces are dominant only at the boundary of the PDMS on the substrate due to the large local curvature. The advantage of spin-coating films lies in the flexibility in preparing different thicknesses and quick turnaround time.

Spin-coating of PDMS has borrowed heavily from the spin-coating of photoresist in the microelectronics industry. For photoresist, the manufacturer usually provides a curve highlighting the best estimated thickness value for spin-coating for a prescribed duration at various spin speeds. Even today, PDMS spin-coating follows a similar approach where users perform several sets of experiments to characterize their spin-coating equipment and obtain estimates of thickness values for various spin speeds. The spin-coating speed and duration are chosen based on an estimate of the final thickness [1]. The sample is then baked in an oven at 85^o for between 20 mins and a few hours. Such an open loop approach to PDMS spin-coating leads to poorly predictable thickness values with large variations.

In Chapter 3, I will analyze the physics of spin-coating of PDMS and show how it is different from that of spin-coating a photoresist. Evaporation of the photoresist solvent occurs while the wafer is spinning. In contrast, PDMS does not have any

[1]For example, spin-coating at 750 rpm for 60 seconds might yield a film of about 90 μm thickness.

solvent evaporation and the spin-coating process of PDMS can be viewed as that of a highly viscous liquid spreading under centrifugal forces. I will show that the spin-coating thickness of PDMS can be described using an analytical model, developed by Emslie *et al*, relating the initial thickness, spin speed, time and material properties [EBP58]. Such a closed-form model cannot be developed for photoresist because of the simultaneous solvent evaporation and centrifugal action. From a review of the literature, there has not been an adequate study of the sensitivity of the PDMS spin-coating process and of possible approaches to improve accuracy and repeatability of the desired thickness.

2.2.2 Peeling of Thin PDMS Films by Hand

Here, I describe a typical sequence of steps for the manual peeling of a film that has been cured following spin-coating on a surface. The operator first scrapes away the portion of film that has overflown the substrate edge. She[2] then cuts away the capillary ridge portion of the film all around the substrate. After both these preliminary steps, the operator inserts a sharp edge of a razor underneath the PDMS to separate a small 'lip' of the film (Figure 2-7). By holding the lip between her fingertips or using the ends of a pair of tweezers and by applying a combination of pulling and twisting, she attempts to peel the film from the surface. In mechanics parlance, the operator is peeling the film by applying either a force and/or a moment. From a control-theoretic viewpoint, one could also say that the operator is applying force or displacement control on the film with visual feedback of the film's state.

While peeling under such conditions, if the film encounters a region of higher adhesion to the substrate, the applied force on the tweezers must increase. The tweezers contact the film at two sharp tips and an increase in applied force might result in the tweezer tips poking through the film. Tearing of the thin PDMS film

[2]I mention the operator as feminine throughout this thesis as a literary choice and not on account of any bias.

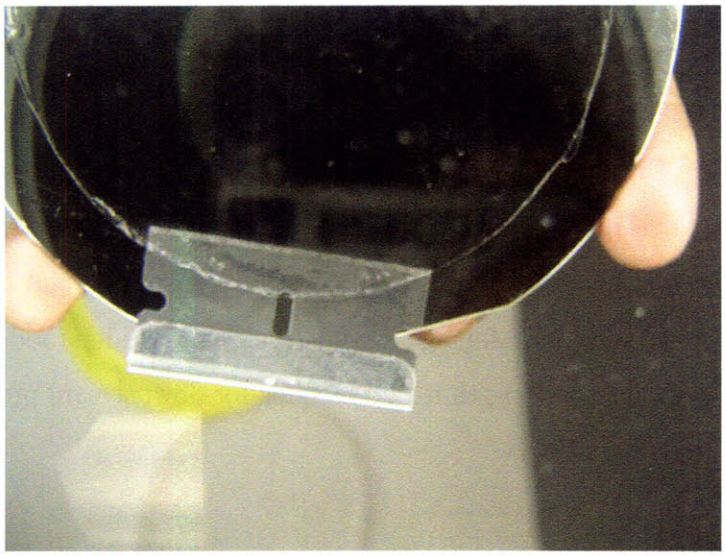

Figure 2-7: It is common to insert a razor blade under the film to free a small portion of the film and initiate the peel.

is possible due to locking over the wafer edge or at the capillary bead, or when encountering stress intensities, or dynamic effects.

In Section 2.3 of this Chapter, I elaborate on the process-level challenges while peeling thin PDMS films and discuss implications for a manufacturing process.

2.2.3 Handling of Thin PDMS Films

After peeling the thin PDMS film by hand, the operator transports the film for futher processing or for assembly on a device using a pair of tweezers. The process of transporting the film has many opportunities for damaging the film: the tweezers can poke through the film, or the film can wrinkle or self-adhere. The operator must exercise caution to separate any self-adhered portions before the film could be used. If the thin PDMS film needs to be stored, it is kept in a petridish. Here again, the film could adhere to the surface it is supported on and the user may have to peel the film off again.

2.3 Macroscopic Process Challenges

The existing PDMS film fabrication process described in Section 2.2 has several challenges. First, the thickness of the film may not be accurate, hampering its performance. Second, the challenges in the manual peeling process demand the intervention of a skilled operator, making the process both time-consuming and labor-intensive. Third, the factors causing film damage are not yet clearly understood. Finally, there has been little work on handling thin PDMS films for downstream processes. I elaborate on these challenges below.

2.3.1 Thickness Variation During Open-loop Spin-Coating

In Section 2.2.1, I discussed how users presently prepare very thin PDMS films by open-loop spin-coating. The open-loop approach for spin-coating does not result in a repeatable film thickness because of the following factors, which are not possible to monitor closely by users:

- initial pour (volume and location of pour on substrate);
- material properties (density and viscosity);
- spin coating conditions (spin speed and duration).

The variation in material properties of PDMS, combined with sensitivity to the spin-coating conditions lead to relative variations of $\sim 20 - 30\%$ in the final film thickness. In many applications, the performance of the PDMS film critically depends on the accuracy of thickness.

2.3.2 Gripping the Film for Peeling

Any device that we develop must accomplish three steps in the peeling process:

1. initiate the peel,

2. separate the film from the wafer, and

3. transport the peeled film away from the wafer.

Unfortunately, the first and second stages are complicated by the inherent physics of peeling that I will discuss further along in this chapter. Let us begin by looking at the initiation of separation. This is a difficult step because the PDMS film adheres over the entire area of the substrate, leaving no 'lip' to hold the film or to start the separation. When an operator introduces a lip by inserting a razor, she must be careful not to scrape the film or inadvertently cut through it. Once she initiates separation, the operator may pull the film at point-contacts which may cause excessive stresses and risk tearing around the contacts. If the film is adhered well to the substrate, she may need to pull hard on the PDMS film which could also cause tearing.

2.3.3 Tearing at the Capillary Bead

Even after a portion of the film has been peeled off the substrate (the peel-initiation step), thin PDMS films tend to tear from the periphery. The edge bead formed during spin-coating is one important cause of such damage. Along with the edge bead, there is also the overflow of the polymer over the substrate's edge. Upon curing, the overflow region locks the film around the edge and prevents uniform separation as the peeling process proceeds. The uneven separation is another cause of tearing. To avoid such tearing, the substrate edge must be scraped manually. Depending on the speed of spin-coating, the edge bead could be twice as thick as the PDMS film being peeled. The comparatively thin PDMS film is unable to provide sufficient strain energy for the edge bead to peel, resulting in tearing.

2.3.4 Difficulty of Advancing the Film During Peeling

The stability of a peeling process in response to actuation disturbance has been analyzed using on a 2-D beam model on a uniform substrate [Bol96]. When peeling

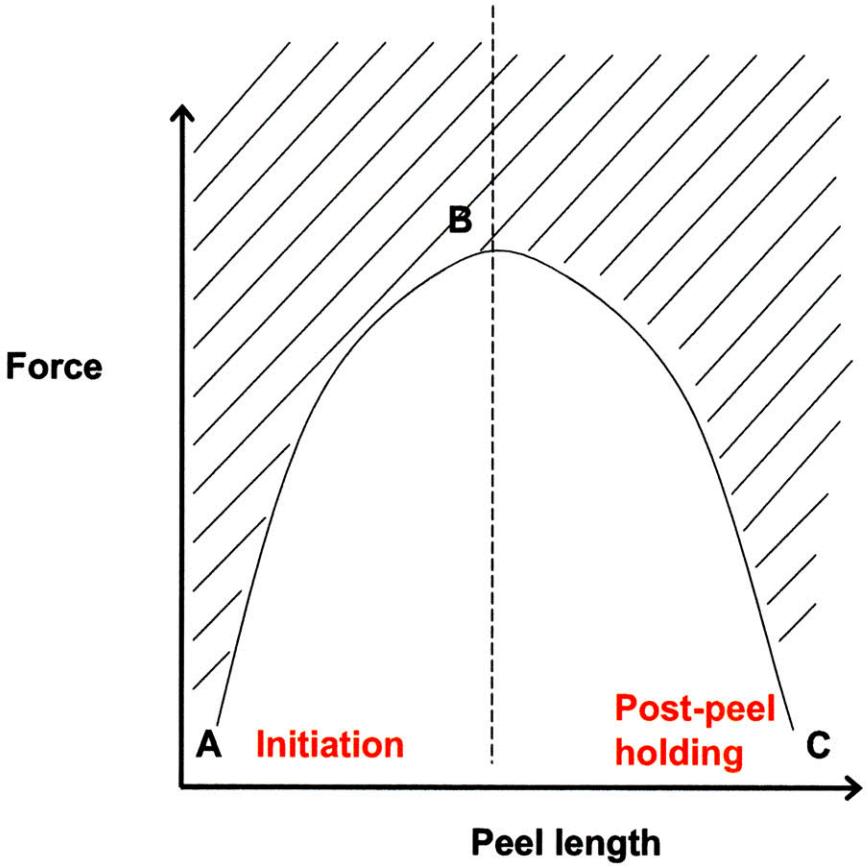

Figure 2-8: Force actuation versus peel length during peeling off a film from a circular wafer. As the film is peeled off the wafer, the applied force must first increase and then decrease.

a thin PDMS film, the overall geometry of the substrate impacts the actuation that needs to be applied. In Figure 2-8, I show that when peeling a film over a circular silicon wafer, the applied force must increase to account for the gradually increasing width of film. Once more than half the film has been peeled, the amount of force required to peel starts decreasing. If the operator does not diligently adjust her effort accordingly, the film peels off in an uncontrollable fashion and could tear.

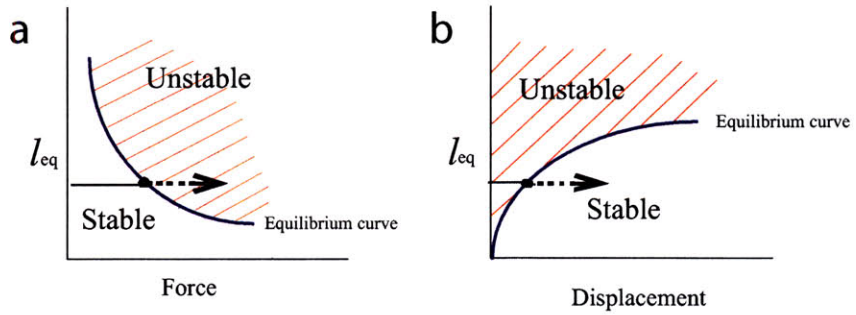

Figure 2-9: Stability analysis for peeling over a uniform substrate [Bol96]. Under force actuation, the peeling process is unstable to disturbances while under displacement actuation is stable.

2.3.4.1 Dynamic Effects

Once separation has been initiated, the peel front must be advanced at a controlled pace. Unfortunately, here too, the physics dictate otherwise. Based on a 2-D model of a beam adhered to a uniform substrate, force actuation is unstable while displacement actuation is stable [Bol96]. By this definition (Figure 2-9), unstable means that the actuation no longer has control over the location of the peel-front. In Figure 2-9, we plot the equilibrium location of the peel-front as a function of actuation. In Figure 2-9 (a), consider the situation when the actuation force suddenly increases, *e.g.*, when the actuator has an overshoot to a step input before settling at the final value. When the actuation force increases, the equilibrium peel-length that can be sustained is reduced. At the peeled length, the film is no longer at equilibrium and the peeling process is hence unstable under force actuation. In Figure 2-9 (b), when the displacement actuation increases by a small amount, the equilibrium peel length increases as well. As the applied displacement increases, the overall system can still achieve a state of equilibrium and hence displacement actuation is stable. Unstable peeling results in advance of the peel front at very high speeds. When the substrate is no longer uniform, such as one with islands of micro-features, stability can be further influenced by the geometry and directionality of the pattern.

2.3.4.2 Sharp Features

One of the consequences of the uncontrolled advance of the peel-front is the whiplash where the film could peel at high speeds until it encounters a feature, a bead or any obstruction. When there are features on the substrate such as a boss or a sharp corner, there is a stress concentration around the feature. When the peel-front advances in a dynamic manner, the stress intensity around the sharp features could be amplified causing tearing. Tears in PDMS film propagate at very high speeds and thus, a more serious consequence of uncontrolled peeling will be damage to the entire PDMS film.

2.3.5 Handling of Film After Peeling

After the operator has diligently managed to peel the PDMS film off the substrate, the next task for them will be to hold the PDMS film without contact or damage at the important surfaces. A thin PDMS film is very flimsy, self-adhering and can easily wrinkle. The use of a backing material such as a thin plastic film on top of the PDMS film has been recently reported [HCF04]. The backing material is removed once the film is placed at its desired location (Figure 2-10).

2.3.6 Alignment of Thin PDMS Films

Thin PDMS films carrying topographic features such as microchannels need to be aligned precisely before being assembled into devices. In order to avoid trapped air pockets while attaching thin films, it is necessary to attach the film by propagating a contact line from one end, a process almost the inverse of peeling.

2.4 Underlying Process Physics

So far, we have seen the process level challenges involved in the preparation of thin PDMS films. PDMS is a relatively new material and since the development of many of

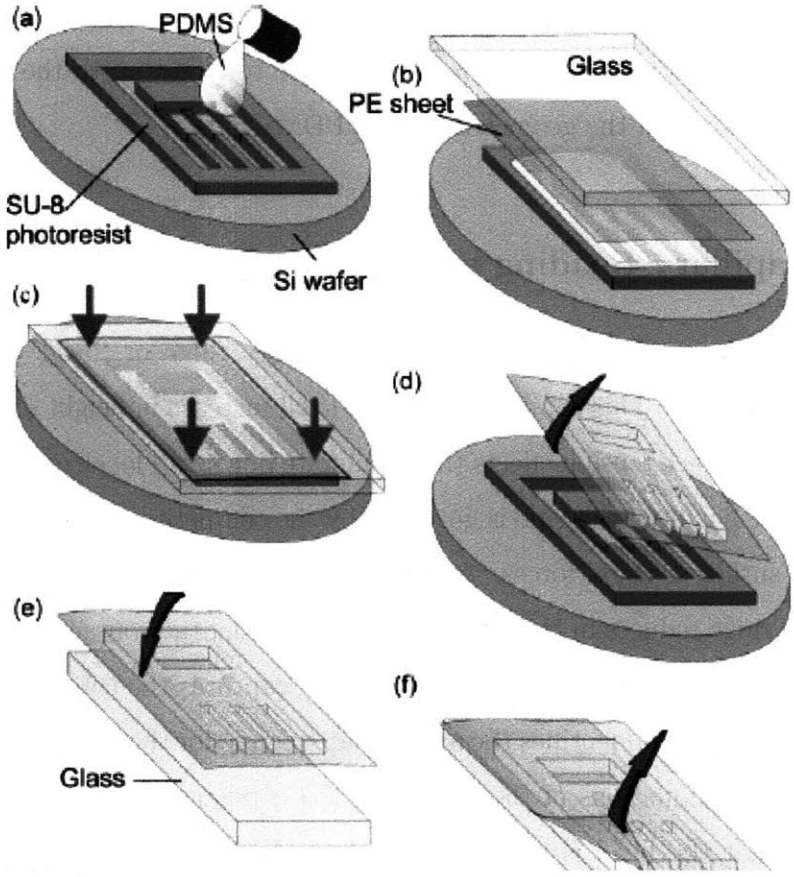

Figure 2-10: A thin backing material made of polyester is adhered to the PDMS surface at the top and the film is peeled from the substrate by holding on to the backing. The film must subsequently be released from the backing [HCF04]. ©Royal Society of Chemistry.

its applications is incipient, the lack of understanding of the process physics of PDMS film preparation is problematic. The material properties of PDMS are also not yet clearly understood and the physics of PDMS peeling has not been well characterized. All these factors render PDMS film preparation more of a 'craft'. Here, I list some of the key physics and show how they influence the design of robust, PDMS film manufacture. Furthermore, the discussion on material properties in Section 2.1.2 suggests that any process we develop must be able to stand up to the variations in material properties and the geometries of the PDMS films.

2.4.1 Capillary Beading at the Substrate Edge

During spin-coating of a blob of PDMS, a capillary ridge or 'bead' forms at the boundary of the blob. This capillary ridge is a local increase in height of the film and is the result of surface tension effects that dominate in a small localized region of high curvature. The height of the blob is governed by the competition between centrifugal, viscous and surface tension forces. As the PDMS blob spreads during spin-coating, the capillary ridge reduces in thickness while maintaining the contact angle boundary condition. The modified Ohnesorge number (Oh) captures the competition between the different effects and identifies the appropriate regime for the dynamics of the bead size. Numerical simulations of the evolution of a capillary bead on a flat substrate have shown that the bead is much thicker than the rest of the PDMS film and it extends over a region several times in thickness. The capillary length as applicable to spin-coating is,:

$$l_{cap} = \sqrt{\frac{\sigma}{\rho\omega^2 R}} \tag{2.1}$$

where l_{cap} is the capillary length, σ the surface tension, R the radius of substrate, ρ the density and ω is the spin-speed respectively.

For PDMS spin-coating at 750 rpm on a 4" Silicon wafer substrate, the above equation provides a capillary length estimate of about 250 microns. However, this

calculation does not account for the reduction in bead thickness once the blob of PDMS reaches the edge of the substrate accompanied by expulsion of material. In practice, it is observed that the capillary bead at the periphery causes the PDMS film to overflow the substrate. When the film cures, the overflow region typically locks the film over the edge. Users of PDMS films are often aware of such overflow and at present must scrape the edge of the substrate to remove the overflow region before peeling. Some users attempt to remove the capillary bead region by scraping with a razor edge. If the capillary bead were not removed, it could cause problems during peeling as the bead, which is thicker, is harder to peel by holding on to the much thinner film. The bead could then cause the film to potentially tear during peeling.

2.4.2 Singular Stress Zone at Peel-front

Boundary conditions differ on either side of the peel-front. On one side, the surface of the film is unattached and has zero shear stress. On the other side, the film adheres to the surface and shear stress is imposed on it by the substrate. This results in a singularity at the peel-front , which means there is a very small and narrow zone around the peel-front where the stress values change rapidly. In particular, during peeling the normal stress is tensile at the peel-front and rapidly decays to zero or to a comparably much lower average stress state. This stress singularity in the normal stress causes the separation of the film at the peel-front.

When viewed close to the peel front, peeling of PDMS could be formulated as a boundary value problem with the appropriate boundary conditions at the rigid substrate and at the actuator. Consider the 2-D case of a rectangular film adhered to the surface and to which a tensile force is applied as shown in Figure 2-11.

The 2-D elasticity problem is formulated as the biharmonic equation:

$$\nabla^2\nabla^2\phi = 0 \tag{2.2}$$

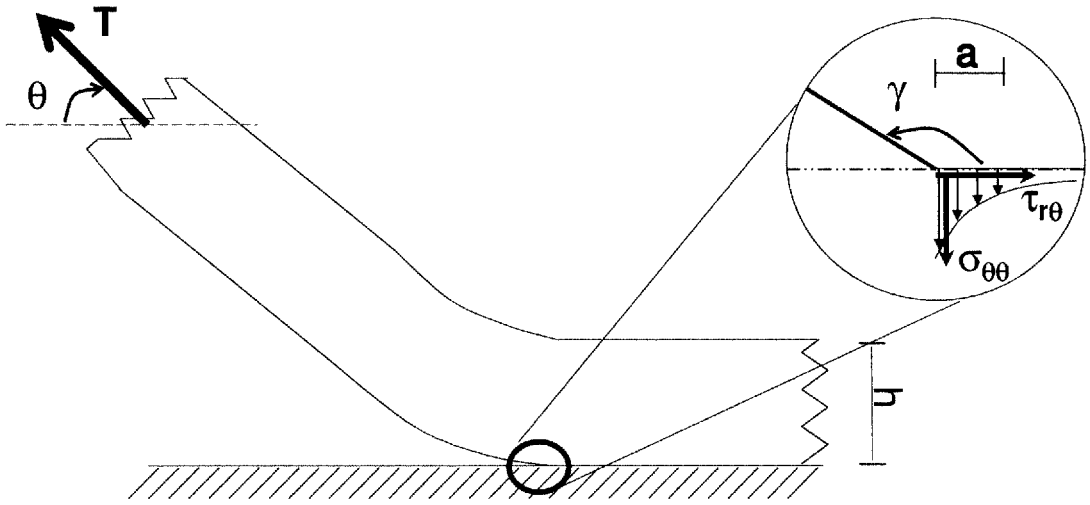

Figure 2-11: At the peel-front, there is singularity – where large stress values are concentrated in an infinitesimal region. The order of singularity depends on the peel angle γ. The size of the singular stress zone a is much smaller than the film thickness and can not be accurately evaluated. Here $\sigma_{\theta\theta}$ indicates the hoop stress (tensile) and $\tau_{r\theta}$ indicates the shear stress.

, where ϕ is the stress function, with appropriate boundary conditions of stress and displacements.

A length scale for the strained zone during peeling is found by choosing a stress function of the form:

$$\phi = Ae^{-\frac{\epsilon x}{h}}\left(Kcos\frac{\epsilon y}{h} + \frac{\epsilon y}{h}sin\frac{\epsilon y}{h}\right) \tag{2.3}$$

where h is the thickness of the film, ϵ is a parameter that identifies the size of the characteristic lengthscale.

Based on an eigenvalue analysis, $\epsilon_{minimum} \approx 1 \Rightarrow a \sim O(h)$ gives an upperbound for the deformation region size [TG70]. In many cases, higher eigenvalues dominate the solution to Equation 2.3 and we find that $a \ll h$. Near the peel-front, the film can be analyzed as a wedge adhered to the substrate. The singularity in stress can be solved using the Williams' asymptotic analysis [Wil52]. Alternately, by using an integral transform – the 'Mellin' transform, we can rewrite the biharmonic equation and the associated boundary conditions using transformed variables [Bog68]. The

solution for the system of equations under Mellin transform gives the order of singularity but not the critical stress intensity factor. We find that for the order of singularity depends on the peel angle and does not necessarily equal 0.5. The stress field around the peel-front, though similar, is not the same as that of stress fields surrounding a crack-tip. The stress field can be described in terms of the order of the singularity but the region over which singularity is important is a few orders of magnitude smaller than the film thickness, and is difficult to estimate.

2.4.3 The Difficulty of Initiating Separation

Any peeling device must accomplish three steps in the peeling process: initiate the peel, part the film separately and handle and transport the peeled film away from the wafer. Unfortunately, the first and second stages are complicated by the inherent physics of peeling. In the previous section, I have identified the presence of the singularity at the peel-front (the edge of a PDMS film prior to initiation) and shown that the bulk of strain deformations is limited to a small region at the peel-front. Based on the singularity in stress, I now assert that the edge of the film is the most promising location to initiate a peel. Upon initiating the peel, the peel-front location still retains the stress singularity (sometimes referred to as stress concentration) which causes further separation of the film from the substrate. I further show that the stress singularity at the peel-front could get amplified around sharp inclusions, increasing the risk of tearing and damage.

We begin by looking at the initiation of separation. This is a difficult step because the PDMS film adheres over the entire area of the substrate, leaving no 'lip' to hold the film or to start the separation. During peel initiation, the goal is to separate a small portion of the spin-coated film from the substrate and attach it to an actuator. Current manual approaches involve using a razor blade or the ends of a pair of tweezers to separate the film at the periphery of the wafer. The ends of a razor blade apply a shear force at the interface between the PDMS film and the substrate.

The shear force causes separation of the PDMS film from the substrate. Sometimes when the razor edge is not precisely at the PDMS-substrate interface, the operator can tear or smudge the film with the razor edge. If the operator has skilfully avoided damaging the film, she could then hold the separated portion of film using a pair of tweezers to continue the peel. In some applications of peeling with surface features, the stress singularity around sharp features could aggravate the risk of tearing. This can be shown analytically by assuming sharp surface variations to be sinusoidal. The amplitude and the wavelength of the sinusoid approximate the effect of sharp features. The surface energy term depends on the arc length of the curve and captures the increase in strain energy during peeling around sharp corners [GK03].

Alternatively, the operator could attempt to initiate the peel by applying an upward force on the top surface of the film. For such an approach, the upward force could be applied by either a negative pressure (say, a vacuum) or by using a strong adhesive to attach to the top surface. The schematic of these approaches is shown in Figure 2-12. The success of either approach depends on how close the applied force is to the vertical plane of the peel-front. Only when the force is applied in the same vertical plane as the edge, the singularity at the edge results in peel-initiation.

If the location of the negative pressure is not directly over the peel-front, but over the adhered portion of the film, it can be shown that the effective load decreases as the inverse of the distance of offset.

The surface stresses on an elastic half-space under a line load are given by:

$$\sigma_z = \frac{2P}{\pi} \frac{z^3}{(x^2+z^2)^2} \tag{2.4}$$

$$\tau_{xz} = \frac{2P}{\pi} \frac{xz^2}{(x^2+z^2)^2} \tag{2.5}$$

where σ and τ are the normal and shear stresses, P is the applied line load, and x, z are the spatial coordinates [Joh87]. When P is positive upwards, σ_z is tensile. With the application of an upward force at the top surface, we hope to cause initiation

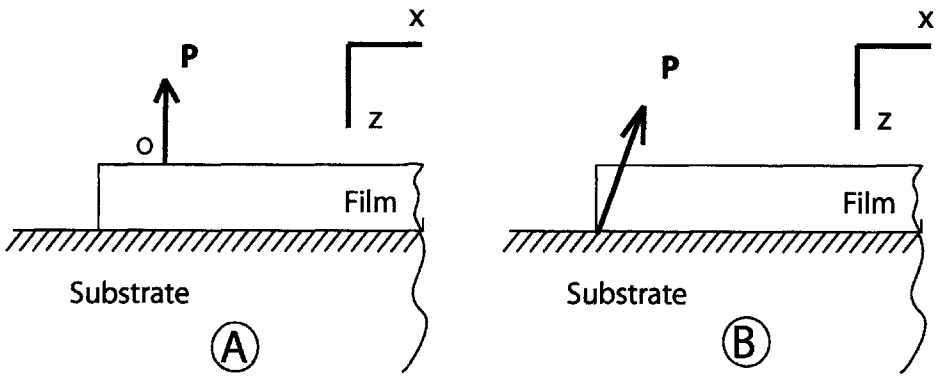

Figure 2-12: For peel initiation, one could apply either, A. An upward force on the top surface of the film or B. A force applied at the edge on the bottom surface (the rest of the bottom surface of the film are not directly accessible)

at the bottom surface of the film. While the above equations are valid only far away from the ends of the elastic half-space, their implications are applicable to peel initiation. The maximum tensile stress is along the vertical line under P and has a strong attenuation once we move away from the edge over the adhered portion of the film. If, however, the load is applied on the separated portion of the film, it helps in peeling because of the moment arm. Even then care must be taken not to introduce an excess of tension in the film as that might cause a tear at the peel-front, or near the points of attachment.

2.4.4 Identifying a Criterion for Separation

Initiating the separation of a PDMS film from a substrate is intrinsically difficult. It would be useful to understand the criteria for separation – as we would if we were studying crack propagation. The adhesion of PDMS to a silicon or glass surface occurs mainly through the formation of hydrogen bonds and with van der Waal's attraction forces [Isr03]. When we peel a PDMS film from a substrate, the work done to overcome molecular interactions over a unit area can be averaged as a surface energy term, γ . Based on the Johnson-Kendall-Roberts (JKR) theory applied to experiments with flexible hemispherical lenses [JKR71], the work of adhesion of PDMS to PDMS has been estimated to be about $40 \sim 45\ mJ/m^2$. Thus, the surface free-energy of PDMS becomes $20 \sim 22\ mJ/m^2$ [FZCS05]. The surface energy of PDMS on silicon surface has been estimated as $44\ mJ/m^2$ [CW91].

Except for the surface energy value, we are not aware of any other experimentally verified interface separation models for PDMS on silicon or glass substrates.

2.4.4.1 Surface Energy

As the PDMS film peels, two new surfaces are created and work needs to be done to overcome the increase in surface energy. Such a macroscopic view of peeling gives rise to the surface energy term describing peeling. The surface energy approach is also known as the Griffith's surface energy approach following Griffith's early work in understanding the rupture and failure of solids [Gri21]. When two different solid materials are in contact, the region of influence of adhesion is modelled differently by two theories: the Johnson-Kendall-Roberts (JKR) theory and the Derjaguin-Muller-Toparov (DMT) theory . In the JKR theory, the surface energy term is assumed to act everywhere within the region of contact between the surfaces, but nowhere outside. In the DMT theory, the surface energy term is assumed to act at the contact line and a little ahead of it, but nowhere else. While these two theories are seemingly in conflict, it has been shown by Tabor that the correct choice of surface energy model

is determined by the Tabor parameter μ describing the adhesion between two elastic spheres is given by:

$$\mu = (\frac{R\gamma^2}{E'^2 z_0^3})^{\frac{1}{3}} \tag{2.6}$$

where R is the effective radius of the two spheres, $\frac{1}{R} = \frac{1}{R_1} + \frac{1}{R_2}$, γ is the surface energy between the two materials, E' is the composite modulus $\frac{1}{E'} = \frac{1-\nu_1^2}{E_1} + \frac{1-\nu_2^2}{E_2}$ and z_0 is the intermolecular separation distance at equilibrium. The Tabor parameter characterizes the relative influence of adhesion, elasticity, curvature and the atomic separation. It has been shown that for large Tabor parameter values, *i.e.*, for soft solids with large radius of curvature, the JKR theory is applicable. For small Tabor parameter values, *i.e.*, for hard solids with small radius of curvature, the DMT theory is applicable [MB78]. Surface energy models that are used to describle PDMS peeling use the JKR model and often use the deformation of the contact patch on a hemispherical lens to estimate the energy value [FZCS05] [CW91].

Beyond these theories of surface energy model of adhesion, conventional peel-tests have also been used to experimentally measure the adhesion energy. In the peel-test model, a rectangular tape of width b is peeled off a surface under the application of a tensile force F. The tape is assumed to have negligible bending stiffness. As the tape peels at a constant angle under equilibrium conditions, the work done by the applied force equals the surface energy increase. This approach has been reported as accurate in the range of angles from 30° to 140° [LS81]. PDMS, being hyperelastic, may not be an easy candidate for such a peel-test approach, as the work done by the force could elastically stretch the PDMS film long before there is any peeling.

2.4.4.2 Critical Stress Intensity to Initiate the Peel

In order to initially separate the film that is adhered everywhere to the surface, we need to apply a tensile load on the film. The point of application of this tensile load is critical to the success of initiation. One could imagine a negative pressure applied as a vacuum load or as a pulling force through an adhesive layer on the top surface

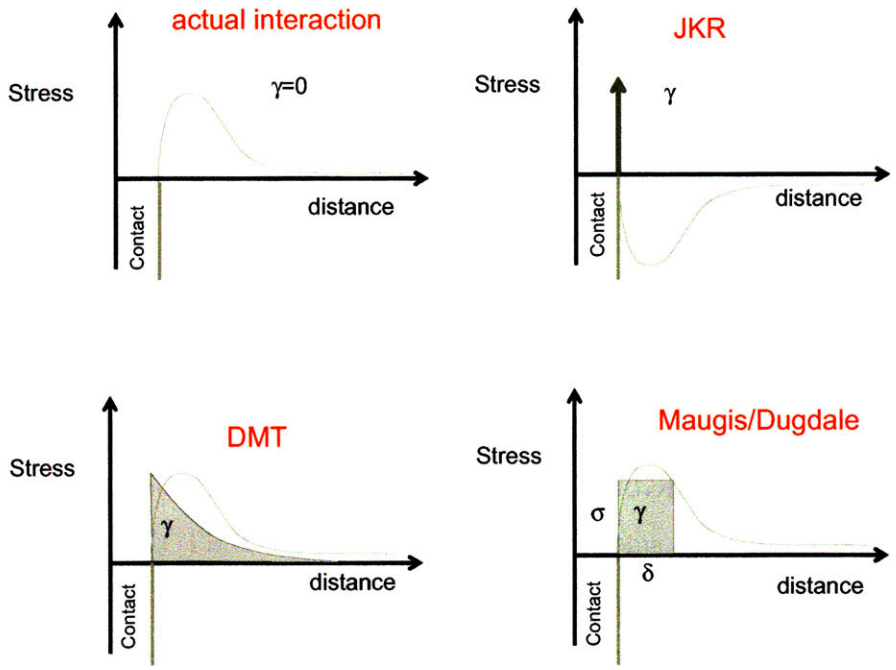

Figure 2-13: Comparison of the surface energy models used for defining adhesion and their associated region of definition.

of the film. The applied vertical force on the top surface of the film is most effective if the point of application of the force is in the same vertical plane as the peel-front. However, the exact value of the force applied on the top surface depends on the film thickness, its modulus and the adhesion level. Even though we could use a critical stress intensity term to identify the peeling behavior, it is not possible to estimate the intensity or to calibrate individual samples during peeling.

2.4.4.3 Cohesive Zone Model

An interface constitutive model called the cohesive zone model has been used more recently to describe the combined effects of a limiting tensile stress value as well as a surface energy term. The cohesive zone model provides an estimate of the traction-displacement relationship in a very small region at the peel-front. It has been successfully implemented in many commercial finite element packages. Instead

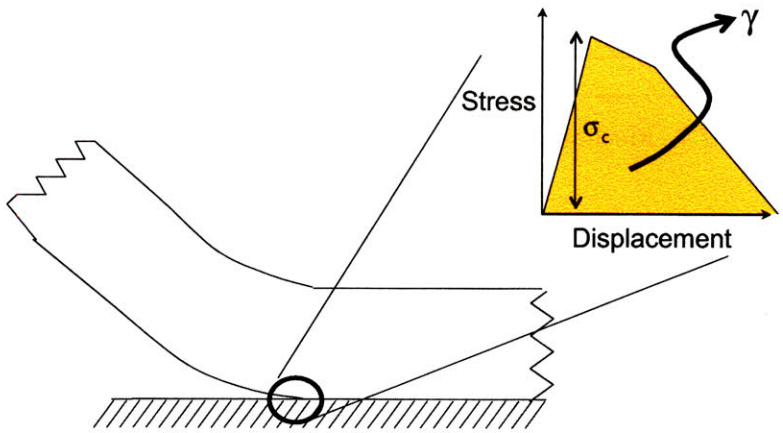

Figure 2-14: The interface constitutive model for the cohesive zone consists of an elastic response region, a damage initiation criterion based on critical stress and a damage evolution region which encloses an area equal to the surface energy.

of modelling the stress singularity, the cohesive zone has an elastic deformation zone and a damage accumulation zone, once the traction stress has exceeded a critical value. The damage accumulation zone can be modelled in several ways, all of which ensure that the total energy dissipated in the cohesive zone is related to the energy required to separate the two surfaces (often termed the 'adhesion energy' instead). The cohesive zone model allows for better understanding of surface separation, fracture or crack propagation. However, calibrating real life scenarios to a cohesive zone model is very challenging. Specifically, it is not possible to directly estimate the critical stress value in the stress-displacement law in the cohesive zone. For the case of PDMS, an experimentally verified interface constitutive relationship is an open question [CWHT02].

	PDMS	Silicon	SiO_2
Elastic modulus(E)	$1 \sim 3$ MPa	165 GPa	73 GPa
Poisson's ratio(ν)	.498	.3	.3
Yield Strength (σ_y)	$2 \sim 4$ MPa	7 GPa	8.4 GPa
Density (ρ)	897 kg/m^3	2330 kg/m^3	2500 kg/m^3

Table 2.1: Mechanical properties of PDMS and substrate

2.4.5 The Behavior of the Separated Film

I now move on to discuss the mechanics of the film after peeling. The silicon or glass substrate is essentially rigid when compared to the PDMS film (Table 2.1). The peeled section of the film is affected by bending, stretching and shear deformations in different regions. However, these deformations are dominant at different length-scales and no single analytical model can capture them. For understanding the mechanics of the peeled film in 2-D, a small-deformation linear analysis using a beam model or large-deformation non-linear analysis using an elastica model may be used. A 2-D peeltest model captures stretching effects [Wil97].

2.5 On Process Automation

So far I have outlined the challenges and the intrinsic physics of peeling thin PDMS films. In order to design an automated process for PDMS film manufacture, I briefly introduce some related machines. The process of peeling, handling and attaching thin films is common in industrial applications such as photographic film manufacturing, paper spooling in printers and removing protective films from electronics. I highlight some of the design insights from these machines that could be relevant for PDMS film manufacture.

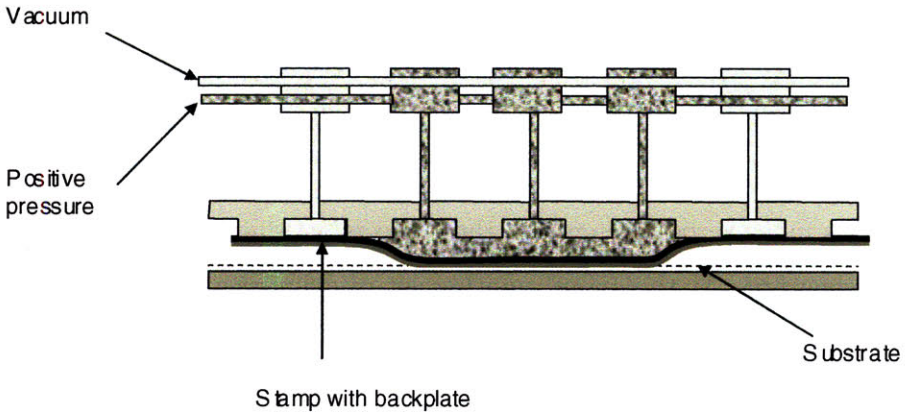

Figure 2-15: A 'wave printing machine' uses a travelling one-dimensional wave of positive pressure to selectively achieve contact between part of the micro-contact template and the substrate. Figure adapted from [DSB+04], ©Materials Research Society

2.5.1 Micro-Contact Printing Machines

For micro-contact printing, the main process requirements are conformal contact without trapped air pockets, accuracy in registration of the stamp over several trials and controlled advance of the contact area. The Offset Liquid Embossing machine makes use of rock and step motion using a locally convex PDMS stamp [BWH+01]. The wave printing machine (Figure 2-15) employs a series of pressure taps that are triggered sequentially to stamp specific regions of a thin, flat polymer stamp with a glass coverplate [DSB+04]. Kendale automated the micro-contact printing machine process by precise parallel alignment of the stamp with the substrate [Ken04].

2.5.2 Web Handling Machines

Paper and web-handling machines are designed to handle thin sheets of material – webs. Webs are kept taut (in tension) with cylindrical rollers for support, to minimize the formation of wrinkles. Further, air cushions using the Coanda effect are used to minimize traction while the webs that move over cylindrical rollers.

Of particular interest to this work is the paper spooling mechanism for printers.

In a printer, the machine has to precisely pick one sheet of paper at a time from a stack to spool under the print-head. By using two sets of rollers, the printer spooling mechanism first pushes out a few sheets of paper from the top of the pile. These sheets could be stuck to each other due to eletrostatic or surface stiction effects. A set of bristles move across the ends of these sheets causing flutter and ensuring that the sheets separate. At this piont, another set of cylindrical rollers catches the top most sheet and feeds it to the printer.

2.5.3 Machines for Peeling Protective Films

The microelectronics industry, the photographic film industry and the printing industry have used thin films as protective coating for many years. For the sake of accuracy and mass-manufacture, many machines that peel protective films exist. One-off removal of protective films is very common and I present a few examples from the patent literature. In [IFK96], we find the use of a cylindrical roller for removing protective films on either side of a printed circuit wiring board. Pressurized fluid is sprayed underneath the protective film to induce separation. In [Ohs94], we find the use of a saw-toothed roller to induce delamination in a coated film and subsequent separation.

2.6 Requirements for a PDMS Manufacturing Machine

In order to make the preparation of PDMS films production ready, I outline the process plan involved during sample preparation, spin-coating, peeling and handling. For the sake of automation, each of these process steps is unique and important, if we are to avoid damage to the film.

2.6.1 Process Requirements

A manufacturing process for PDMS films should achieve the following requirements:

- robustness to material property variations and operator errors,
- thickness accuracy during spin-coating,
- thickness uniformity over the surface of the wafer,
- high yield,
- repeatability across different production runs, and
- high throughput.

2.6.2 Design Requirements

In order to achieve the process requirements outlined in Section 2.6.1, I identify the following design requirements at various stages of the film manufacture.

2.6.2.1 Requirements during Spin-Coating

During spin-coating, variations are possible in the pre-polymer sample, the spin-up conditions of the motor, the flatness and horizontal inclination of the substrate and the wafer chuck. The requirements to ensure repeatability during spin-coating are:

- prepare the PDMS pre-polymer and ensure the spin-coating process is completed within the pot life of the PDMS sample (4 hours),
- place the substrate centered on the spin-coating chuck,
- pour the PDMS pre-polymer on the substrate in a near-concentric manner,
- spin-coat for the prescribed time based on the first-order estimate, and
- when finished spin-coating, remove the substrate carefully from the spin-coater and place it in the oven for curing.

2.6.2.2 Requirements during Peeling

Upon curing, the PDMS film with the substrate and the peel-initiator are taken for the peeling step, which has the following requirements:

- minimize stress in the peeled film,
- avoid tearing at the boundary between the film and the peel-initiator,
- avoid locking of the film over the edge of the substrate.

2.6.2.3 Requirements during Handling of Film

While handing thin PDMS films, the requirements are:

- hold the film while avoiding wrinkling or self-adhesion,
- hold the film without contact or contamination on the top and bottom surfaces,
- provide features for aligning the film for future operations,
- provide a minimal biaxial tension on the film to avoid tearing or damage.

2.7 Chapter Conclusions

From a systematic study of the individual process steps, the following are key problems associated with the current approach to PDMS film preparation:

- material property variation;
- thickness variation;
- peel initiation;
- gripping the film;
- tearing due to beading and dynamic effects;

- handling and storage of the film.

The analysis of the process deficiencies can be used as a guideline to help define requirements for a PDMS film manufacturing process. Further, a review of a few related machines in soft lithography and in web handling is presented.

THIS PAGE INTENTIONALLY LEFT BLANK

Chapter 3

Towards Robust Spin-Coating

3.1 Introduction

The main requirements during spin-coating are to make films of uniform accurate thickness over the entire substrate area. The stiffness of a film scales as the cube of thickness and variations in the thickness have an aggravated non-linear effect on the performance of the films. For example, when used in microfluidic valves, a variation of thickness from 15 μm to 20μm causes a change in actuation pressure from 18 kPa to 30 kPa [SHP+04]. The spin-coating process of PDMS has inherited many of the concepts commonly used for spin-coating photoresist in microelectronics industry. Borrowing from spin-coating of photoresist, many users of PDMS spin-coating rely on tables, which prescribe estimates of thickness for spin speed and time.

In this chapter, I will discuss how the spin-coating of PDMS is different from that of photoresist mainly because PDMS does not contain volatile components. The spin-coating of PDMS can be captured with an analytical model, relating initial thickness, spin speed and time. Such an analysis is not possible for photoresist due to the evaporation mechanism of the solvent. Based on the analytical model, I will present guidelines for improving robustness of spin-coating whereby the film thickness depends only on material properties, spin speed and time duration. I will show how

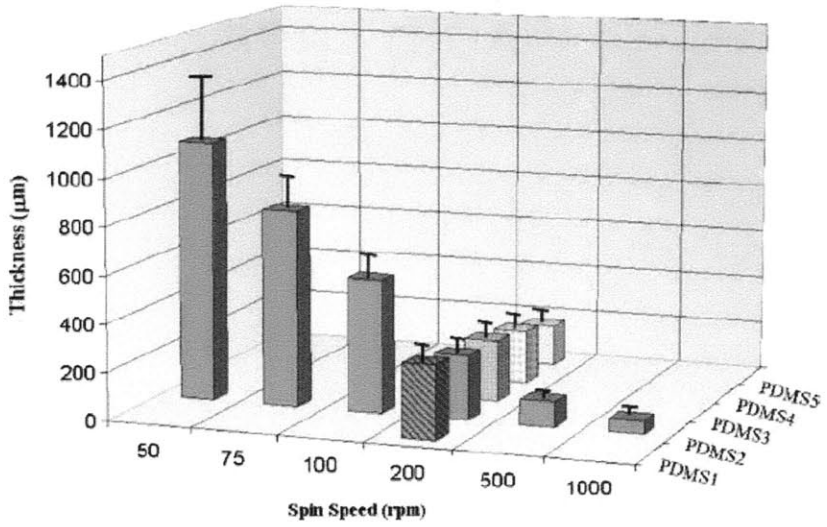

Figure 3-1: Study of PDMS spin-coating thickness for different cross-linker ratios, by [MFR05], shows $\sim 20 - 30\%$ variation in thickness for the same sample and spin speed. Included with permission from the publisher. ©Springer.

$\omega^2 t$, can be used as a single design parameter to determine a particular thickness value.

In collaboration with the Physical Optics and Electronics group in the Research Lab for Electronics (RLE) at MIT, I have performed experiments using low-coherence interferometry as a metrology tool to measure PDMS film thickness in real-time. Based on my robust spin-coating approach, I show my ability to obtain films with thickness variation of about 5%. The variation can be attributed to material property values and disturbances in processing. In order to improve the resolution of spin-coating thickness to about 1 μm, I discuss the use of a real-time metrology setup using reported interferometry techniques, such as low-coherence interferometry (LCI).

3.2 Need for Thickness Control

At present, spin-coating of PDMS films typically involves the use of look-up tables. Look-up tables are prepared by spinning PDMS samples at different rpm values for

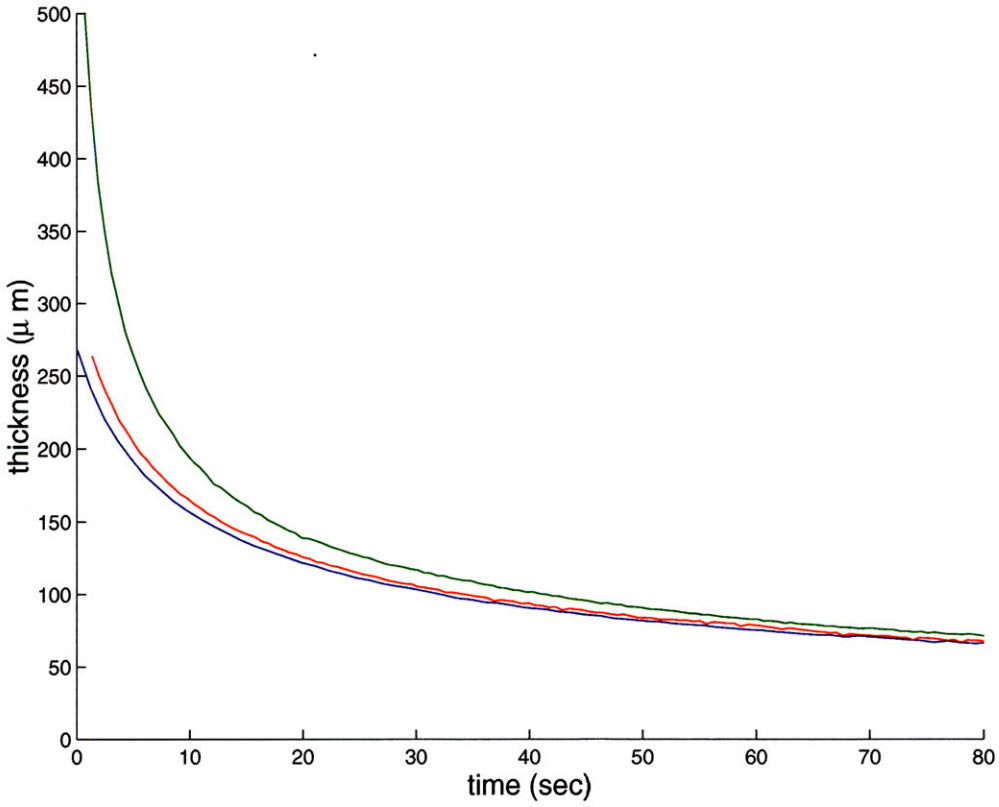

Figure 3-2: For the same sample spincoated at 750 rpm during different experiment runs, the measured thickness values are different. The initial thickness values affect the height variation during spin-coating.

a fixed duration of time, curing them and then measuring the thickness of the solid film using a contact probe. The shrinkage of PDMS during the curing process from a viscous liquid into a solid film is about 1% [ACJ+00]. Based on the shrinkage factor, the final thickness of the spin-coated film is estimated and a look-up table is prepared, giving an estimate of thickness as a function of rpm for a fixed duration of spin-coating. With look-up tables for open-loop PDMS spin-coating, the user assumes that the material properties of PDMS is repeatable across all samples and furthermore that the processing conditions during spin-coating are identical. The material property variations in PDMS discussed in Section 2.1.2 and processing variations contribute to very poor control of PDMS thickness using this approach. Some of the reported

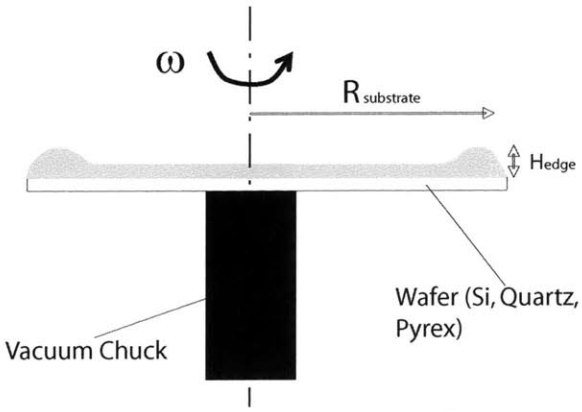

Figure 3-3: PDMS spin-coating is done on a wafer mounted on a spinning vacuum chuck. The film is nearly uniform over the most part of the substrate and at the periphery, there is a capillary ridge or 'bead'.

thickness values for PDMS (Figure 3-1) indicate upto 30% variation [MFR05]. In Figure 3-2, I show measurements of the thickness of PDMS films spin-cooated under identical conditions. The variation in the thickness values highlight the need for better understanding of PDMS spin-coating and more robust approaches to thickness control.

3.3 Model for Spin-coating Thickness versus Time

In this section I analyze the spreading dynamics of PDMS on a substrate . The typical profile of the PDMS liquid covering the entire substrate during the spin-coating process is shown in Figure 3-3. As the substrate is spun, PDMS fluid is expelled at the sides and the film progressively thins.

3.3.1 Key Assumptions

For the sake of simplicity, I will make the following assumptions:

- the initial volume of PDMS is a cylinder of height, h_0, on a flat substrate;
- the axis of the cylindrical volume of PDMS and the axis of rotation of the substrate are coincident;
- the effect of surface tension at the ends of the cylinder are negligible in this analysis;
- the flow of PDMS during spin-coating is in a viscous-dominated regime;
- the flow of PDMS is incompressible.

3.3.2 Height Variation with Time

We write the equations of motion for an axi-symmetric spinning volume of PDMS in cylindrical coordinates. For an incompressible fluid:

$$\nabla \cdot \bar{v} = 0, \tag{3.1}$$

where $\bar{v}$ is the velocity of the fluid.

The complete Navier-Stokes equation for this system is:

$$\rho\left(\frac{\partial \bar{v}}{\partial t} + \bar{v} \cdot \nabla \bar{v}\right) = -\nabla p + \mu(\nabla^2 \bar{v}) + \nabla(\sigma \nabla \cdot \bar{\mathbf{n}}) \tag{3.2}$$

where ρ is the density, μ is the dynamic viscosity, p is the static pressure, σ is the surface tension, $\bar{\mathbf{n}}$ is the normal at a point on the surface of the fluid and $\nabla \cdot \bar{\mathbf{n}}$ estimates the local curvature.

Taking the component along the radial direction and since $v(\theta)$, the azimuthal

component of velocity is zero due to axisymmetry,

$$\rho\left(\frac{\partial v(r)}{\partial t}+v(r)\frac{\partial v(r)}{\partial r}\right)=-\frac{\partial p}{\partial r}+\mu(\nabla^2 v(r))+\sigma\left(\frac{(rh_r)_r}{r}\right)_r \tag{3.3}$$

where $\bar{v}$ is the velocity of the fluid, h is the thickness at a radial location r, ∇ is the gradient operator, ∇^2 is the laplacian operator and subscripts denote partial derivatives. The effect of surface tension is dominant only at the boundary of the cylinder of fluid as the local curvature is large. Solving the complete system is hard and so the solution is divided into two regimes:

1. the inner region where surface tension effects dominate, and,

2. the outer region where surface tension effects are negligible.

At the limit of zero surface tension, and with viscous dominated flow, Equation 3.3 reduces to:

$$-\rho\omega^2 r=\mu\frac{\partial^2}{\partial z^2}(v(r)) \tag{3.4}$$

with no-slip boundary condition imposed on $v(r)$, the radial velocity component, at the solid surface and shear stress continuity at the top surface.

Thus, the boundary conditions are:

$$\frac{\partial v(r)}{\partial z}=0 \text{ at } z=h(r) \tag{3.5}$$

$$v(r)=0 \text{ at } z=0 \tag{3.6}$$

Upon integrating Equation 3.4 we obtain:

$$v(r)=\frac{\rho\omega^2}{\mu}(-\frac{1}{2}rz^2+rhz) \tag{3.7}$$

By mass conservation of the entire fluid volume:

$$r\frac{\partial h}{\partial t}=-\frac{\partial(rQ_r)}{\partial r} \tag{3.8}$$

where:

$$Q_r = \int_0^{h(r)} v(r)\mathrm{dz} \tag{3.9}$$

is the flow per unit length of circumference at a radius r.

Expanding Equation 3.8:

$$\frac{\partial h}{\partial t} = -\frac{\rho\omega^2}{3\mu}\frac{1}{r}\frac{\partial}{\partial r}(r^2h^3) \tag{3.10}$$

$$\frac{\partial h}{\partial t} = \frac{\rho\omega^2}{3\mu}(\frac{2rh^3}{r}) \tag{3.11}$$

$$-\frac{\mathrm{dh}}{\mathrm{dt}} = \frac{2\rho\omega^2h^3t}{3\mu} \tag{3.12}$$

This final equation can be integrated to obtain the height variation as a function of time and the result is valid everywhere except close to the outer boundary of the spin-coating liquid volume where a capillary ridge is present.

$$\frac{1}{h_t^2} - \frac{1}{h_0^2} = \frac{4\rho\omega^2t}{3\mu} \tag{3.13}$$

The above equation is commonly written as:

$$h_t = \frac{h_0}{\sqrt{1+\frac{4\rho\omega^2th_0^2}{3\mu}}} \tag{3.14}$$

The height variation equation (Equation 3.14) indicates that the height of the film does not depend on the radial coordinate. This implies that the film is nearly uniform during the process of spin-coating. The no-slip boundary condition (Equation 3.5) might imply that the contact angle and the contact line location do not change during the entire spin-coating process. Despite this anomaly, the approximation of zero surface tension in this model gives a closed-form solution (Equations 3.13 and 3.14) which matches experimental trends such as those shown in Figure 3-2. A physically correct simulation will include additional constitutive laws relating the velocity of the contact line and the contact angle.

3.3.3 Numerical Simulations of Spin-coating

The numerical procedure for solving the spin-coating problem under axisymmetric conditions was first proposed by Melo *et al* [MJF89]. More recent work has focused on using boundary layer theory to solve the system in surface tension free and surface tension dominated regimes, on modeling surface tension force singularity, the no-slip boundary condition and constitutive laws relating contact angle variation and contact line velocity [SR04], [WHD00]. These simulations are helpful in developing a size estimate of the region where surface tension forces are dominant.

3.4 Deviation from Height Variation Model

We have conducted spin-coating experiments with real-time monitoring of thickness using LCI and observed the lack of repeatability in spin-coating PDMS. In Figure 3-2, we see that the spin-coating thickness for the same spin speed is not repeatable. For example, after spin-coating for 60 seconds, the thickness values were $\sim 80\mu m$ with $\sim 7\%$ variation. In Figure 3-4, we validate our robust spin-coating model by plotting $\frac{1}{h_t^2}$ versus $\omega^2 t$, which from Equation 3.15 should yield a line with slope equal to $4/3\nu$. Variations in the slope indicate a different kinematic viscosity was obtained for the PDMS samples for the trials at 600 rpm compared to the PDMS for the trials at 500 rpm and 750 rpm (15% difference). These trials were conducted on different days from two separately prepared batches, and are an example of the variability that can lead to look-up table errors.

3.4.1 Effect of Initial Slug

By solving the Navier-Stokes equation with quasi-static assumptions in the viscous dominated regime (Section 3.3.2), we obtain the following relation for variation of

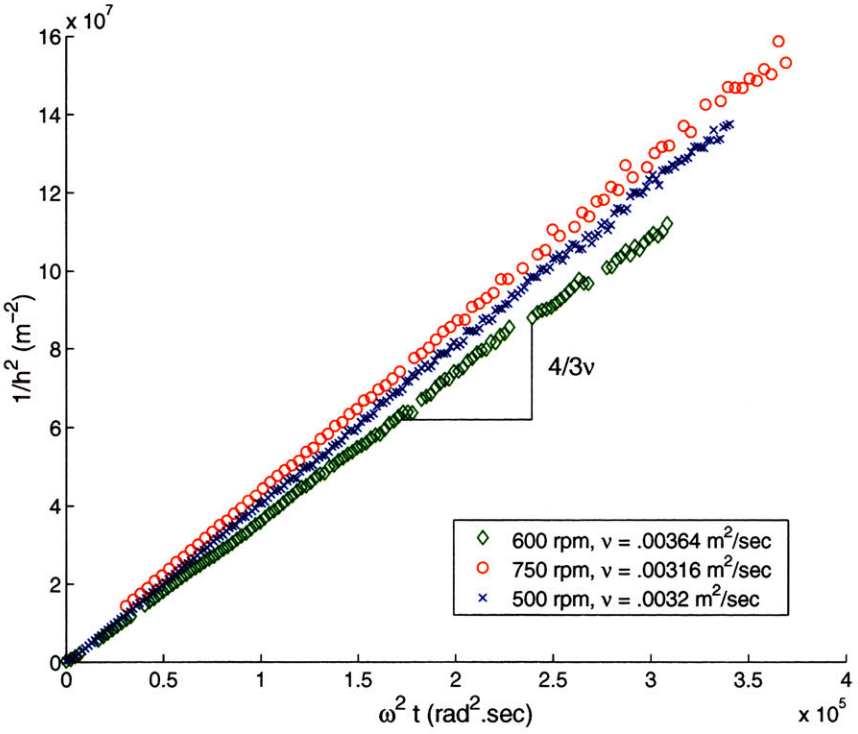

Figure 3-4: Inverse squared thickness varies linearly with $\omega^2 t$. This graph shows the effect of large initial pour – the offset due to initial thickness is negligible. The difference in slopes is caused due to viscosity variations during PDMS preparation.

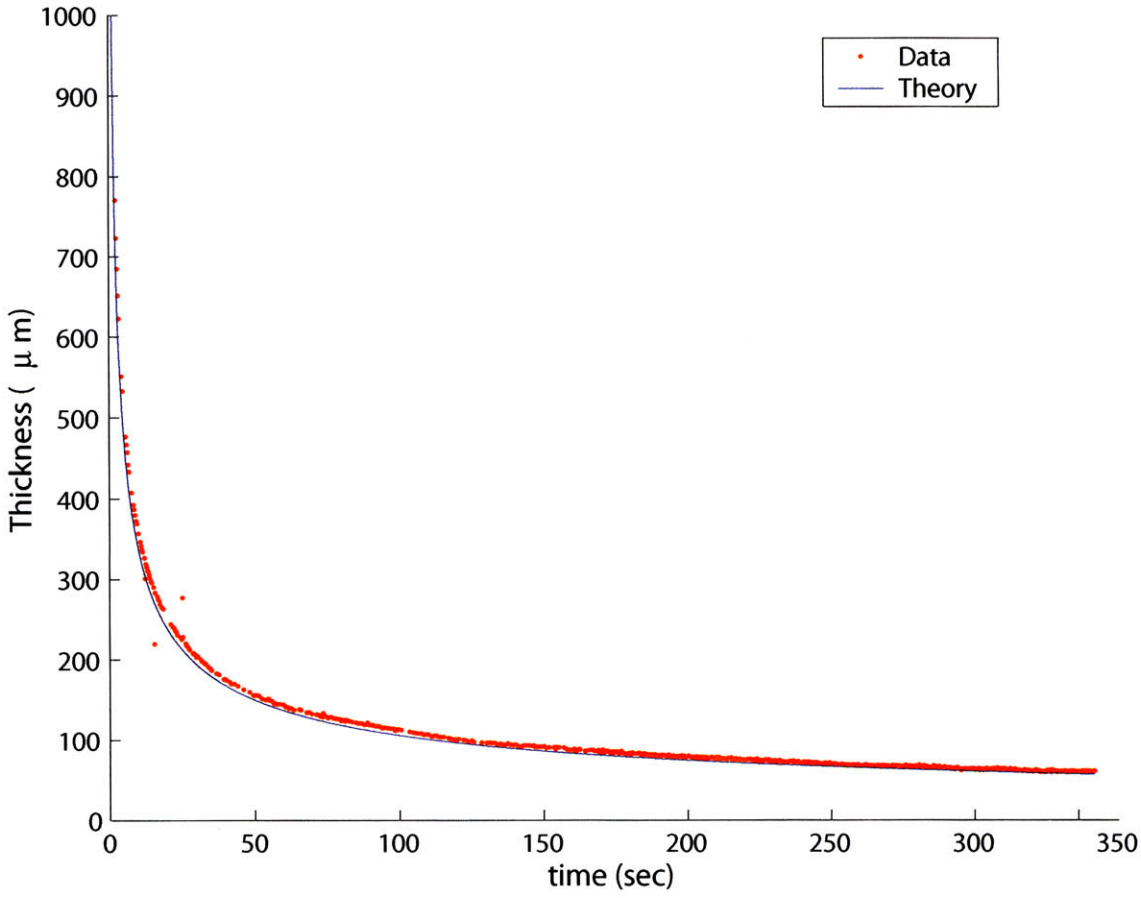

Figure 3-5: Thickness variation with time and comparison with theory. When the initial pour volume is large, the spin-coating model can predict the film thickness to within 5 % error.

height with time in the differential equation form:

$$-\frac{\mathrm{dh}}{\mathrm{dt}} = \frac{2\omega^2 h^3 t}{3\nu} \tag{3.15}$$

which upon integrating yields:

$$-\int_{h_0}^{h(t)} \frac{\mathrm{dh}}{h^3} = \int_0^t \frac{2\omega^2}{3\nu}\mathrm{dt} \tag{3.16}$$

$$\Rightarrow \frac{1}{h(t)^2} - \frac{1}{h_0^2} = \frac{4\omega^2 t}{3\nu} \tag{3.17}$$

From equation 3.15, we observe the following:

- the rate of thinning is proportional to the thickness cubed;
- the height evolution of the film is independent of the radial location or size of the film;
- the height evolution of the film is sensitive to the initial thickness.

As a result, local height variations get rapidly evened out and the spin-coating process produces films that are nearly even in thickness everywhere. In addition, we find that the height variation is sensitive to the initial height h_0. If we make the initial thickness very high, that is, if $h_0 \gg h_t$, we can see that:

$$h_t \approx \sqrt{\frac{3\nu}{4\omega^2 t}} \tag{3.18}$$

Thus, when we pour a large volume of PDMS on the substrate at the start of spin-coating, we could use equation 3.18 as a design guideline in the choice of rpm and time for our spin-coating. From our thickness measurements, we have found that this method provides an accuracy of$\sim$ 5% in film thickness. To further improve the accuracy, we can monitor thickness in real-time using low-coherence interferometry.

3.4.2 Effect of Eccentric Slug

One possible source of non-uniformity in spin-coating is the eccentricity of the center of mass of the initial sample volume to the spinning axis. The analysis outlined in Section 3.3 depends critically on axisymmetry of the problem. When there is an eccentric blob on the substrate, different parts of the blob are subject to a different centrifugal acceleration, $\omega^2 r$ and the shape of the blob is progressively skewed. If the substrate size is such that the blob covers the entire surface, then the spin-coating scenario is axisymmetric again. Such a scenario is made possible by large pour volumes. If there is a very small pour volume that is eccentric, fingering instability occurs and the PDMS may not even coat the substrate completely [MJF89].

3.4.3 Effect of Motor Dynamics

In Section 3.4.1, I have shown how the large pour volume enables the design of the final film thickness based only on material properties and the spin-coating conditions as a single parameter: $\omega^2 t$. In a conceptual model, it is easy to expect the motor to start spinning at the desired spin speed ω beginning at t=0. However, in reality, the motor inertia, friction and power input cause the motor to accelerate initially and reach the desired spin speed after a finite amount of time. For the case of the motor used in our spin-coating setup, the ramp-up time was nearly 5 seconds (an average acceleration of nearly 100 rpm/sec). In a very simple model, we can capture the speed variation of the motor as shown in Figure 3-6. The desired $\omega^2 t$ and the actual value are different because of the initial acceleration of the motor.

$$(\omega^2 t)_{actual} = \int_0^{t_0} \omega(t)^2 \mathrm{d}t + \omega^2 \int_{t_0}^{t_{final}} \mathrm{d}t \tag{3.19}$$

$$< \omega^2 t_{final} \tag{3.20}$$

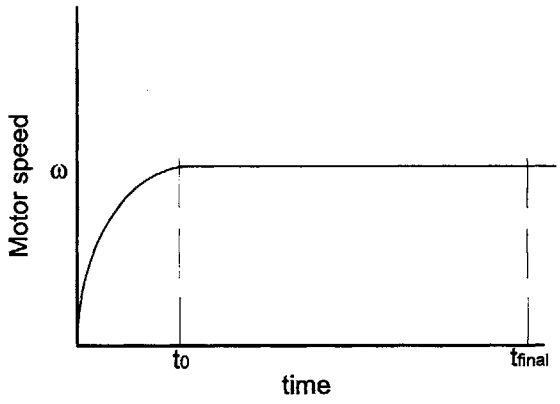

Figure 3-6: When a motor used for spin-coating is set to the desired rpm in open loop, it shows an initial acceleration phase and then reaches a steady speed.

In order to account for the difference in our thickness estimate, we could either calibrate the spin-coater to identify a correction factor (as shown in Equation 3.19) or measure $\int \omega^2 dt$ in real-time for greater precision.

3.4.4 Spreading of PDMS Under Gravity

At the beginning of spin-coating and right at the end of spin-coating, there is a blob of PDMS on the substrate. Left to itself, the blob will tend to spread under the influence of gravity and is opposed by viscous forces and surface tension forces. In this section, we discuss the spreading of a blob of viscous fluid on a surface under the influence of gravity. Based on the interferometric measurements at the start of spin-coating, we observe a thickness decrease of about $4\mu m/sec$ for a blob of thickness $\sim 2000\mu m$ (Figure 3-7). At the end of spin-coating, the height variation was at most $1 \sim 2\mu m$ over several minutes (Figure 3-8).

The theoretical analysis of spreading of a viscous fluid on a surface is complicated by the competing influence of gravity, surface tension and viscosity. Further the sin-

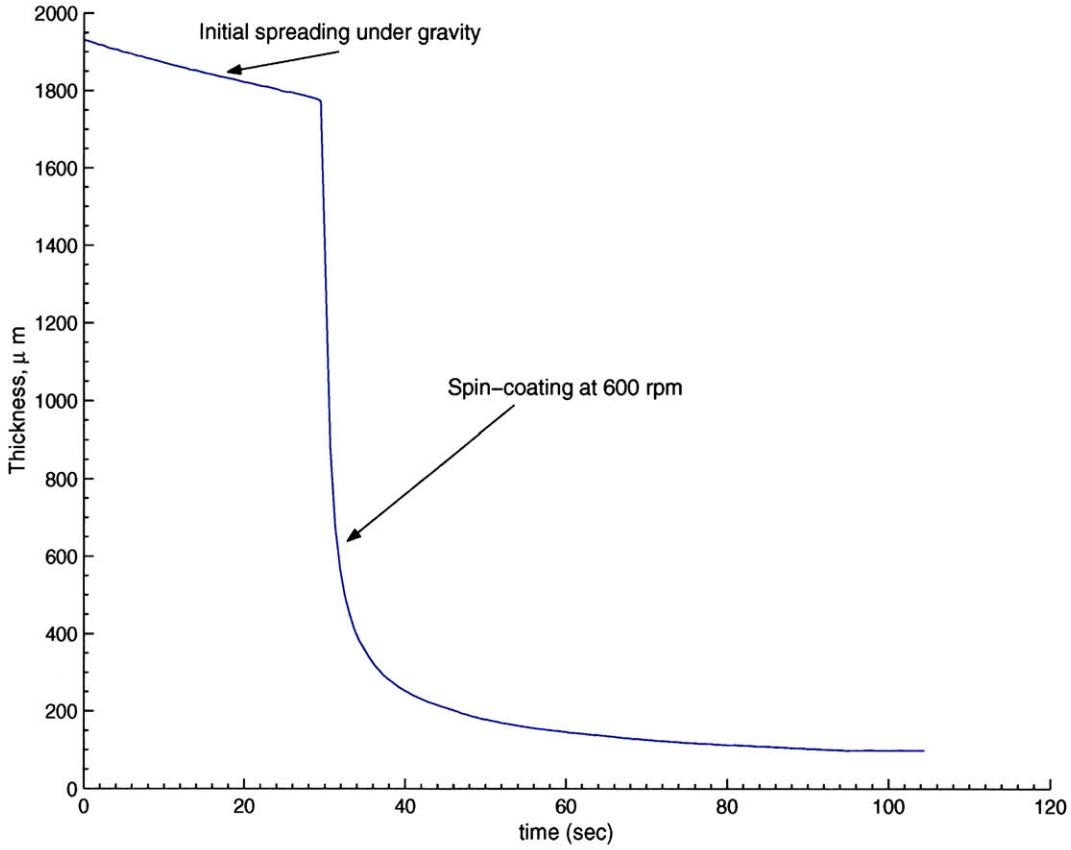

Figure 3-7: Experimental data of the spreading of the spin-coated PDMS film at the start of spin-coating. The PDMS blob thins under gravity at the rate of nearly 4 $\mu m/sec$. However, this spreading does not affect the final spin-coating thickness as the initial volume is very large

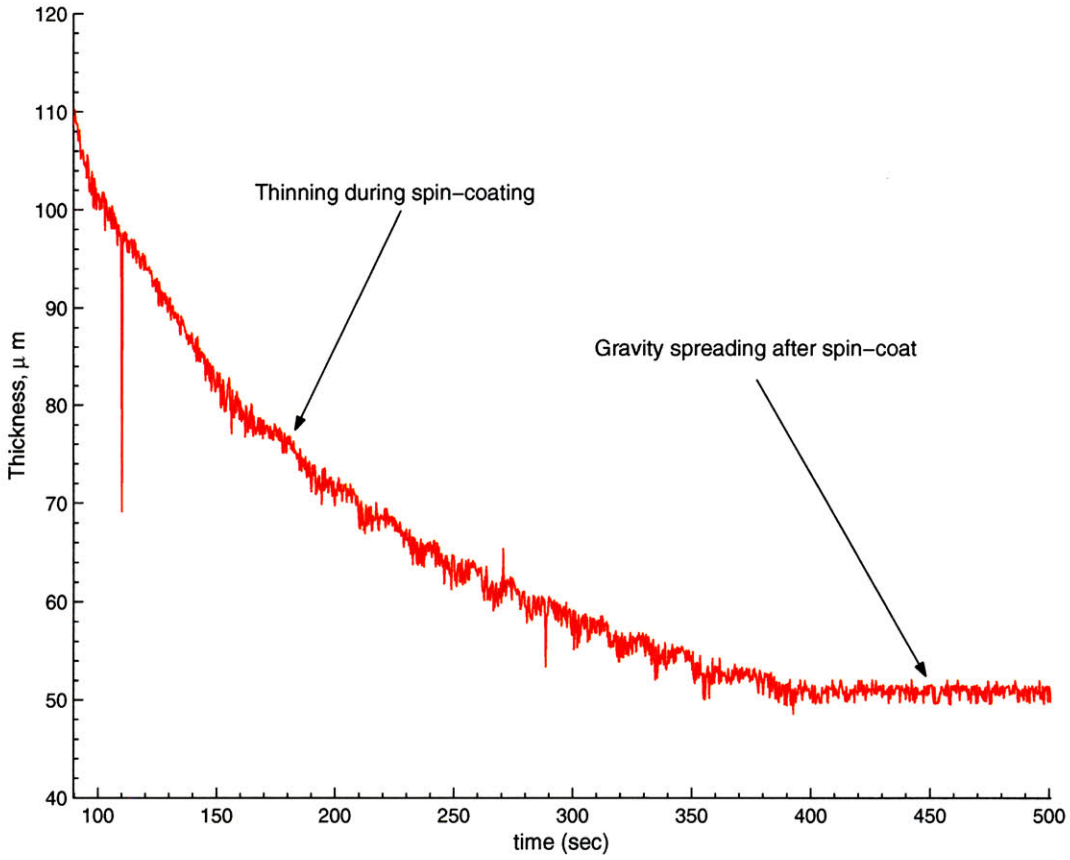

Figure 3-8: Experimental data of the spreading of the spin-coated PDMS film of $50\mu m$ thickness shows negligible spreading under gravity after the spinning.

gularity at the edge (due to the surface tension force acting along a line) can not be captured in analytical solutions. The surface tension boundary condition fixes the contact angle at the ends of the blob. As the blob spreads under the influence of gravity, an infinitely large force will be required to extend the ends while continuously satisfying the contact angle boundary condition. The constitutive relationship describing the variation of contact angle with the velocity at the contact line is still an open problem. Various empirical laws have been proposed including the Voinov-Tanner equation [Voi99].

The known theoretical evolution equation of the radius of a 'pancake' composed

of a viscous liquid spreading on a horizontal surface under gravity is:

$$R(t) \approx 1.09 \left(\frac{\sigma \Omega^3}{\mu l_{cap}^3} \right)^{\frac{1}{7}} t^{\frac{1}{7}} \tag{3.21}$$

where R(t) is the radius of the pancake, Ω is the total volume of sample spreading under gravity, σ is the surface tension, μ the dynamic viscosity of the sample and $l_{cap} = \sqrt{\sigma/\rho g}$ is the capillary length [Kav05]. Based on this equation,

$$h(t) \sim \frac{\Omega}{R^2(t)} \sim t^{-\frac{2}{7}} \tag{3.22}$$

Thus, the spreading of a pancake of viscous liquid on a surface under the effect of gravity is a slow varying function of time. This observation is also further validated by our experimental measurement of height variation.

3.5 Real-Time Metrology for PDMS Spin-coating

3.5.1 Low-Coherence Interferometry (LCI)

In this section, we describe the use of (LCI) for measuring the thickness of the spin-coated PDMS film in real-time. LCI allows for simultaneous measurement of thickness and refractive index of a film. Using LCI, point measurements of thickness are taken to estimate the spin-coating film thickness. Based on Equation 3.15, point measurements of thickness are sufficient for PDMS spin-coating as the height does not vary with the radial location (except near the capillary edge bead).

LCI is well suited for monitoring PDMS film thickness during spin coating because it is a non-contact, high speed (40-100Hz), precise and low-cost method [SG92]. LCI is based on the principle that broadband, or low coherence, light from two arms of an interferometer will only interfere if the difference in optical path length in the two arms is less than the coherence length $l_c = \frac{2ln2\lambda^2}{\pi \Delta \lambda_{FWHM}}$ where λ is the center wavelength

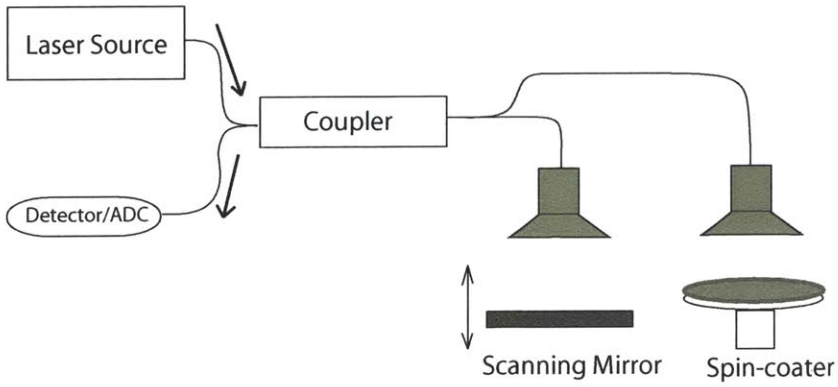

Figure 3-9: Setup of spin-coating with Low-Coherence Interferometry as metrology

and $\Delta\lambda_{FWHM}$ is the spectral bandwidth [FDHL03]. By scanning the path length in one arm of the interferometer(Figure 3-9), reflections from dielectric interfaces can be located as peaks in the interference signal as shown in Figure 3-10. For commonly available light sources, $l_c = 6 \sim 20\mu m$, is easily obtainable, and determines the minimum resolvable film thickness.

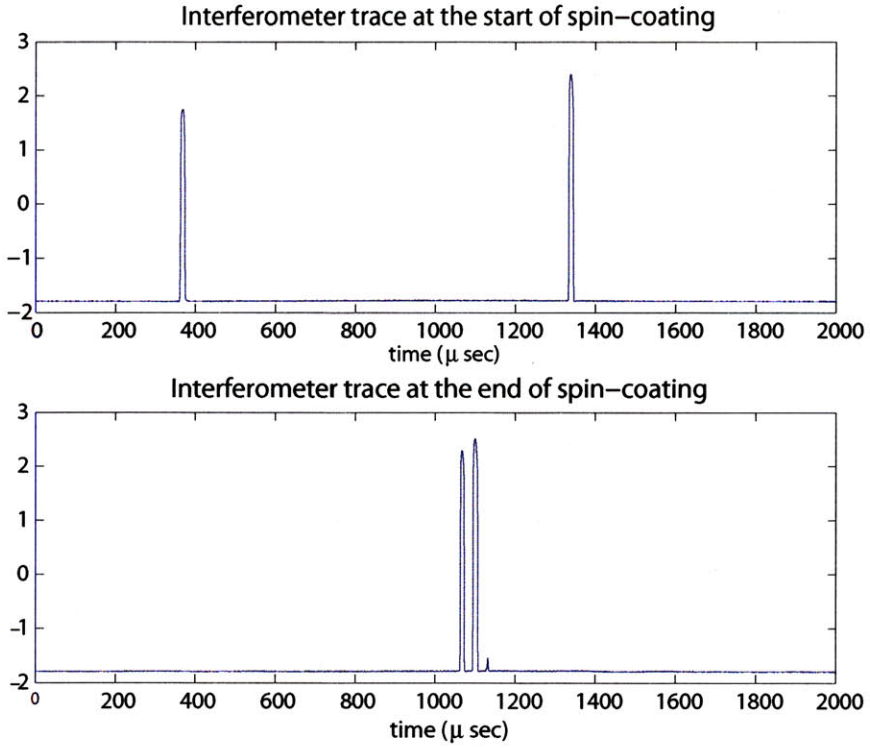

Figure 3-10: Trace from the Low-Coherence Interferometry (LCI) setup

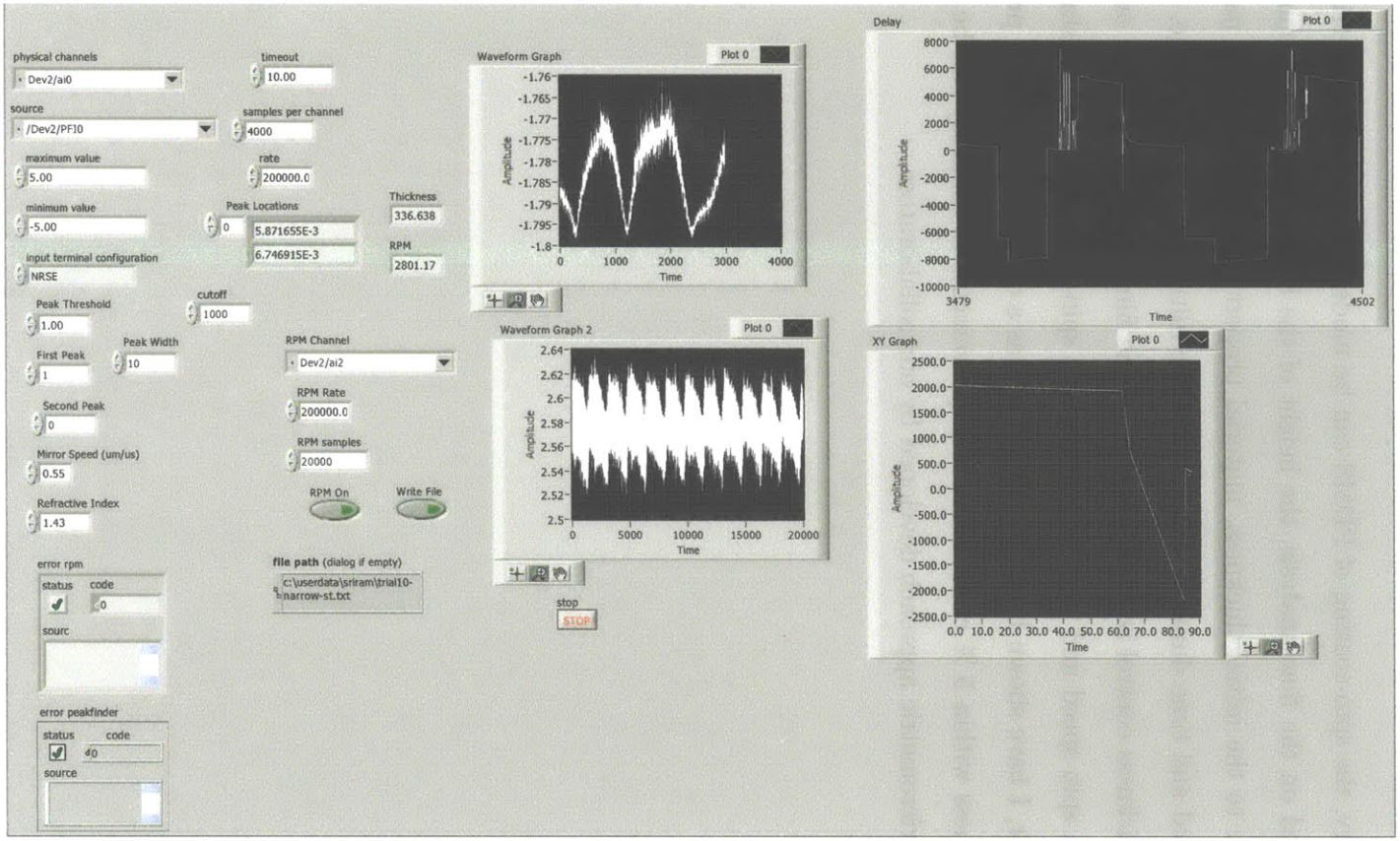

Figure 3-11: Screen capture from the Labview program that interfaces with the LCI setup, the tachometer to the spin-coater. Labview program created by Kevin Lee, Physical Optics and Electronics Group, MIT Research Lab for Electronics, MIT.

3.6 Chapter Conclusions

In summary, the spin-coating of PDMS can be modeled as an axisymmetric viscous flow. Based on the flow analysis, the height of the PDMS film during spin-coating is sensitive to the initial thickness, material properties and the process parameters – spin speed and time duration. By making the initial pour volume large, the spin-coating thickness control is made robust and the film thickness depends only on its properties, spin speed and time. With a robust spin-coating approach using a large initial pour, I have shown how $\omega^2 t$ can be used as a design parameter to predict the film thickness within 5 % error. Further improvements in accuracy can be obtained by an interferometric approach developed by our collaborators.

Chapter 4

The Peel Initiation Process

We have seen in Chapter 2 that many of the challenges inherent in current approaches for thin PDMS film manufacture pertain to the peeling of the film from the substrate. Based on the discussion in Chapter 3, by controlling $\omega^2 t$ and by using a robust spin-coating approach, one can obtain film thickness values within 5% of the design value. Upon spin-coating, the substrate along with the thin PDMS liquid layer is then cured in an oven to convert the PDMS liquid layer into a solid elastomer film (refer Appendix A for manufacturer prescribed curing conditions).

Now, I discuss the peeling of the cured, thin, solid PDMS film from the substrate without damage. I then identify design insights based on the physics and develop some concepts for peeling. Based on peeling experiments with these concepts, I present further guidelines for the design and prototype of a peeling machine. While peeling PDMS films, during each of the stages of initiation, continuous mode peeling and of film handling, there are different process requirements based on the physics and thus it is necessary to design specific components for each stage. For initiation, I introduce the use of a thin, annular scaffold incorporated *in situ* between the PDMS film and the substrate. Based on the physics and bench-top experiments, I discuss the design of such an in-situ scaffold and describe the methods for its manufacture and subsequent integration within an automated peeling process for PDMS films.

For continuous mode peeling, I propose the use of an adhesive roller actuator with compressive preload. An adhesive roller reduces stress concentration and micro-slip in the PDMS film, and avoids potential damage to the film by tearing. The compressive preload provides for a controlled advance of the peel-front, and avoids dynamic effects in peeling such as instability or whiplash. Upon peeling, I show how the *in-situ* scaffold could be used for handling the PDMS film and aligning it for subsequent processing and storage.

4.1 Concepts Motivated by Initiation Physics

Previously (see Section 2.4.4.2), I have shown how the application of a tensile load for peel initiation is most effective when located vertically over the peel-front. For practical reasons, it is not possible for an actuator to attach directly to a thin film on a substrate, let alone over its its boundary or an edge. Together, these factors favor the use of a starting notch for a more deterministic approach to peel initiation. In this section, I present some concepts of a starting notch and then introduce the use of a thin scaffold incorporated between the film and the substrate for peel initiation .

The scaffold enables the separation of the film from the substrate and provides an easy way for gripping the film during and after peeling. Next, I present some scaffold concepts involving different geometries and materials and discuss the observations from peeling tests based on these concepts. I propose the design rules for a scaffold and manufacturing techniques for such scaffolds. Finally, I discuss the viability of manufacturing techniques for both low-volume prototyping and large-volume production, the alignment and attachment of the scaffold to the substrate before spin-coating and after successful peeling from the substrate.

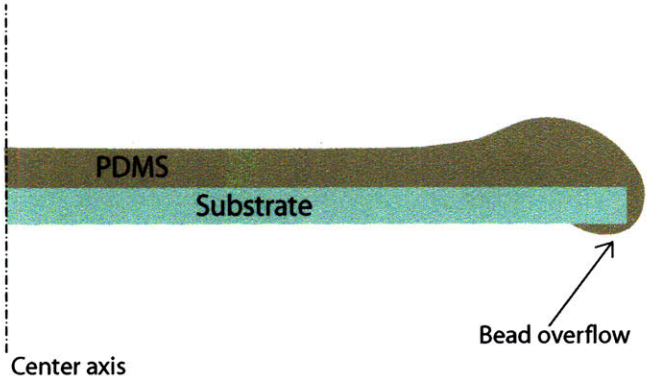

Figure 4-1: At the edge of the wafer, the PDMS film could overflow and spread over both the rim and the underside

4.1.1 Razor Edge for Peel Initiation

When a PDMS film is spin-coated on a substrate, there is a capillary ridge formed at the periphery. The ridge is formed due to the competition between surface tension forces and the centrifugal forces. In Section 2.4.1, I discussed the fluid mechanics of the capillary bead formation. The capillary ridge ('bead') could be several times thicker than the rest of the PDMS film and can extend radially over a distance several times the thickness of the film. In addition, the liquid in the capillary bead may flow around the edge of the wafer substrate and coat on its underside. Such overflow and coating on the rim and underside of the substrate could cause the film to lock over the substrate (Figure 4-1).

During manual peeling, the strain energy for peeling is transmitted entirely through the thin PDMS film. The thin PDMS film may not be able to provide the energy required to peel the bead portion (which is locally several times stiffer than the rest of the thin film). The user may attempt to increase the tension in the film for the sake of peeling a portion of the capillary bead and thus might aggravate the risk of

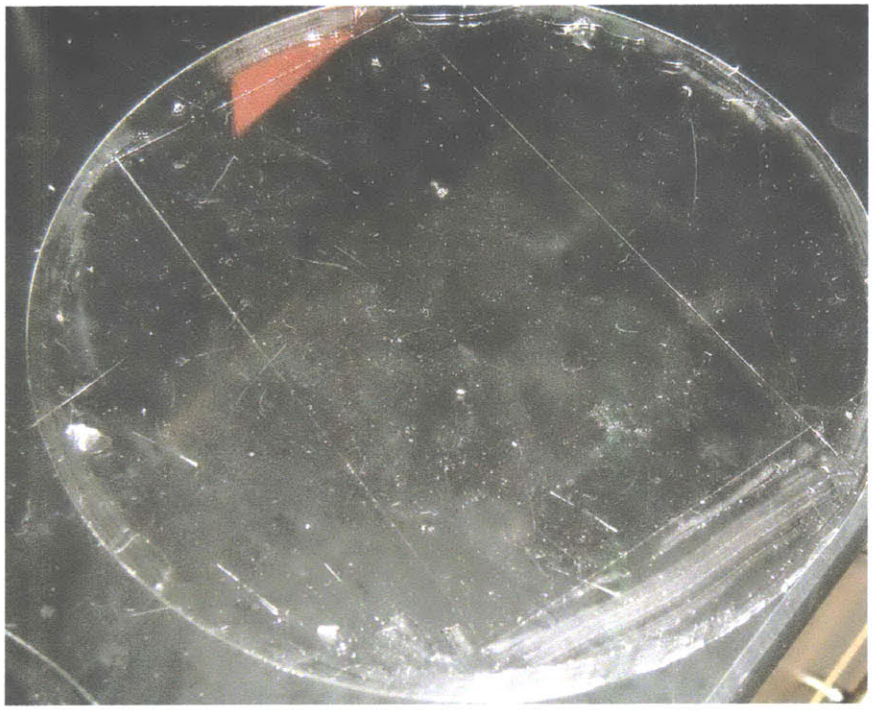

Figure 4-2: When the user uses a razor to release a small portion of the film from the substrate, there is a risk of scraping and tearing the film. Sample provided by Salil Desai, BioMEMS group, MIT Research Lab for Electronics.

tearing. As an alternative, some users use the razor edge to first scrape the edge of substrate to remove the capillary bead and any overflow. They then insert the razor edge under the film to create a small 'lip' for holding the film (Figure 2-7). Figure 4-2 shows an example of a 6" pyrex wafer with a $100\mu m$ PDMS film, where the scraping of the bead can be seen as well as portions of the film that have been scored with a razor edge. When inserting a razor under the PDMS film, unless extraordinary care is taken by the operator, the razor edge could very likely tear the PDMS film and tearing is common.

4.1.2 Need For a Starting 'Notch' for Peel Initiation

A naive approach to peel the film from the substrate would be to 'pull upwards' on it. In other words, we can apply a tensile force on the upper surface of the film and hope to induce peel initiation. We simulate the effect of an applied tensile load on the surface and find that the load is most effective only when it is in the same plane as the peel-front. If the load is away from the peel-front, then its net effect drops inversely with distance. At the same time, the presence of a notch or a pre-crack at the peel-front makes the peel initiation process easier .

4.1.3 An All-Around Scaffold for Starting a Peel

I tested the use of a starting notch for peeling, by including a rectangular piece of material (fiber, paper) under the PDMS film during spin-coating. The PDMS film was nearly $300\mu m$ thick, the fiber was $100\mu m$ thick (.004") and the paper material was $75\mu m$ thick (.003"). Since we grip the PDMS film using the starting notch and since they stay with the PDMS film, we find that they are also useful as scaffolds. When we gripped the PDMS film through these rectangular scaffolds, we were able to initiate peeling, and soon found that the PDMS film tore beginning at the corners. Figure 4-3 shows the rectangular notch incorporated between the PDMS film and the substrate, and Figure 4-4 shows the portions of the film remaining on the substrate after the film tore at the corners of the scaffolds. This test showed that the presence of re-entrant corners on the peel initiator will cause tearing. The only way to incorporate a peel initiator without re-entrant corners would be to have the initiator cover the entire periphery and furthermore, that its inner periphery be convex in shape.

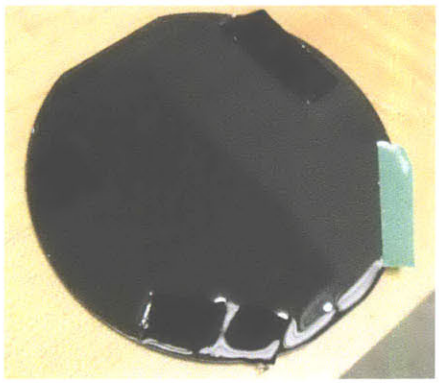

Figure 4-3: When we use a rectangular piece of paper and fiber as initiators, we can induce peeling. However, the corners of the rectangle act as points of damage initiation

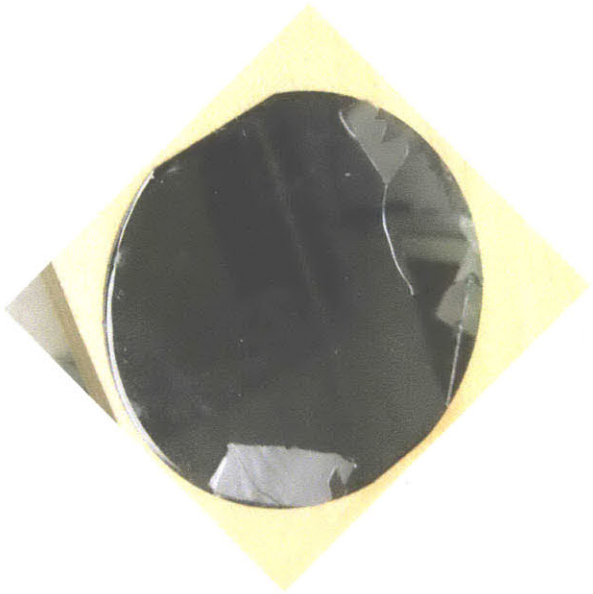

Figure 4-4: Damaged film following the use of a rectangular piece of scaffold

4.1.4 Stiffness and Thickness of Scaffold

In order to avoid rectangular corners, I tested the use of a circular annulus that covered the entire wafer periphery. The sample materials I tried included waxpaper, vinyl, copper foil, polyester film and metal shims made of brass and stainless steel. I spin-coated a nearly $300\mu m$thick PDMS film on substrates with starting notches made of these materials. The $300\mu m$ thick PDMS film was obtained by spin-coating at 300 rpm for 60 seconds.

The key observations from these tests are:

- The polyester scaffold wrinkled easily when attached to the substrate. Like the PDMS film, it was flimsy and difficult to handle. The wrinkles on the inner periphery of the scaffold caused tearing of the PDMS film during peeling.

- The copper scaffold was very malleable and creased when attached to the substrate. When peeling with the copper film, the thin copper film did not bend easily. Instead, at the boundary with the PDMS film, the copper film had a tendency to plastically deform and tore away from the film.

- With a vinyl scaffold, I had limited success while peeling PDMS films. The PDMS film did not cure over the vinyl film, and the scaffold tore from the PDMS film as a result.

- Brass and stainless steel shims were effective as scaffolds and helped peel the PDMS film successfully. The burrs formed during their manufacture often caused tearing between the PDMS film and the scaffold at the inner periphery.

Based on these observations, I identified the following guidelines for the design of a successful scaffold:

- The scaffold material must be stiff so that it does not wrinkle. The scaffold

should not wrinkle when attached to the wafer substrate as the wrinkles could act as defect sites.

- If the scaffold is very stiff, it may behave similarly to a razor and tear the PDMS film.
- The scaffold should bend easily without plastic deformation. Creasing of the scaffold could cause tearing.

4.1.5 Edge Quality of Scaffold

The presence of re-entrant corners, creases, burrs and sharp wrinkles in the scaffolds caused tearing at the inner periphery. These surface features act as damage causing sites during peeling. Thus, during the design of such scaffolds, the convex edge on the inner periphery must be smooth and free of sharp features. When peeling the PDMS film through the scaffold by hand, the operator applies a moment on the scaffold. The moment is transmitted through the scaffold and results in tension and shear forces at the inner periphery. Sharp corner singularities in the inner perimeter could serve as regions for stress concentration and become likely candidates for tearing the film.

4.2 *in-situ* Scaffold-based Peel Initiation

In the previous section, I presented some design insights based on my tests to show the use of very thin scaffold for peel initiation and thin PDMS film handling. To summarize the results, I will first highlight the advantages of using a scaffold for PDMS peeling and handling. Next, I discuss how such thin scaffolds could be designed and manufactured. Newer challenges arise from the use of scaffolds for peeling, mainly for process integration, compatibility and possible risks for film damage. Finally, I present some process windows for scaffold based peeling .

After spin-coating PDMS on the wafer substrate holding a scaffold, the substrate is

left in the oven to bake. The scaffold material and the adhesive used to attach it to the substrate must both withstand the curing temperature range without deterioration in properties or dimensions. Care must be taken to avoid complete contact between the bottom of the substrate with the petridish due to the risk of stiction and the subsequent inability to remove the wafer.

After baking, the overhang of the peel-initiator around the wafer allows for easy initiation of the peeling. The stiffness of the scaffold plays an important role in providing a better purchase on the thin film.

4.2.1 Advantages of Using a Scaffold in Peeling

The use of a scaffold for peeling thin PDMS films offers the following process level advantages:

1. The scaffold acts as a starting notch to initiate peeling deterministically.
2. The scaffold removes the capillary bead away from the starting location for peeling and avoids the risk of tearing by preventing the film locking over the substrate edge.
3. The scaffold allows the gripping of the PDMS film.
4. The scaffold serves as a scaffold for holding the film without wrinkling or self-adhesion.
5. The scaffold provides means for handling the PDMS film without contamination risk.
6. The scaffold accommodates fiducials and features for alignment and kinematic coupling.
7. The scaffold allows different methods for handling PDMS films – positive, magnetic and vacuum attachment.

4.2.2 Design of a Scaffold for Peeling

In this section, I summarize the observations I made during testing different scaffold materials and geometry.

4.2.2.1 Design of Shape and Thickness

From geometry and kinematics-based arguments, the scaffold must:

1. avoid singularities and re-entrant corners at the inner perimeter;

   A convex shape without sharp corners is a good candidate. The inner diameter of the scaffold must be smaller than the diameter of the silicon wafer or glass disk. The outer diameter of the scaffold should be larger than the diameter of the silicon wafer or glass disk.

2. allow for peeling from many directions;

3. have a much smaller thickness than the PDMS film so that the PDMS liquid can cover the scaffold well during coating;

   If the scaffold is too thick[1], only a very thin layer of PDMS film will be deposited and the scaffold may not attach properly at its inner periphery with the rest of the PDMS film.

4. have good edge quality on the inner periphery.

   The outer periphery of the scaffold does not affect the peeling process and thus there are no specific requirements for its geometry. The inner perimeter, which forms a boundary between the scaffold and the thin film, is the most vulnerable location for tearing. A smooth edge on the thin scaffold and prevention of local thinning of the PDMS film will mitigate some tearing risks.

[1]The effect of scaffold thickness relative to the film thickness will be discussed later in this chapter

4.2.2.2 Material Selection

The scaffold is a thin annulus which is attached around the periphery of the substrate. Thin annulus-shaped films have low bending and torsional stiffness and are thus flimsy to handle, prone to wrinkling and crumpling. A possible approach to holding their shape is to apply a low biaxial tension pre-load on scaffold materials of sufficient stiffness to retain their shape.

The material of the scaffold must not degrade or undergo significant deformations. During the baking step (at about 80° C), paper, metal and certain classes of polymer films are good candidates for good performance at elevated temperatures. From a manufacturing point of view, the scaffold material must machine easily and cost-effectively.

4.2.2.3 Manufacturing Approach

For fabrication of the thin annulus scaffold, we investigate the following manufacturing processes:

- scribing,
- shearing (cutting) with scissors,
- stamping,
- wire EDM with sandwich materials for support,
- waterjet machining with sandwich materials for support, and
- chemical etching.

4.2.2.4 Alignment and Attachment

After a scaffold is manufactured, it must be aligned on the wafer substrate and attached. For the sake of alignment and attachment, the scaffold must:

1. apply easily on the perimeter of the substrate,
2. be aligned concentric to the circular edge of the wafer substrate,
3. avoid wrinkling in the radial and tangential directions when attached on the substrate,
4. stay on the wafer without gaps (especially on the inner perimeter), during spin-coating of PDMS,
5. separate from the wafer easily after baking, and
6. must not react adversely with the substrate and the PDMS film material.

For aligning the scaffolds in the shape of a circular annulus, we can use reference outlines if the scaffold material is transparent, *e.g.*, polyester film. For metal scaffolds, we can make fiducials and rectangular pockets for kinematic alignment using cylindrical pins against the wafer edge.

When the thin annular scaffold is fixed to the substrate, it could wrinkle due to trapped air pockets or due to the scaffold softening and expanding under heat. Wrinkling at the inner perimeter could cause the PDMS to seep under the scaffold during spin-coating and potentially tear the film during peeling. A 'smoothing action' on the scaffold could help make sure there is continual and unbroken contact at the inner perimeter.

The choice of adhesive for the scaffold has further trade-offs. We want the adhesive to keep the scaffold in place on the substrate during spin-coating. However, during peeling, we want the adhesive to have very low tack (adhesive strength) so that it comes off the substrate easily. The adhesive should not degrade during the film curing and further, should not outgas or react with the PDMS film. Furthermore, the adhesive should not react with the silicon or glass substrates.

Some approaches for affixing the scaffold on the substrate are:

- surface tension forces due to a thin wetting liquid film,

- adhesive contact, and
- magnetic pre-load using a ferromagnetic scaffold material and magnets located beneath the wafer.

4.2.3 Scaffold Prototyping

From a design viewpoint, the critical parameters that affect overall peeling success are edge quality, relative thickness of the scaffold and material stiffness. Given the very small thickness of the scaffold and its shape as an annulus, these parameters depend critically on the manufacturing approach .

For my experiments, I prepared scaffold samples in the shape of a circular annulus. The concept of having a thin circular annulus situated over the periphery of a circular substrate seems intuitive. However, when we attempt to manufacture such scaffolds of thickness much less than $100\mu m$ each, several practical issues arise. First, the feasibility of conventional manufacturing process for such thin materials is not guaranteed. Second, fixturing the raw material is a challenge and we need to avoid unnecessary deformation in the scaffold during fabrication.

4.2.3.1 Comparison of Scaffold Manufacturing Approaches

I tested the following prototyping approaches for scaffolds made of materials such as metal, vinyl, paper and polyester (PET). For each of these approaches, I list here my key observations regarding feasibility, process success and overall cost.

1. Shearing with scissors or hard blades

   Shearing a thin metal sheet using a pair of scissors resulted in very sharp features as the scissors could not follow the circular path. I used a knife-edge based vector outline plotter (Roland CAMM-1 CAD plotter) for tracing the geometric outline on the scaffold material. The scaffold material was first adhered on a thicker backing material and then the knife-edge cut through the material. Finally, the

scaffold of the desired geometry was peeled off the backing and attached to the substrate. The knife-edge based plotter was useful in preparing scaffolds made out of paper and polyester film.

When cutting a thin metal shim (of brass or steel) using a hardened steel blade, the knife-edge plotter approach failed as the blade dulled easily and could not cut the metal. When the thin metal shim was scribed with the blade edge, stick-slip of the blade on the shim resulted in severe wrinkling of the scaffold.

2. Laser micromachining

   I found it very difficult to cut scaffolds out of thin metal shims using laser micromachining because of the reflection off the metal surface. For paper, polyester and vinyl materials, edge quality and geometry was affected by laser micromachining due to over-heating and/or melting. Furthermore, since laser micromachining is a serial process, and thus the time requirement was high.

3. Wire electrospark discharge machining (wire EDM)

   Using Wire EDM, I was able to trace the outline of the scaffold on metal shims sandwiched between two pieces of 1/16" Aluminum (Al 6061) sheet. The edge quality of the metal scaffold was very poor as the diameter of the wire and the thickness of the shim were comparable. The sparking between the wire and the shim led to random material removal from the metal, resulting in poor edge quality.

4. Stamping

   For stamping a circular annulus out of a metal shim, I first machined a matching set of punch and die for the circular cross section on the inside. The punch and die were not subject to surface hardening or any heat treatment, as this effort was for prototyping and the cost of manufacturing a high quality punch and die set was prohibitive. The shim was supported in a sandwich between two

sheets of 1/16" thermoplastic and stamped using the punch and die. After the second trial, the corners of the punch had rounded off and thus, the edge was both rounded and full of burrs. For my prototyping tests, I found stamping to not be a viable alternative due to the poor edge quality and the setup time in machining a punch and die set..

In the long run, sheet-metal stamping will offer the most cost-effective approach for manufacturing metal scaffolds.

5. Abrasive waterjet machining

   Abrasive waterjet machining offers potential for prototyping scaffolds by fixturing the thin scaffolds between two thin stiff 'sandwich plates' and then waterjet machining through the sandwich thickness. However waterjet machining produces burrs on the inner periphery whose size is sometimes comparable to the thickness of the shim. Figure 4-11 shows a typical edge profile for waterjet machining.

6. Chemical etching

   The chemical etching process involves preparing the outline of the scaffold in a hard photo-mask, attaching the mask on top of the scaffold raw material and then using a 'wet etch' recipe of strong acids to etch away the exposed regions. This leaves behind the scaffold of desired geometry. Chemical etching produces a highly even and uniform edge. There are no burrs since there is no mechanical material removal and variations in edge smoothness are only due to the undercut (of size 10% of the thickness of the shim). Figure 4-12 shows a typical edge profile for chemical etching.

In Figures 4-5 - 4-12, I show some sample results from testing various materials as scaffolds. Based on these tests, I chose chemical etching as the manufacturing approach for the scaffolds. The scaffolds were made out of $25\mu m$ thick shims of stainless steel and low-carbon steel. Vendor information is provided in Appendix B.

Figure 4-5: When I used a scaffold made of vinyl, I found that the vinyl material softens and wrinkles when PDMS was cured in the oven. Further, the vinyl material was not compatible with PDMS and delayed the curing of PDMS over the vinyl.

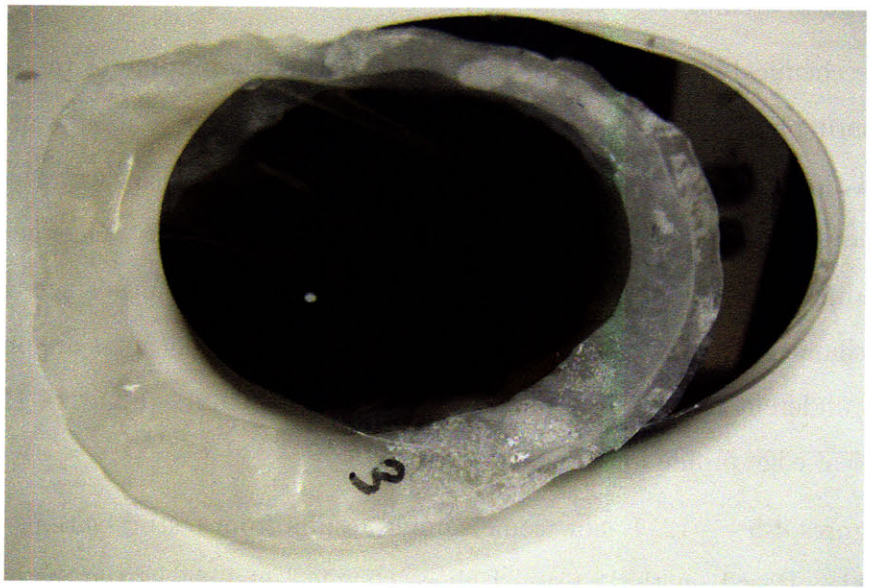

Figure 4-6: Paper scaffold was hard to manufacture and to attach to the substrate.

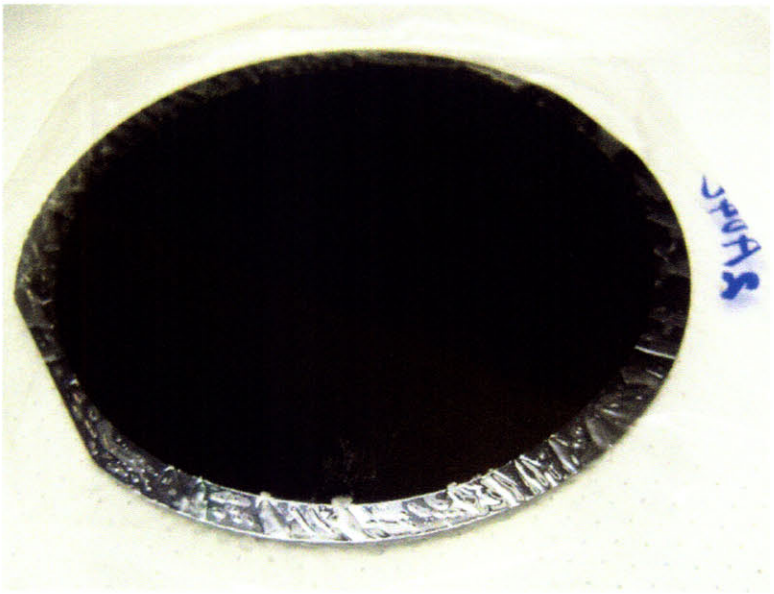

Figure 4-7: When I used a scaffold made of polypropylene, I found that the polypropylene wrinkled a lot when attached and softened under heat forming trapped air bubbles.

Figure 4-8: Polypropylene scaffold had many wrinkles and it allowed seepage of PDMS underneath. During peeling, the seepage caused tearing of the scaffold leaving the film on the substrate.

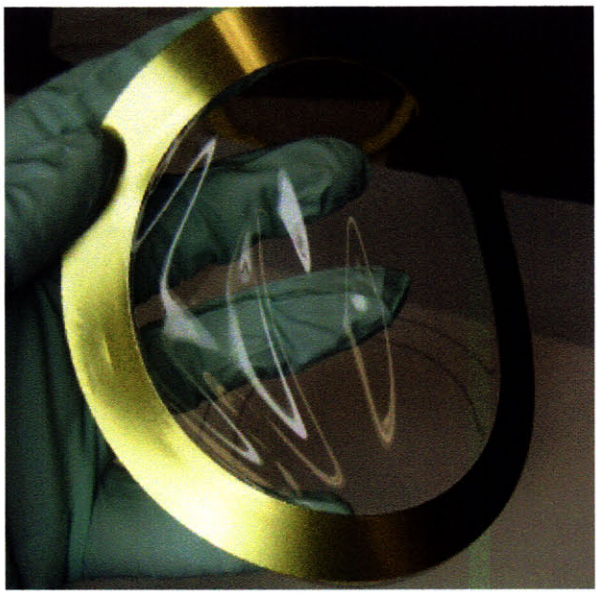

Figure 4-9: A brass scaffold has high stiffness and does not wrinkle much.

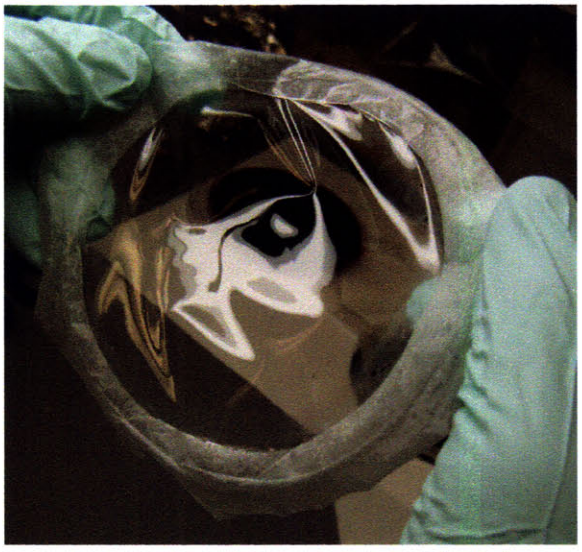

Figure 4-10: Waxpaper scaffold with a $100\mu m$ PDMS film showing the flimsiness of the wax scaffold material.

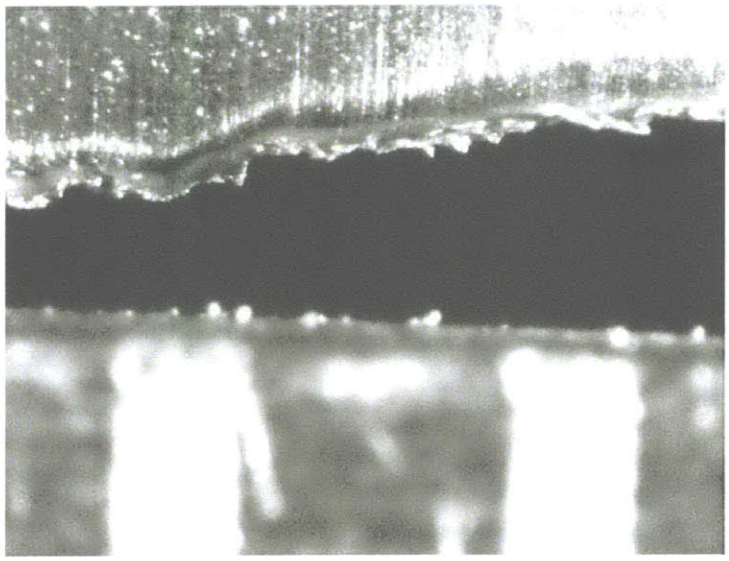

Figure 4-11: Waterjet machining of very thin metal shims requires the use of a sandwich material of high stiffness and low yield strength. The shadow on the edge indicates the size of the burrs which are comparable to the thickness of the shim. The vertical lines on the bottom are the incribed lines on a ruler 1mm apart.

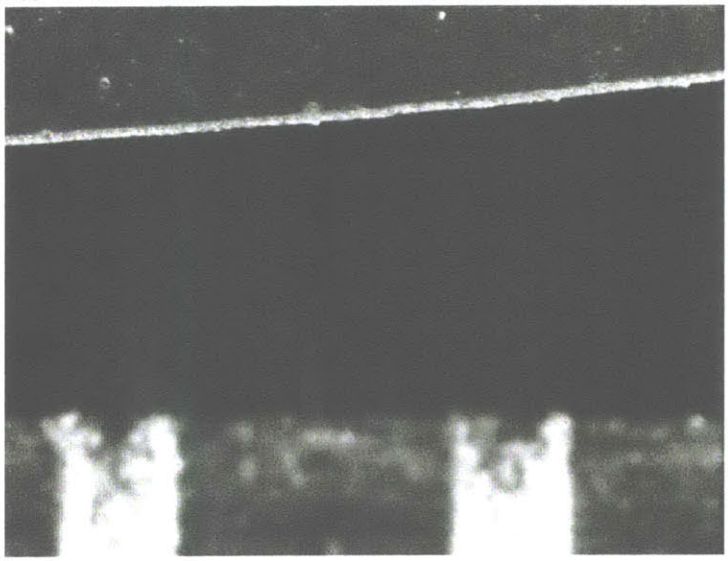

Figure 4-12: Chemical etching causes burr size equal to that of the undercut, which is about 10% of the thickness of the shim. The vertical lines on the bottom are the inscribed lines on a ruler 1mm apart.

4.2.4 Alignment and Attachment to the Substrate

The scaffolds were attached to the wafer substrate using adhesives. For the case of metal scaffolds, a silicone based spray adhesive, (3M Repositionable 75 spray adhesive), was used (refer Appendix B). The polyester, vinyl and copper films had pre-coated layer of adhesive on their surface. The spray adhesive was pointed at grazing incidence to the scaffold to minimize its amount. The substrate was dropped onto the adhesive surface of the scaffold.

4.2.5 Further Challenges

When the scaffold is attached to the substrate, the adhesive used for attachment and the geometry of the scaffold could affect the spin-coating process as well as the PDMS polymer.

4.2.5.1 Adhesive Outgassing

The use of a scaffold provides a deterministic approach for peel initiation, for gripping the film and for handling the film for downstream processing. When preparing PDMS films, the compatibility with PDMS of the materials for the scaffold, the adhesive and any by-products of these materials produced during spin-coating and curing is important. The adhesive used for the scaffold must not adhere permanently to the substrate or leave debris on the substrate (a phenomenon called 'ghosting' in the adhesives industry). It is well known that platinum is a catalyst for the cross-linking reaction of PDMS [CW87] and it has been observed that PDMS on vinyl does not cure into a solid readily. PDMS also swells in organic solvents. Such properties serve as constraints for process integration when choosing the material for the scaffold as well as the adhesive that attaches the scaffold to the substrate. In our case, steel and stainless steel do not react adversely with PDMS and the non-volatile content of the spray adhesive does not outgas in the operating temperatures for PDMS curing.

4.2.5.2 Ridge at the Inner Periphery

With the scaffold attached, the viscous PDMS polymer spreading over the wafer surface during spin-coating encounters a radial step at the scaffold's inner periphery. The presence of this step causes the formation of a trough and a ridge on the profile of the PDMS film. When the PDMS liquid spreads and encounters the step at the scaffold, surface tension effects are pronounced both at the bottom and the top of the step.

When a highly viscous fluid flows over a 'step up', a local thickness reduction has been observed ahead of the step [KBH00]. The capillary number Ca is helpful in studying the dynamics of the PDMS film flowing over the step.

$$Ca = \frac{\mu U}{\sigma} \tag{4.1}$$

where μ is the dynamic viscosity, U the radial velocity component in PDMS during the spin-coating and σ is the surface tension. For spin-coating PDMS films of thickness about $100\mu m$, the following are the typical range of parameters: $\mu \sim 3 - 5Pa.s.$, $\sigma \sim 20 - 40mN/m$, $U \sim 0.1 - 1mm/sec$ and $Ca \sim .05 - .2$.

In this range of Capillary number values, [KBH00] have reported numerical studies in a dimensionless form of a viscous fluid over a step-up. When the fluid flows over a step of relative thickness 1 (step height equals far-field film thickness), the film has a trough before the step, with a relative thickness reduction of about 30%. The distance on either side of the step over which such a thickness reduction occurs is about $10 \sim 20$ times the film thickness [GMH04],[MGH04]. For PDMS films of thickness $100\mu m$, the distance over which such thickness reduction and the presence of the step is felt, is a few millimeters. Far away from the step, both on the substrate and on the step, the film thickness is nearly identical and is dictated by the spin-coating dynamics. The trough and ridge are formed due to the competition between surface tension and centrifugal spreading. This scenario is similar to the formation of a capillary ridge at

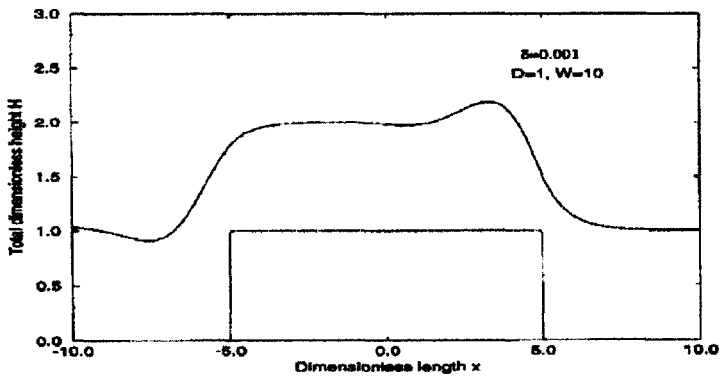

Figure 4-13: At the scaffold step, the PDMS film forms a local trough before the step and a ridge on top of the step. The particular example shown above depicts a step equal in height to the fluid film thickness far-away and shows local thinning of the film near the step. Used with permission of the publisher. ©American Institute of Physics.

the edge of a spin-coated cylindrical volume of fluid.

Next, I present some experimental data showing the presence and the size of the ridge. Figures 4-14 and 4-17 show an isometric view of the interferometric measurements over a portion of the scaffold reinforced film's top surface imaged using an interferometer. To enhance reflection a thin layer of gold was sputtered on top of the PDMS film. Figures 4-15 - 4-16, and Figures 4-18 - 4-19 show the respective top view and cross section thickness profiles for two samples. From the figures, we see the presence of the ridge as well as sharp variations in the thickness profile near the scaffold step. Beyond such representative data, we suggest further interferometric measurements to characterize the behavior of the PDMS film thickness near the scaffold step. The trough formed at the inner periphery reduces the effective thickness of the PDMS film attached to the scaffold. This aggravates the risk of tearing at the inner periphery of the scaffold. In order to counter the negative effects of the trough, I propose to locally reinforce the ridge by pouring PDMS over it all around the inner periphery (Figure 4-20).

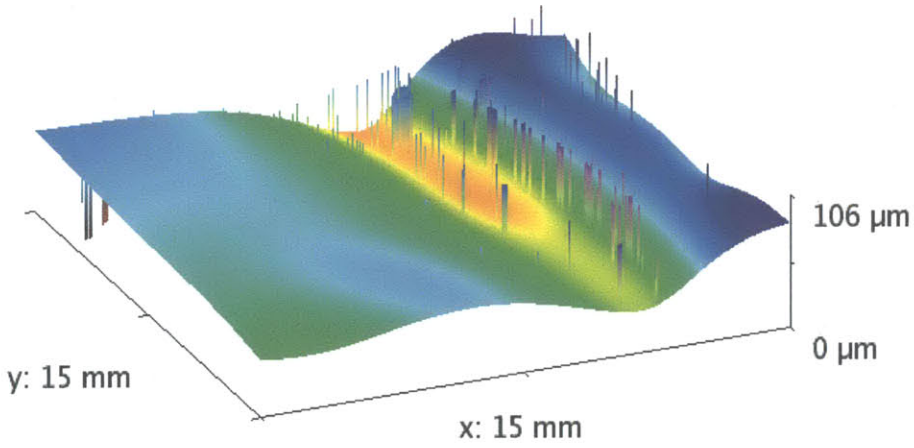

Figure 4-14: Near the step of the scaffold, the PDMS film forms a trough and a ridge. The ridge thins by about $40\mu m$ compared to the design thickness of $90\mu m$ everywhere on the PDMS film

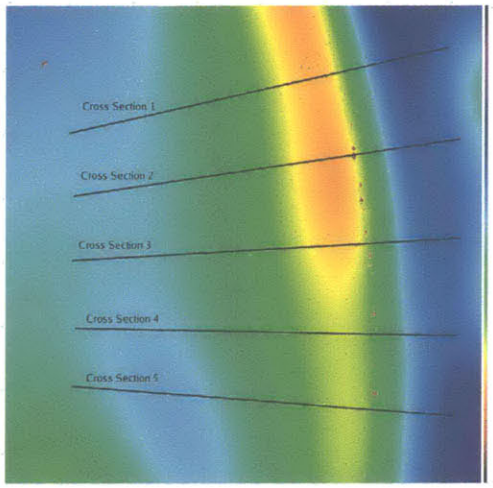

Figure 4-15: Near the step of the scaffold, the PDMS film forms a trough and a ridge. The film thins by nearly $40\mu m$ while its thickness elsewhere is $90\mu m$

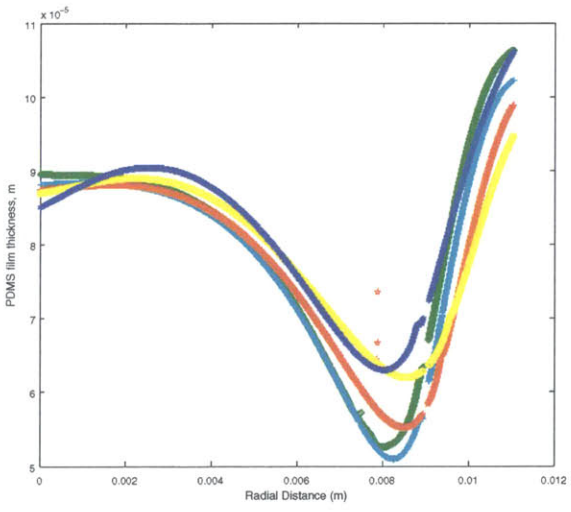

Figure 4-16: The height variation plot at cross sections indicated in Figure 4-15 show that the PDMS film forms a trough and a ridge near the step over the scaffold.

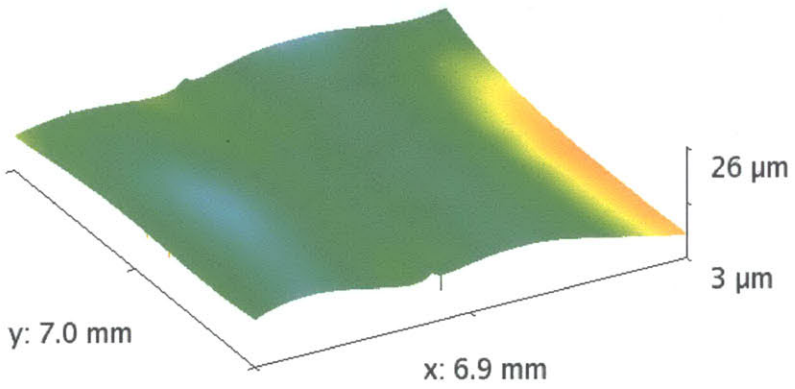

Figure 4-17: Isometric view (exaggerated) of the ridge near the inner periphery of $25\mu m$ scaffold carrying a $80\mu m$ thick film. Near the step of the scaffold, the PDMS film forms a trough and a ridge. The local thinning in this portion is not so pronounced as in Figure 4-15.

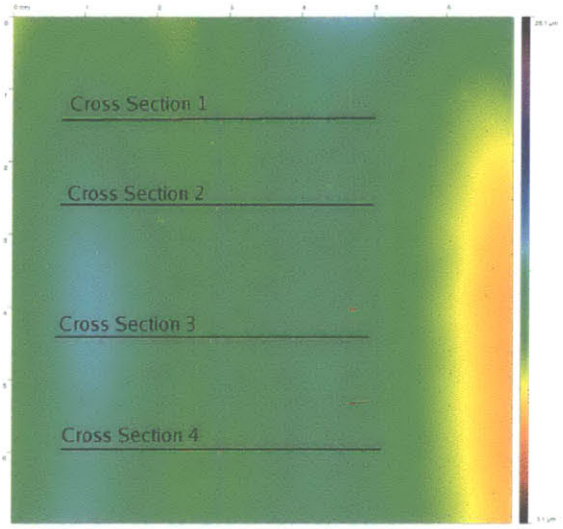

Figure 4-18: Near the step of the scaffold, the PDMS film forms a trough and a ridge.The local thinning in this portion is not as pronounced as in Figure 4-15.

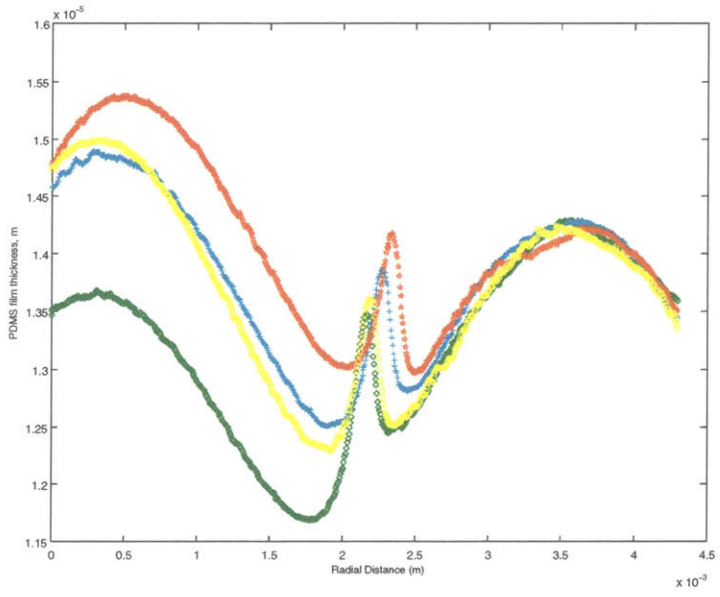

Figure 4-19: The height variation plot at different cross sections indicated in Figure 4-18 show that the PDMS film forms a trough and a ridge near the step over the scaffold.

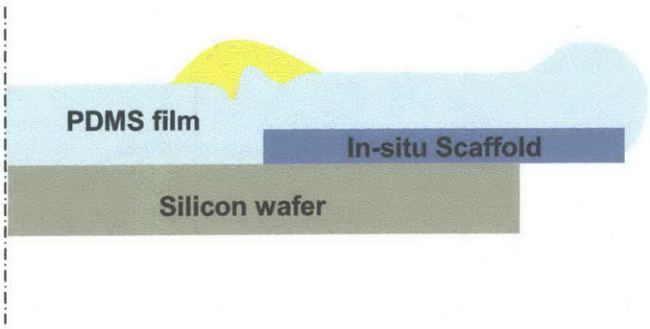

Figure 4-20: At the scaffold step, the PDMS film forms a local trough and a ridge. The local thinning of the film could be a tearing risk. By pouring PDMS using a syringe locally over the ridge, we reinforce the thin region and reduce the risk of tearing.

Material	Manufacture	Attachment	Observations
vinyl	CAD plotter	pre-coated adhesive	vinyl does not allow proper curing of PDMS
waxpaper	scissors	thin coat of PDMS	wax of the waxpaper did not melt at the temperatures of PDMS curing
copper film	CAD plotter	pre-coated adhesive	copper crimped excessively due to plastic deformation and tore through the PDMS film
paper	scissors	water	water surface tension is not sufficient to hold paper scaffold in place during spin-coating; water layer thickness difficult to control
PET tape	CAD plotter	pre-coated adhesive	easy to manufacture, but scaffold wrinkled easily when applied and handling of scaffold had similar problems as that of handling thin PDMS films
polypropylene	CAD plotter	pre-coated adhesive	easy to manufacture, but polypropylene deforms plastically under tension and loses shape; It also softens and loses shape under heat
brass	waterjet machining	3M Repositionable 75 Spray adhesive	brass held its shape; burrs due to waterjet machining were unpredictable
stainless steel	waterjet machining	3M Repositionable 75 Spray adhesive	stainless steel is stiffer than brass and held its shape; burrs due to waterjet machining were unpredictable
low carbon steel	waterjet machining	3M Repositionable 75 Spray adhesive	burrs due to waterjet machining were unpredictable

Table 4.1: Comparison of scaffold materials

4.3 Process Windows for Scaffold Manufacture

For the manufacture of thin scaffolds for use in thin PDMS film preparation, I discuss some of the material choices, the design space of key parameters and process windows based on practical considerations.

For the material choice for the scaffold, I present a summary of peeling experiments in Table 4.1. For the design of a scaffold, the main requirement is that the thickness

of the scaffold material be much smaller than the design thickness of the PDMS film:

$$h_{scaffold} << h_{PDMS} \tag{4.2}$$

Based on the discussion in Section 4.2.5.2, the thickness of the scaffold can be at most equal to the final thickness of the film, to guarantee that the fluid will overflow over the step. In such extreme cases, the ridge formation and the 'pinch-off' region near the step are critical locations. By designing the scaffold thickness to be much smaller than the PDMS film thickness, we can guarantee coating over the scaffold and a less pronounced effect due to the ridge at the scaffold step.

If we use a scaffold in the shape of a circular annulus, we have the following requirement so that the scaffold both attaches to the substrate and leaves room for gripping the scaffold outside the substrate:

$$R_{inner}|_{scaffold} < R_{substrate} \tag{4.3}$$

$$R_{outer}|_{scaffold} > R_{substrate} \tag{4.4}$$

The adhesive used to attach the scaffold to the wafer substrate must be weaker than that of the PDMS adhesion so that the scaffold separates easily. In practice, it is very hard to identify commercial adhesives of specific adhesive strengths. However, the following guideline can serve to compare choices of scaffold adhesives:

$$\gamma_{scaffold-substrate} < \gamma_{PDMS-substrate} \tag{4.5}$$

4.4 Chapter Conclusions

In summary, a thin, stiff scaffold is a component that helps solve the problem of peel initiation and of handling very thin PDMS films. The inclusion of a scaffold in a PDMS film manufacturing process offers several advantages. We list them here:

- The scaffold avoids the problem of beading around the periphery or overflow over the rim of the substrate. Thus the risk of tearing during initiation is minimized when using a scaffold for peeling.

- The scaffold is made of a thinner, yet stiffer material than the PDMS film. The flexural rigidity of the scaffold helps determine the shape of the PDMS film. By holding or by fixturing the scaffold, one can easily constrain the PDMS film to be planar. The scaffold thus prevent self-adhesion in thin PDMS films.

- The use of a scaffold enables peeling through kinematics as the stiffness of the scaffold dominates that of the PDMS film. The use of the scaffold thus circumvents the problem of material property variation in PDMS. It is well known that the material properties of PDMS are not repeatable from one experiment to the other, even when the same experimental protocol is used. By not depending on a specific parameter value for separation, the scaffold based film manufacturing process is applicable to any elastomer that is spin-coated, not just PDMS.

- The scaffold can be used even in a completely manual process to obtain a better grip on the thin PDMS film.

The process windows for scaffold design, manufacture and attachment presented in this chapter can help identify candidate materials for scaffolds and their associated geometry. The inclusion of a scaffold introduces additional questions regarding compatibility and spin-coating dynamics that must be addressed in order to implement a manufacturing process. For both prototyping applications as well as mass manufacture, thin steel shims offer a lot of potental as a scaffold material. For prototyping scaffolds out of thin steel shims, chemical etching provides a good edge quality. For production scale manufacturing of scaffolds, stamping will offer economies of scale.

Chapter 5

Continuous Peeling of PDMS Films

Following peel initiation, I focus on how to peel the PDMS film progressively and continuously from the substrate. The challenges in this task are to avoid the risk of tearing due to excessive tension or dynamic effects, to advance the peel-front in a controlled manner, to avoid wrinkling the peeled portion of the film and to hold the peeled film in a way suitable for subsequent processing. In the following section, I will discuss some of the dynamic effects in peeling (*e.g.* instabilities) and the non-linear geometry of the peeled film on non-uniform adhesion substrates. I will show how the use of a compressive pre-load provides for a controlled advance of the peel-front.

5.1 Process Level Challenges

Once we have initiated peeling the scaffold from the substrate, our objective is to control the location and advance of the peel-front and to mitigate any causes of damage for the remainder of the peeling process. I analyze both these topics here.

5.1.1 Controlled Advance of Peel Front

The process of peeling can be seen as the propagation of a peel-front, a planar curve across the area of the film separating the film from the substrate. Traditional stability

analyses have only focused on peeling over uniform substrates. Using a 1-D beam model, it can be shown that force actuation is unstable while displacement actuation is stable [Bol96]. I present a brief summary of the stability analysis here. Consider a beam of width b and length l acted upon by a force F at the free end. The beam is being peeled off the substrate of adhesion energy γ.

At a particular location, the energy (U) of the beam and substrate system is:

$$U_{total} = U_{bendingenergy} + U_{surfaceenergy} \tag{5.1}$$

$$= \int_0^l \frac{M^2}{2EI} \mathrm{dx} + \gamma \mathrm{bl} \tag{5.2}$$

where M is the moment at a cross section, EI is the flexural stiffness. For the two cases of force actuation, 'F' and displacement actuation at the free end 'd', we can write the following expressions for total energy:

$$U_{total} = \frac{F^2 l^3}{6EI} + \gamma bl \tag{5.3}$$

$$= \frac{EId^2}{2l^3} + \gamma bl \tag{5.4}$$

At equilibrium:

$$\frac{\partial U_{total}}{\partial l} = 0 \tag{5.5}$$

.

From this we obtain the equilibrium peel length of a 1-D beam under a force actuation as:

$$l_{equilibrium} = \frac{\sqrt{2EIb\gamma}}{F} \tag{5.6}$$

and under a displacement actuation as:

$$l_{equilibrium} = \sqrt[4]{\frac{9EId^2}{2b\gamma}} \tag{5.7}$$

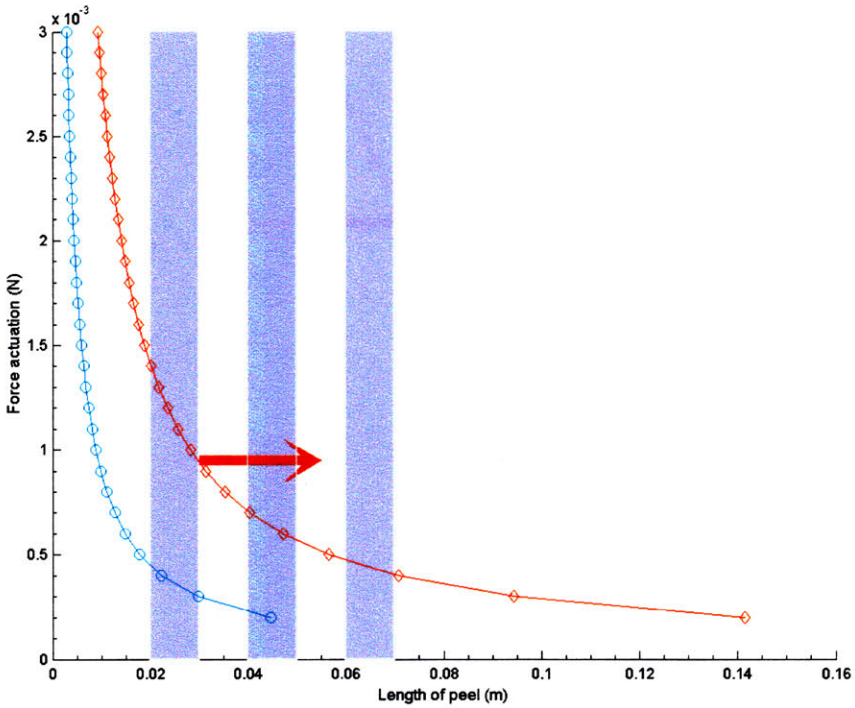

Figure 5-1: For a non-uniform substrate, transition from a sticky to a less sticky region is unstable under force actuation. The red arrow indicates the unstable transition from a stickier region to a less sticky one. The shaded columns are more sticky than the white columns. This analysis, building on the work of Bolotin on uniform substrates [Bol96], shows instability on non-uniform substrates.

.

At these respective equilibrium peel lengths, we investigate the stability by perturbing the actuation and find that force actuation is unstable while displacement actuation is stable. This simple 1-D beam model is approximate, but still captures some of the key insights regarding peeling stability.

If we consider peeling over a non-uniform substrate with different regions of variable stickiness, we find that peeling is unstable, no matter what kind of actuation is used. In Figure 5-1, I analyze the peeling over a substrate with alternating regions of adhesion under force actuation. The two curves indicate the force actuation versus equilibrium peel-length dependence, if the substrate were uniform with the particular

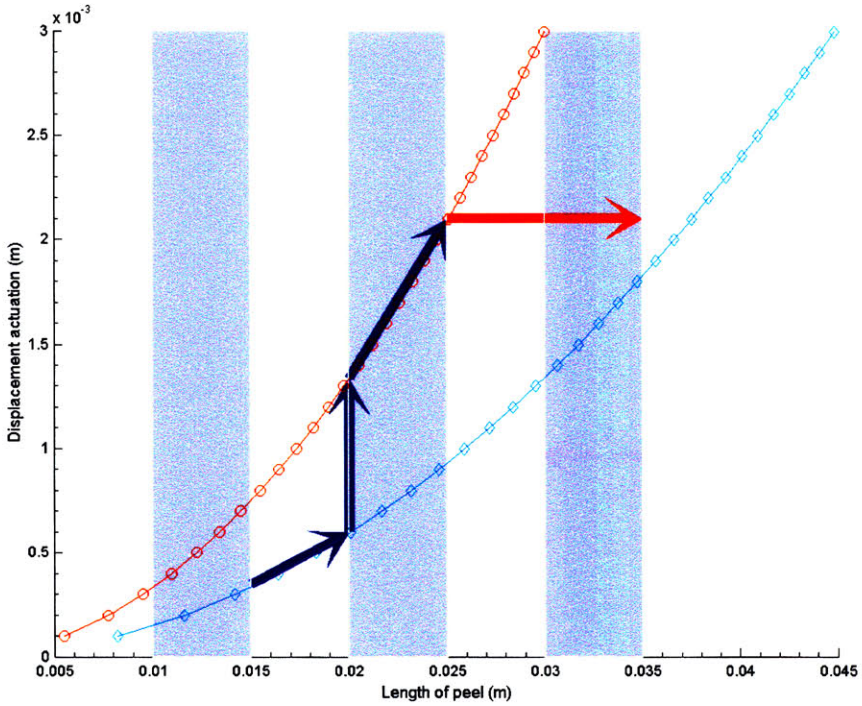

Figure 5-2: For a non-uniform substrate, transition from a sticky region to a less sticky region is unstable under displacement actuation. The blue lines indicate the peeling actuation under quasi-static conditions. The red arrow indicates the onset of unstable peeling from a stickier region to a less sticky one. The shaded columns are more sticky regions than the white columns.

adhesion energy. The curve for the larger surface energy value is on top. When the film transitions from a less to more sticky region, the new actuation force to sustain peeling is higher and, as a result, the peel length remains constant while the actuation force increases. When the film transitions from a more sticky region to a less sticky region, the new actuation force necessary for peeling is lower. As a result, the film peels uncontrollably leading to possible whiplash and tearing. In Figure 5-2, the two curves show the displacement actuation versus equilibrium peel-length dependence if the substrate were uniform with the particular adhesion energy. The curve for the larger adhesion energy value is on top. The transition of the film from a less to more sticky region only results in an increase of actuation with the peel length remaining constant. Similar to the case of force actuation, the transition from a more to less

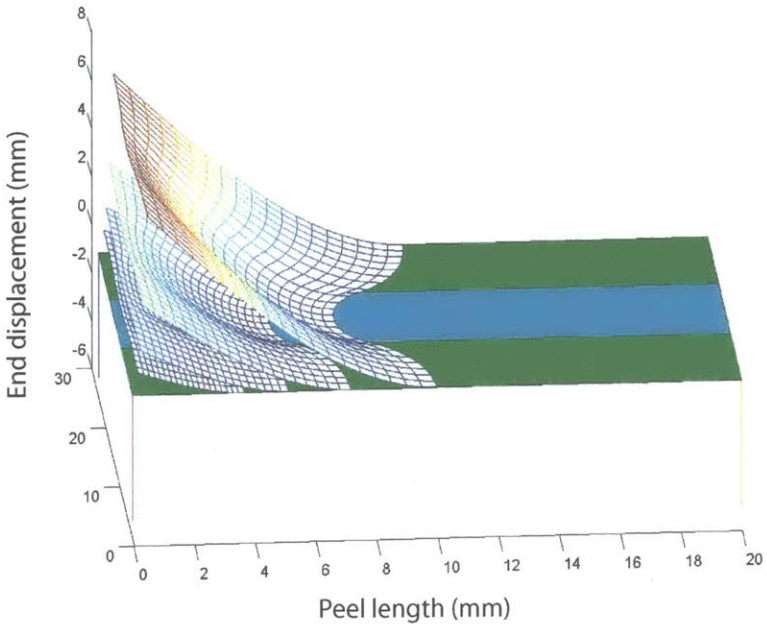

Figure 5-3: When peeling over parallel regions of different adhesion energies, the film stays more on the more adhesive region. As a result, the peel-front geometry is non-linear and the free-standing film could wrinkle.

sticky region leads to an uncontrolled peeling. In summary, for a substrates of different adhesion energies, the transition from a more to less sticky region will always be unstable (indicated by the red arrows in Figures 5-1 and 5-2).

The above stability analysis implies that pre-load constraints may be needed to prevent the uncontrolled advance of the peel-front over non-uniform substrates.

5.1.2 Non-linear Geometry of the Peel-front

When we peel a free-standing film off a substrate with different grades of adhesion, the extent to which the film will separate locally may depend on the local adhesion energy beneath the portion of the film. It is not possible to capture such 3-D behavior analytically since the shape of the film is non-planar and the shape of the peel-front

is non-linear. However, we can numerically simulate the approximate behavior of the film by using an approach similar to the 'finite strip method'. We divide the film into a series of long thin beams and assume they are all peeled off the substrate with the same displacement boundary conditions at the end. Figure ?? shows the result of an approximate numerical analysis showing the non-linear nature of the peel-front as well as the wrinkling of the free-standing film. If the peel-front is non-linear there is a risk of stress concentration around features and micro-slip at the boundary with the scaffold.

In order to avoid the non-linear peel-front geometry and the associated risk due to tearing, we may need to apply geometric constraints so that the peel-front location is controlled and the shape constrained to a straight line.

5.2 Concepts for Continuous Mode Peeling

Upon attaching the actuator to the scaffold, and subsequent initiation of peeling of the film from the periphery, I define the remainder of the process as 'continuous-mode peeling'. During continuous-mode peeling, the film could potentially tear due to unstable propagation of the peel-front, or a boss or a sharp feature on the surface or the scaffold edge, or a failure to release from the surface (excess adhesion). I present concepts for the continuous-mode peeling process and discuss fixturing, actuation degrees of freedom and pre-load constraints.

5.2.1 Fixturing the Substrate

The method of fixturing the circular wafer or a glass disk depends on the degrees of freedom we impose on the substrate. If we want to constrain the substrate in the plane of its lamina, we can use a vacuum chuck and an appropriate placement of two pins for fixturing the wafer. If we want to allow for small displacement adjustments, we can leave the substrate unconstrained on a flat surface with a low friction coefficient.

5.2.2 Degrees of Freedom for Peeling

When peeling the film manually, the operator could grip the scaffold between her fingers and roll the film gently. In a manual approach, it is not necessary that the peel-front moves in the direction of motion of the fingers. The operator could apply forces and moments in all three directions in a manual peeling process. Using a machine, one might expect the attachment of the peel initiator constraining the applied force and moment to a single direction if applicable.

5.2.3 Peeling with Compressive Pre-load

Earlier, I have shown the possible dynamic effects in peeling that are possible if we encounter different regions of adhesion. Further, different actuation approaches could also cause instabilities. In order to control the advance of the peel-front in a deterministic fashion, I used a cylindrical roller to hold the scaffold against and roll along the surface. As the roller rolls, the scaffold and the PDMS film it carries are peeled off the substrate. The roller applies a compressive pre-load, which 'pinches' the peel-front and prevents it from advancing any further.

5.2.4 Peeling with an Adhesive Roller Surface

Building on the concept of a roller to apply a pre-load onto the film, one could include an adhesive surface on the roller. Such a concept accomplishes few additional design goals. Adhesive attachment minimizes the excess tension in the peeled portion of the film. It also prevents the scaffold and film from lagging behind the roller surface, a condition that could lead to tearing.

5.3 Continuous Peeling Using Adhesive Roller

In this section, I analyze the physics of peeling a scaffold reinforced PDMS film using an adhesive roller. First, I present the energy balance during such a peeling process. I then discuss the prototype I assembled as part of my research and identify design guidelines for such machines.

5.3.1 Mechanics of Continuous Peeling

When the adhesive roller actuator is pressed against the scaffold, it adheres to the roller and begins to separate from the wafer substrate and onto the roller's adhesive surface. I analyze the energy balance of this process comparing the bending of the scaffold and PDMS film, the adhesion of the PDMS film to the roller and the separation of the PDMS film from the wafer substrate.

The incremental energy (ΔW) provided when the roller rotates by an angle $\Delta\theta$ is:

$$\Delta W = \Delta W_{Bending\ Energy} + \Delta W_{Surface\ Energy} \tag{5.8}$$

$$\begin{aligned}\Delta W \;=\; & \frac{\Delta\theta}{R}\left[\frac{Ebt^3}{12(1-\nu^2)}\right]_{Scaffold} + \frac{\Delta\theta}{R}\left[\frac{Ebt^3}{12(1-\nu^2)}\right]_{PDMS} \\ & + \gamma_{PDMS-Substrate}(R+t/2)b_{PDMS}\Delta\theta + \gamma_{Scaffold-Substrate}(R+t/2)b_{Scaffold}\Delta\theta \\ & - \gamma|_{Roller-PDMS}(R-t/2)(b_{PDMS}+b_{Scaffold})\Delta\theta\end{aligned}$$

where R is the radius of the roller actuator, t refers to the thickness, E refers to the Young's modulus, $b_{scaffold}$ is the total width of the scaffold at a particular cross section, b_{PDMS} is the width of the PDMS film at a particular cross section and the subscripts to the surface energy γ indicate the pairs of surfaces of interaction. As the roller rotates by $\Delta\theta$, the widths $b_{scaffold}$, b_{PDMS} change with the change in b_{PDMS} being much larger. Based on typical material properties for a steel scaffold and the

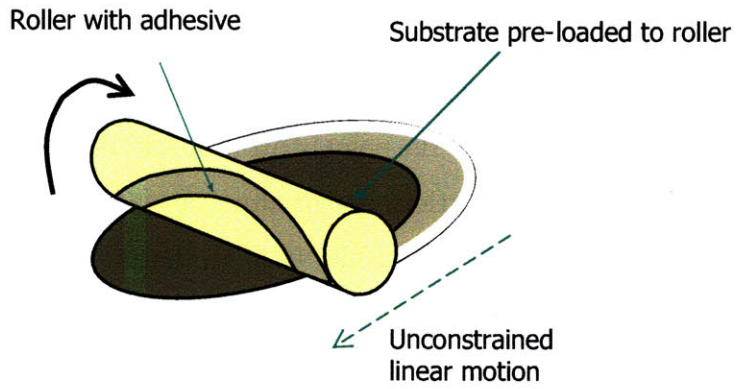

Figure 5-4: Schematic of an adhesive roller actuator with compressive preload

geometry we designed, we find that:

$$\left[\frac{Et^3}{12(1-\nu^2)}\right]_{Steel} \gg \left[\frac{Et^3}{12(1-\nu^2)}\right]_{PDMS} \tag{5.9}$$

and

$$R \gg t \tag{5.10}$$

Thus, we can simplify Equation 5.9 to:

$$\begin{aligned}\Delta W &= \frac{\Delta\theta}{R}\left[\frac{Ebt^3}{12(1-\nu^2)}\right]_{Scaffold} + \gamma_{PDMS-Substrate} R b_{PDMS} \Delta\theta \\ &+ \gamma_{Scaffold-Substrate} R b_{Scaffold} \Delta\theta - \gamma|_{Roller-PDMS} R(b_{PDMS} + b_{Scaffold})\Delta\theta\end{aligned}$$

The above energy balance is applicable mainly during the peeling of the PDMS film from the substrate. For the energy balance expression to be valid, it is necessary that the adhesion of the roller adhesive provide the necessary bending energy on the scaffold as otherwise the scaffold will not attach to the roller actuator – a condition necessary for successful peeling. The individual terms in an energy balance expression are modified when we consider that both the roller and the PDMS film undergo Hertzian-elastic deformations at the point of attachment. However, during continuous operation, the hertzian deformations do not alter the overall energy balance given by Equation 5.11. When peeling a thin film from the substrate, the risk of instability must be carefully avoided. Next, I present the design of an adhesive roller that pinches the film just ahead of the peel-front so that there is no uncontrolled advance of the peel-front.

5.3.2 Roller Geometry

The geometry of the roller is designed mainly based on the energy balance during the attachment of scaffold and PDMS film to the roller. The roller radius can be designed using Equation 5.9 as a guide. For practical reasons, the roller width and circumference should be greater than the film size. The roller radius should not be too small such that there is a risk of permanent plastic deformation in the metal scaffold as it is attached to the roller. Later in this chapter, I will present these competing influences on an adhesive roller design in a process window.

5.3.3 Compressive Pre-load Design

The pre-load applied by the roller on the wafer substrate must ensure contact between the roller and the substrate at all times. However, the pre-load must not be too large that there is excessive friction underneath the wafer. During the design of the peeling machine, a constant force spring is used to pre-load the surface carrying the wafer against the adhesive roller.

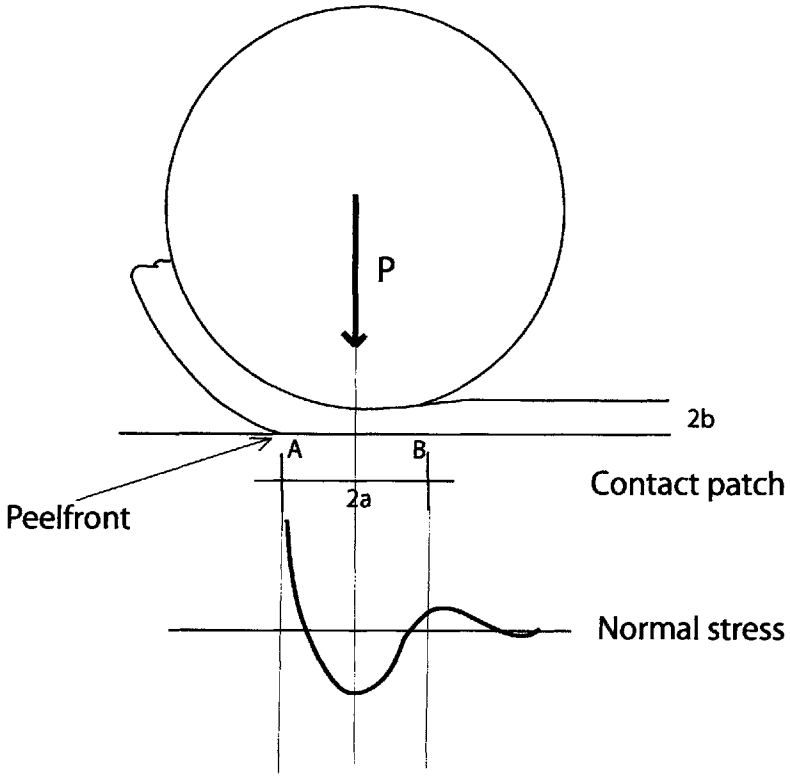

Figure 5-5: Typical normal and shear stress profile under the film when actuated with an adhesive roller

5.3.4 Speed of Operation

The maximum speed of advance of the peel-front is given by the wave-speed at the interface. For typical values of adhesion energy as encountered in $PDMS - SiO_2$ systems, the surface wave speed is nearly $20cm.s^{-1}$ and determines the maximum speed at which the adhesive roller actuator could operate for peeling. From practical considerations during experiments, we want to operate the roller at such a speed that allows manual inspection and intervention. If we use time-sensitive adhesives then the roller speed can not exceed a limit. Even before the wave-speed based limit, the roller might cause excess flutter or centrifugal action on the scaffold and PDMS film if it is rotating at a very high velocity.

5.3.5 Motor Selection

The roller is driven with a geared DC motor (**escap** motor M22 10) with a gear ratio of 1:125. While designing the actuation for the roller, I considered the use of a linear stage for the wafer substrate and using position feedback from the linear stage to drive the roller. Given the complexity of such a feedback control setup, I decided to drive the roller in open-loop and have the wafer substrate be pulled onto the surface by the scaffold.

5.3.6 Roller Surface Adhesive Selection

For the roller surface, I chose adhesive tapes carrying acrylic pressure-sensitive-adhesives (PSAs). The key requirements of the adhesive on the roller are that it is non-ghosting, non-reactive and has a low tack. I used adhesive tapes sold commercially by 3M (Product Code 3126C medium-tack adhesive tape) and attached the tape to the roller surface using scotch tape on the boundary.

5.3.7 Surface Carrying Wafer

In my proposed approach, the wafer substrate is not constrained on the inclined surface. The requirements on this surface are that it is stiff and has low friction so that the wafer moves freely, has low thermal expansion and has low cost.

5.3.8 Comptatibility with PDMS

The materials for the peeling machine, the scaffold and the adhesives we have discussed so far must be compatible with PDMS, not affect its performance adversely and not leave any debris on the film. The use of metal shims with steel, stainless steel or brass is similar to the metals used in tweezers or wafer holders. PDMS is contaminated by platinum during its curing process but any other metal is not known to react adversely with PDMS [CW87]. The tack on the roller surface must be strong enough to stay attached to the film, but be sufficiently weak to release the film easily and not to allow transfer of particulate matter or debris to the PDMS film surface.

5.4 Process Windows for Peeling with an Adhesive Roller

A process window for the adhesive roller can be developed based on Equation 5.9 relating the radius of the roller and the adhesion energy of the roller surface. In addition, avoiding plastic deformation in the scaffold or the film wrapping around itself on the roller provide limits on the roller size. A schematic of the process window for an adhesive roller peeler is shown in Figure 5-6.

5.5 Chapter Conclusions

In summary, the key observations regarding continuous peeling are as follows:

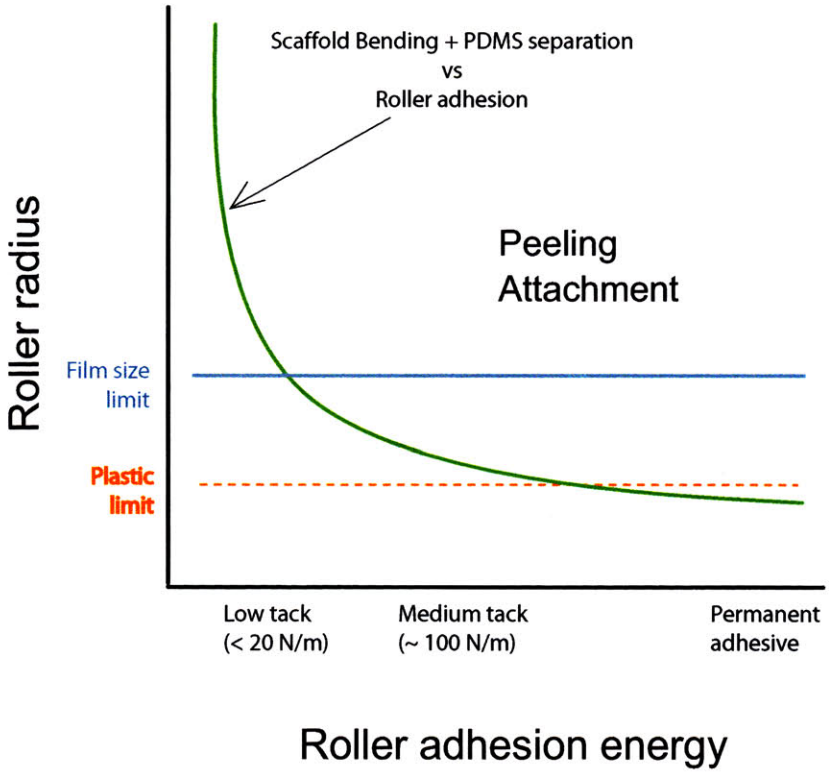

Figure 5-6: The process window for the adhesiver roller peeler compares the radius of the roller with the adhesive strength on the roller surface. The roller circumference must be greater than film size and the roller radius must also avoid the risk of plastic deformation in the scaffold. The downward sloping curve are the equilibrium solutions to Equation 5.11.

- The controlled advance of the peel-front is an important challenge during continuous peeling as there is a risk of whiplash and tearing.
- When the substrate has different regions of adhesion, the geometry of the peel-front could be non-linear and there is a risk of stress concentrations in the film.
- An adhesive roller attaches to the film and prevents excessive tension during peeling.
- The peel-front can be constrained to be linear and advanced in a deterministic fashion using a compressive pre-load.
- During peeling with a scaffold, the stiffness of the scaffold dominates that of the PDMS film. Thus, the bending of the scaffold when adhered to the roller surface determines the shape of the PDMS film.
- The roller geometry can be designed by considering the energy balance during peeling and being mindful of practical design issues such as film size.
- The compressive pre-load values can span a wide range so long as we maintain contact between the roller and the film at all times, and avoid excess friction between the substrate and thesupport.

THIS PAGE INTENTIONALLY LEFT BLANK

Chapter 6

Handling PDMS Films after Peeling

6.1 Offtake from the Adhesive Roller

In my proposed process, the scaffold reinforced PDMS film is attached to the adhesive surface of the roller for peeling from the wafer substrate. Before the PDMS film could be used, the film and scaffold must be separated from the roller. Such separation can be done by attaching to the scaffold and pulling it away from the roller. We broadly define these process steps as 'offtake' of the PDMS film and scaffold. The challenges in offtake center around how we will initiate the separation of the scaffold from the roller and how we will attach to the scaffold and peel it off the roller. Here again, we need to do offtake while avoiding tearing of the PDMS film or having permanent deformation to the scaffold.

6.2 Mechanics of Offtake

During 'offtake', we face a problem similar to peeling the scaffold reinforced PDMS film from the wafer, with the key difference being that the substrate is now cylindrical

and adhesive. Similar to the energy balance presented in Section 6.1, I identify the energy balance for a scaffold reinforced film on a cylindrical roller. Here, the competing physics is between the (un)bending of the scaffold and the adhesion with the roller surface. Such an energy balance is valid everywhere except at the point of initiation. The beam or plate theory assumes a finite width of the material – a condition that is not satisfied at the point of initiation off a circular scaffold. Thus initiation is a challenge during off-take and must be specifically addressed in the design. Assuming the width of the scaffold and film is finite and non-zero everywhere, the incremental energy change in unbending the film is,:

$$\Delta W = \Delta W_{bendingenergy} + \Delta W_{surfaceenergy} \tag{6.1}$$

$$= \gamma|_{roller-PDMS}(R - t/2)(b_{PDMS} + b_{scaffold})\Delta\theta - \frac{\Delta\theta}{R}\left[\frac{Ebt^3}{12(1-\nu^2)}\right]_{scaffold} \tag{6.2}$$

where b_{PDMS} and $b_{scaffold}$ are the instantaneous widths of the PDMS and scaffold portion of the peel-front respectively. Because of circular geometry of the PDMS film and the annular geometry of the scaffold, both these widths are continuously changing during the offtake process.

If we neglect the scaffold thickness relative to the roller radius:

$$\Delta W = \Delta\theta\left(\gamma|_{roller-PDMS}R(b_{PDMS} + b_{scaffold}) - \frac{1}{R}\left[\frac{Ebt^3}{12(1-\nu^2)}\right]_{scaffold}\right) \tag{6.3}$$

,

If we pull on the scaffold in a straight line with a tensile force, F, for offtake, this incremental energy ΔW equals the work done for offtake:

$$\Delta W = FR\Delta\theta \tag{6.4}$$

An estimate of the tensile force needed for offtake is:

$$F = \gamma|_{roller-PDMS}(b_{PDMS} + b_{scaffold}) - \frac{1}{R^2}\left[\frac{Ebt^3}{12(1-\nu^2)}\right]_{scaffold} \quad (6.5)$$

,

Equation 6.5 shows that the unbending of the scaffold contributes to the offtake mechanism. Further, this equation could be used to design suitable offtake mechanisms, concepts of which I will discuss in the following sections.

6.3 Initiation of Offtake

The analysis presented in Section 6.2 is valid everywhere except at the initial point of attachment of the scaffold. At the initial point of attachment, the width of the peel-front tends to zero and thus Equation 6.1 will be redundant with each term being zero. The initiation of the scaffold off the cylindrical adhesive surface can not thus be predicted or designed by energy balance. In order to deterministically initiate offtake, we must design the starting width of the adhered portion of the scaffold-PDMS film setup to be finite.

We can design for such a non-zero starting peel-front width using three possible concepts that can be incorporated at the time of starting the adhesion of the scaffold to the cylindrical roller (right before the PDMS film has even begun to be peeled off the wafer substrate):

- allowing small freehang of the scaffold,
- crimping the end portion of the scaffold upwards, so that the crimp leaves a small starting length of the scaffold unadhered, or
- temporarily attaching a spacer wire on scaffold which leaves a portion of the scaffold unadhered at the start.

6.4 Attachment to Scaffold for Offtake

After we design the initiation of offtake, we can use Equation 6.3 and Equation 6.5 to design concepts for continuous offtake of the scaffold and PDMS film from the roller. I list three potential approaches below:

- A large diameter roller for peeling off the wafer substrate connected by a continous web to a smaller diameter roller. The scaffold and film will peel off the substrate and onto the roller, then onto the adhesive web. When the adhesive web encounters the smaller roller, the curvature can be designed to cause the scaffold to peel off the second roller (Figure 6-2).

- By using a rare-earth magnet and the scaffold made out of a ferromagnetic material, *e.g.* low carbon steel, we can attach to the scaffold and separate the scaffold and film from the roller. The magnetic attachment could then be an approach for handling the scaffold as well.

- By using a clamp, we can attach to the scaffold and separate the scaffold and film from the roller for the sake of offtake.

6.5 Process Windows for Offtake

The process window for offtake from the roller is shown in Figure 6-1. The offtake region's boundary is obtained from the roots of Equation 6.5. The dotted line shows the process window for attachment using a roller. The two design regions being separate indicate that we can not achieve spontaneous peel attachment and offtake. There is no plastic deformation limit for offtake as smaller rollers will favor separation of the scaffold from the roller surface.

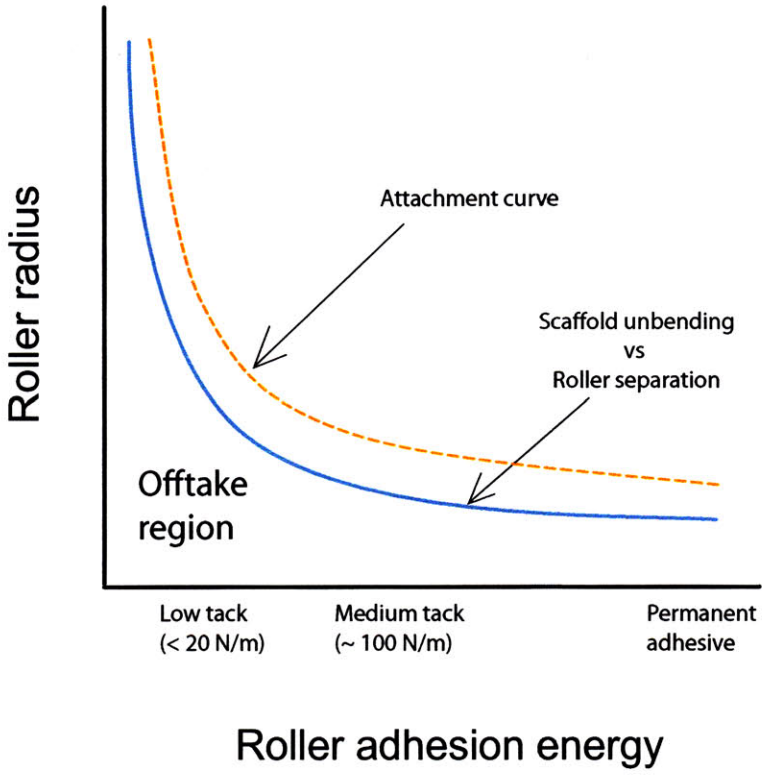

Figure 6-1: During offtake, the energy balance is between the straightening of the scaffold and the separation from the adhesive roller surface.

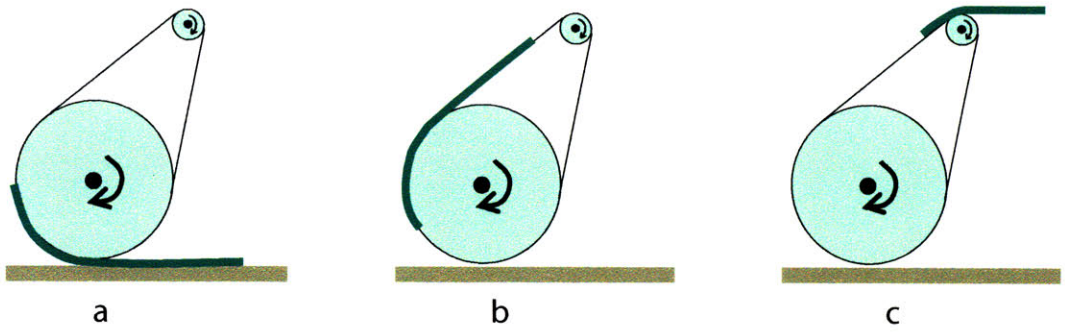

Figure 6-2: With a large roller and a small roller connected by an adhesive belt, we can implement automatic offtake. The radius of the small roller is designed using the process windows such that the scaffold unbends while moving over the small roller. In the above schematic, a) shows peeling of the scaffold reinforced film from the substrate; b) shows the film conveyed on the adhesive belt to the smaller roller; c) shows the scaffold separating from the adhesive belt while moving over the small roller.

6.6 Registration and Alignment

The scaffold can be used to obtain a direct control over the shape and planarity of the PDMS film. When the scaffold is constrained against a surface then both the scaffold and the film retain their geometry and avoid any out of plane deformations. Similarly the scaffold orientation and location can be used to fix the location and orientation of the PDMS film it carries. Such an approach will be useful for aligning PDMS films with features, as part of a multi-layer device. We can incorporate fiducials for directionality and features for kinematic placement of the scaffold.

6.7 Transport and Storage

PDMS films with scaffolds can be easily stored, handled and transported by attaching exclusively to the scaffold alone and never to the PDMS film. When films are prepared in anticipation of a demand, they can be stacked with spacers around the scaffold. When PDMS films need to be handled one at a time, a pick-and-place strategy could

be implemented by attaching to the scaffold through positive attachment or alternate methods like magnetic handling or vacuum chucks.

6.8 Chapter Conclusions

Based on the discussion so far, we make the following observations:

- Offtake is necessary when peeling using an adhesive roller.
- Offtake initiation is challenging and we must incorporate concepts such as an end-wire or a crimp to start the offtake from the roller.
- Offtake can be done by hand or in an automatic manner using magnetic attachments.
- The scaffold can be used for holding, handling and transporting thin PDMS films.
- Handling thin PDMS films using the scaffold avoids contamination of the film surface.
- Fiducials included in the scaffold can be used to align the PDMS films.

Successful offtake completes the implementation of the PDMS film peeling process. In addition, offtake of a scaffold reinforced film also provides the first step towards handling and subsequent storage of thin PDMS films.

THIS PAGE INTENTIONALLY LEFT BLANK

Chapter 7

Experiments and Discussion

Based on the theoretical analysis and design insights discussed so far, I have prototyped an automatic peeling machine. In this chapter, I present the details of the machine using which I have peeled PDMS films of thicknesses down to $50\mu m$. The key components of an automatic PDMS film manufacturing process are a scaffold incorporated between the film and the wafer, a pre-loaded adhesive roller for peeling the PDMS film, an offtake approach to get the film off the adhesive roller and methods for storage and handling.

I have conducted an extensive array of experiments using the peeling machine for peeling PDMS films of thickness down to $50\mu m$ and off of glass and silicon substrates. Here, I present some results from experiments of peeling thin PDMS films under different process conditions – film thickness, substrate choices, adhesive choices, damage mitigating factors and geometry of the peeling device.

7.1 Proof of Concept Peeling Machine

The prototype peeling machine is shown in Figure 7-1. The wafer is placed on a 12 " long delrin sheet that is hinged at one end and spring-loaded against the roller using constant force springs. The roller is made out of delrin and it is 1.6" in diameter

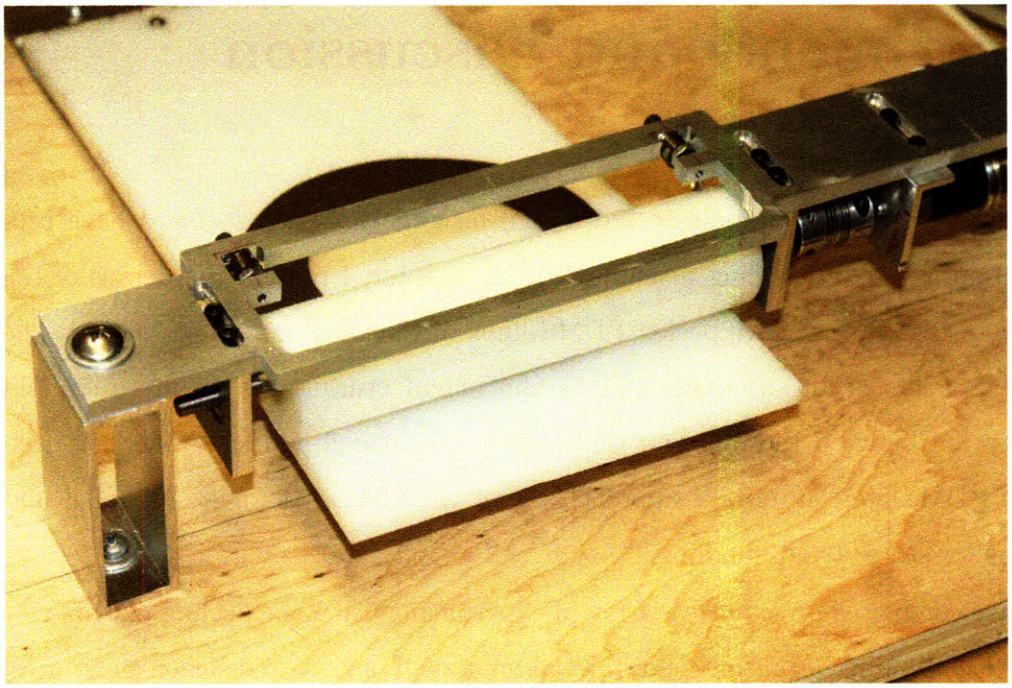

Figure 7-1: The prototype of an automatic peeling machine developed in this thesis includes an adhesive roller peeler and a wafer carrying surface spring-loaded against the roller.

(for handling 4" substrates). The delrin is supported by 6mm dowel pins press-fitted at the ends and driven by a geared DC motor. A flexible shaft coupling corrects misalignment between the motor and the roller. The motor and the roller are mounted on a .25" Aluminum plate. A window is cut out in the plate to allow access to the top surface of the roller and for visual inspection. Medium tack adhesive sheets (3M adhesive tape 3126C) are attached to the roller surface using scotch tape. The DC motor is driven using a variable voltage power supply.

As a summary of the requirements, an automatic process for PDMS film manufacture involves the individual steps of a robust approach for preparation of films of accurate thickness, repeatable initiation of peeling of the film from the substrate, peeling of the film in a steady, controlled manner and finally, handling the film for subsequent processing. Although, the attachment of the scaffold to the substrate, the spin-coating process and the curing process steps are separate from the peeling machine, one can conceive of a scenario where all these individual process steps are integrated within a manufacturing cell.

7.2 Experimental Results

7.2.1 Automatic Peeling

	Substrate										
	Glass				**Si**				**Patterned Si**		
	Ridge reinforcement		No reinforcement		Ridge reinforcement		No reinforcement		Ridge reinforcement		
	Scaffold Adhesive		Scaffold Adhesive		Scaffold Adhesive		Scaffold Adhesive		Scaffold Adhesive		
Thickness (μm)	Ageing	No Ageing	Ageing	No Ageing	Ageing	No Ageing	Ageing	No Ageing	Ageing	No Ageing	Height data
300	√	√	√	√	√	√	√	√	?	√	?
100	√	√	√	√	√	√	√	√	?	√	√
90	√	√	√	√	x	√	x	√	?	√	√
80	√	√	√	x	x	√	x	x	?	x	√
70	√	√	√	x	x	√	x	x	?	x	√
60	√	√	?	x	x	√	x	x	?	x	√
50	?	√	?	x	x	x	x	x	?	x	√

Table 7.1: Experimental validation of the scaffold reinforced elastomeric film manufacturing process

Film Thickness (microns)	Offtake Approach		
	Manual	Magnetic	
		No Crimping	Crimping
300	√	?	?
100	√	x	√
90	√	x	√
80	√	x	√
70	√	x	?
60	√	?	?
50	√	?	?

Table 7.2: Experimental validation of offtake from the adhesive roller

In Table 7.1, I summarize the various tests that I conducted using my automatic peeling machine. '√' indicates successful peeling, 'x' indicates damage during peeling and '?' indicates further tests are needed. In this series of experiments, I focused more on thinner films more. While this set of experiments may not be exhaustive from a statistical viewpoint, we are confident based on our results that our peeling machine is capable of peeling PDMS films of thickness 100 microns and less. We do recommend further testing to quantify the yield of this approach.

7.2.2 Offtake

In Table 7.2, I summarize the various tests that I conducted using my automatic peeling machine. '√' indicates successful peeling, 'x' indicates damage during peeling and '?'indicates further tests are needed.

7.2.3 Handling of thin PDMS films

Using the scaffold the PDMS film can be held by hand easily without the risk of contamination. When we use steel scaffolds, we can further use a magnetic attachment to hold the PDMS film. Figure 7-2 shows an $80\mu m$ thick PDMS film that was peeled using the automatic peeling machine with magnetic offtake by hand.

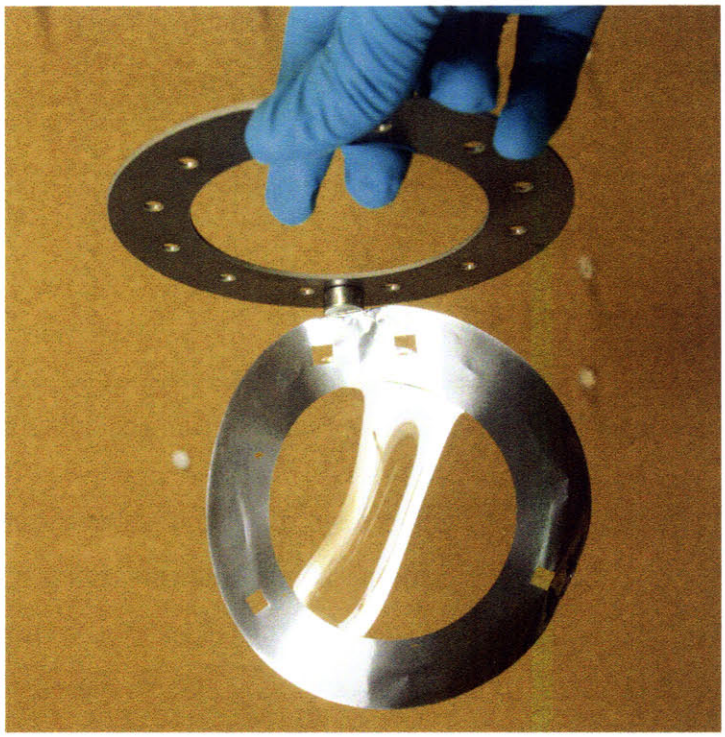

Figure 7-2: This picture shows an $80\mu m$ PDMS film supported by a steel scaffold and held using a magnet on a steel frame

7.3 Key Observations

7.3.1 Spin-Coating Study

Here we showed the variation of thickness with time. We showed the robustness in spincoating using a large initial slug. Under such conditions, we show the viability of using $\omega^2 t$ as the design parameter. For the same spin speed, we show that time for spin-coating varies as the inverse square of thickness. *E.g.* it takes four times as long to spin-coat a film down to half as much thickness.

7.3.2 Effect of Adhesives

From our experiments, we make the following observations regarding the choice of adhesives between the scaffold and substrate and on the roller surface,:

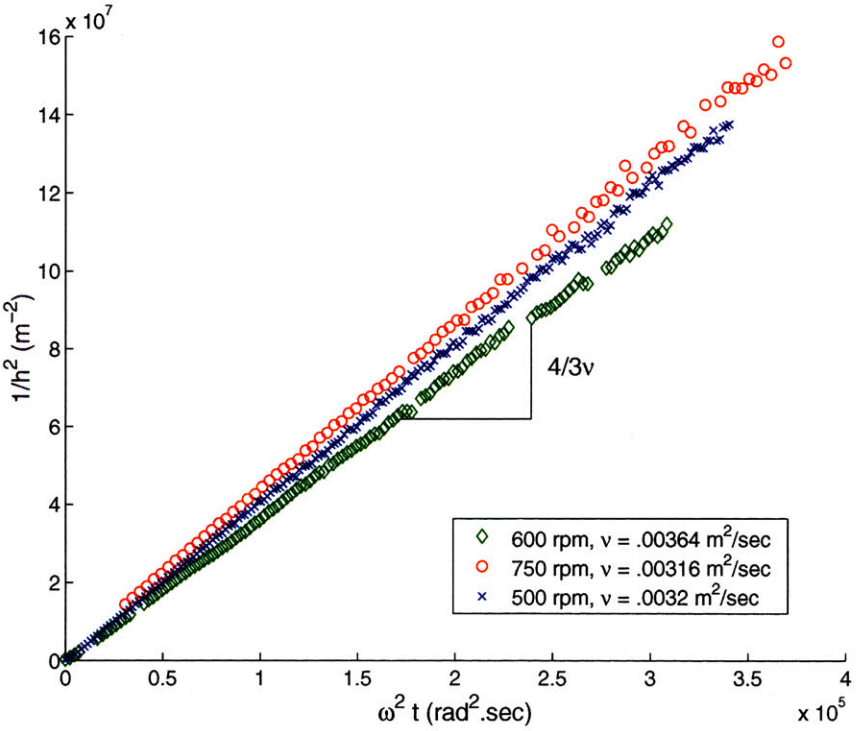

Figure 7-3: Inverse squared thickness is linear in variation against $\omega^2 t$. Repeat of Figure 3-4

- If the scaffold is attached with a stronger adhesive then the scaffold does not separate easily from the substrate. As a result, the film does not peel and attach to the roller. The peeling process fails if the scaffold is attached too strong.
- The stronger the adhesive on the roller, the better are the conditions for peeling the film from the substrate. However, for the sake of offtake the roller adhesive must not be permanent.
- The use of low to medium-tack pressure sensitive adhesives are potential choices for use with PDMS film peeling

7.3.3 Effect of Reinforcing the Inner Periphery of Scaffold

From experimental measurement of the profile of the PDMS film, we find a local reduction in film thickness near the step caused due to the scaffold. This locally thin region weakens the attachment of the scaffold to the PDMS film and causes tearing. To reinforce this portion, a very small volume of PDMS is applied all over the inner periphery of the scaffold using a syringe. The local reinforcement avoids the tearing risk at the inner periphery and does not affect the thickness of the rest of the PDMS film.

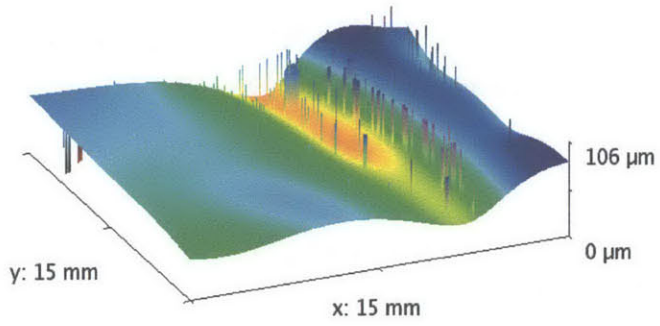

Figure 7-4: Near the step of the scaffold, the PDMS film forms a trough and a ridge. The ridge thins by about 40 microns compared to the design thickness of 90 microns everywhere on the PDMS film. Repeat of Figure 4-14

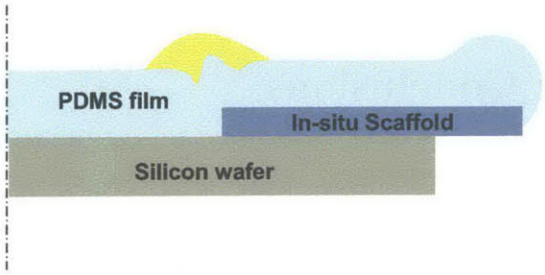

Figure 7-5: At the scaffold step, the PDMS film forms a local trough and a ridge. The local thinning of the film could be a tearing risk. By pouring PDMS using a syringe locally over the ridge, we reinforce the thin region and reduce the risk of tearing. Repeat of Figure 4-20

7.3.4 Effect of Substrates

During my experiments I was able to peel thin PDMS films off of glass substrates, silicon substrates – both plain and with topography. The adhesive we used for scaffold attachment (3M Repositionable 75) had a noticeable ageing behavior on silicon wafers. In situations when the scaffold with adhesive was left for long durations on the silicon wafer, the adhesion of the scaffold to the wafer was very strong and resulted in tearing during peeling. From patterned silicon wafers with surface micromachined features of upto $5\mu m$ depth we were able to peel PDMS films of $90\mu m$ thickness. There is a caveat here, however. The success in peeling films off one particular patternis no guarantee that we will peel from other surfaces. We recommend more extensive tests to identify specific limitations to peeling films off patterned wafers.

7.3.5 Effect of Initiation Features for Offtake

When we crimp the scaffold for initiation in the offtake stage of the process, the crimp directed upwards avoids peeling of a small portion of the scaffold at start and helps offtake. However, the crimp directed downwards causes adhesion everywhere except the crimp and is not so effective by comparison.

7.4 Chapter Conclusions

In my dissertation, I have presented a prototype of an automatic peeling machine. Using this automatic peeling machine, I have validated my manufacturing process for thin PDMS films that includes robust thickness control, is insensitive to material property variations and can peel PDMS films off of glass and silicon wafers. Although the implementation shown is for 4" wafers, the peeling machine concept is capable of handling 4 inch as well as 6" wafers.

Chapter 8

Conclusions

In this thesis, I have developed the elements of an automatic process for manufacturing thin PDMS films. By assembling a prototype peeling machine and through extensive experiments, I have shown evidence that the proposed process is capable of manufacturing PDMS films of thicknesses down to $50\mu m$. Here, I present a brief overview of – the process steps and process windows – PDMS film manufacture. I envision an end-to-end automation of thin PDMS film manufacture and critique my research in this context. I conclude with the key research contributions in this thesis.

8.1 A Summary of the Process

8.1.1 Process Steps

The manufacturing process developed in this thesis consists of:

1. Robust thickness control in spin-coating.

    - Spin-coating of PDMS with a large initial pour volume and $\omega^2 t$ as the design parameter
    - Real-time monitoring of spin-coating thickness using an approach developed by our collaborators.

2. A Scaffold-Reinforced Elastomeric Film Manufacture (SEFM) process consisting of:
   - an *in-situ* Scaffold for peel initiation and gripping the thin PDMS film,
   - an adhesive roller with compressive pre-load for peeling the film continuously, and
   - an automatic approach for offtake of the film and scaffold from the adhesive roller.
3. Storage and handling of thin PDMS films using features on the scaffold, *e.g.* fiducials on the scaffold for kinematic alignment.

8.1.2 Process Windows

In this section, I summarize the key process windows,

- For the scaffold design,:

$$h_{scaffold} << h_{PDMS} \tag{8.1}$$

$$R_{inner}|_{scaffold} < R_{substrate} \tag{8.2}$$

$$R_{outer}|_{scaffold} > R_{substrate} \tag{8.3}$$

- For the adhesive to attach scaffold to the substrate,:

$$\gamma_{scaffold-substrate} < \gamma_{PDMS-substrate} \tag{8.4}$$

- For the design of the adhesive roller and for the offtake mechanism,:

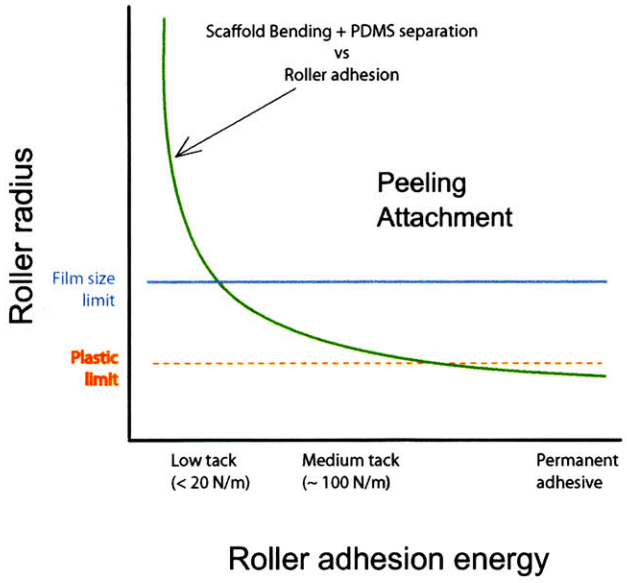

Figure 8-1: Process window for adhesive roller peeler. Repeat of Figure 5-6

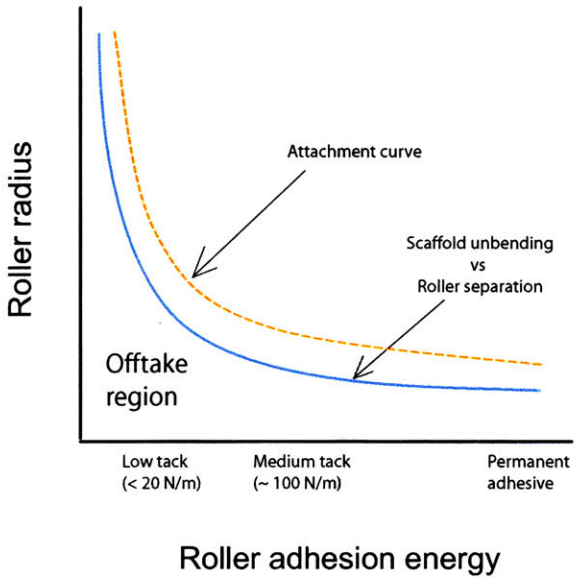

Figure 8-2: Process window for offtake. Repeat of Figure 6-1

8.2 Requirements for Automation

8.2.1 Towards a 'Fab'

As an outcome of our research, we envision a production system for thin PDMS films which satisfies the key requirements of modern manufacturing such as accuracy, yield and rate. One can imagine a PDMS 'fab' consisting of key machines based on the process steps we have identified or invented. The individual process steps are:

1. an automatic scaffold manufacturing sub-unit with scaffold design from the masks;
2. robust spin-coating of PDMS film over wafer substrates carrying concentric scaffolds;
3. automatic peeling machine using the adhesiver roller;
4. a magnetic offtake mechanism that transports the film for further processing and/or storage.

All these sub-units might constitute a single manufacturing cell; alternatively, each of these could be scaled up for a production line.

Figure 8-3: Schematic of a fab for thin PDMS film production

8.2.2 Gaps between our Work and the Vision

In this research, we have shown test results for each of the steps of a PDMS film manufacturing process, but we have not built the complete setup for peeling automation. Here, we mention the key components of the manufacturing system we envision and the scope and limitations of our work:

1. Stamping the scaffold

   The scaffolds can be manufactured cost-effectively by stamping thin metal shims out of a library of stamping molds. We did not use stamping for making the scaffolds because of the high setup cost. During prototype tests with different scaffold designs, machining the punch/die set was time consuming and expensive. Furthermore, the molds could not be surface hardened in a lab setting and the scaffolds we stamped had poor edge quality.

2. Production-ready closed-loop spin-coating

   We showed both a robust open-loop spin-coating approach and showed the use of a real-time monitoring approach using low-coherence interferometry. We did not build a spin-coating setup with feedback control.

3. Peeling

   For our experiments, we assembled a device for peeling using an adhesive roller which showed how automatic peeling and offtake could be implemented. For our adhesive roller, the adhesive tapes were affixed manually. We built this device as a research prototype, but did not design and build a full-fledged automatic peeling machine.

4. Offtake

   Through our analysis of the offtake process, we showed how a 'large-small' roller concept can achieve automatic offtake but did not build the double roller offtake

setup. Through experiments, we have shown how a magnetic offtake approach can be implemented. Our tests involved holding a magnetic chuck by hand for offtake. Automatic magnetic offtake can be timed based on the adhesive roller's rotation. We did not build such an automatic magnetic offtake step.

5. Alignment

   We showed how thin PDMS films could be aligned using fiducials and cutouts in the scaffold. We did not build a machine for aligning thin PDMS films.

6. Yield analysis

   The experiments I have summarized in Table 7.1 suggest strongly that the manufacturing process I have presented is applicable for thin PDMS films. Our experiments were selective and focused more on critical and damage prone areas. It will be useful to study the yield of the proposed Scaffold Reinforced Elastomeric Film Manufacture (SEFM) process in a systematic manner over film thickness, substrate choices and other variations. Such a study will help characterize this process and help pave the way for adoption of this process.

8.2.3 Confidence in Process Steps

Based on the theoretical analysis, the assembly of a prototype and through extensive experiments, we feel confident that the manufacturing process presented is capable of peeling very thin PDMS films of thickness down to $50\mu m$. The peeling machine we built is a bench-top research prototype. We identify limitations to our experiments and suggest improvements here.

For spin-coating, the use of a motor with closed-loop feedback will improve the spin-speed accuracy. The samples that we used in our experiments were prepared and used within the prescribed pot life. Using PDMS samples with known age (time since mixing) will provide more confidence in interpreting the experimental results on viscosity variation. Instead of bench-top experiments, testing the process in more

controlled environments will also reduce the risk of the material getting contaminated. For the peeling machine, the stiffness of the roller assembly can be increased and with a servo motor for better speed control. The spring-loaded surface can be modified to have more torsional compliance to ensure it provides a line contact against the adhesive roller. In addition, larger roller geometry could be used to test both 4" and 6" substrates. In order for the scaffold reinforced elastomeric film manufacturing process to be adopted, there still remain more detailed studies that characterize the process windows, that identify the yield of the process and that include alternate film materials.

8.3 Contributions in this Thesis

In this thesis, I have developed a new manufacturing process for very thin elastomeric films. Below, I list the specific contributions. In this thesis I have,

I have,

- outlined the specific process steps for the manufacture of thin PDMS films ,
- demonstrated the variability in spin-coating thickness, explained a mechanics model for height variation and improved the robustness of the spin-coating process using the mechanics model,
- described the challenges in PDMS manufacture due to its material property variation,
- analyzed the problem of low yield in manual peeling, due to tearing and beading,
- explained the physics of initiation and introduced concepts for peel initiation based on the physics,
- explained the risk of instability in the peeling process and have shown how such instability could cause damage in the film,

- demonstrated the application of a roller with pre-load for controlling peel-front advance,
- introduced a new component – ' an *in-situ* Scaffold', for repeatable initiation of a peel, for attaching to the film during peeling, for use as scaffolding to avoid wrinkling of peeled film and for registration and alignment,
- introduced the use of an adhesive roller actuator with compressive pre-load for peeling films with a peel initiator,
- implemented these components in a prototype of an automatic peeling machine for peeling PDMS films down to 50 microns in thickness.

In summary, I hope that this dissertation will take us a step closer to the vision of a fab for thin PDMS films.

THIS PAGE INTENTIONALLY LEFT BLANK

Appendix A

Data Sheet for PDMS

Product Information

DOW CORNING

SYLGARD® 184 Silicone Elastomer

Optically clear elastomer

FEATURES

- Two-part, 10:1 mixing ratio
- Medium viscosity
- Room temperature cure or rapid heat cure
- Addition cure system: no cure by-products
- Stable and flexible from -50°C (-58°F) to +200°C (392°F)
- Clear
- Flexible rubber - protects against mechanical shock and thermal cycling stress at components
- Excellent dielectric properties

APPLICATIONS

- Designed to protect against moisture, environmental attack, mechanical and thermal shock as well as vibration especially when optically clear product is required.
- Typical applications include: encapsulation of amplifiers, coils, connectors, circuit boards, equipment modules, ferrite cores, solar cells and transformers.

TYPICAL PROPERTIES

Specification writers: These values are not intended for use in preparing specifications. Please contact your local Dow Corning sales representative prior to writing specifications on this product.

CTM*	ASTM*	Property	Unit	Value
		As supplied		
0050	D1084	Viscosity at 23°C (Base)[1]	mPa.s	5500
		Mixing ratio by weight (Base:Curing Agent)		10:1
0050	D1084	Viscosity at 23°C, immediately after mixing with Curing Agent	mPa.s	4000
0055	D1824	Pot life at 23°C[2]	hours	2
		Physical properties, cured 4 hours at 65°C		
0176		Color		Clear
0099	D2240	Durometer hardness, Shore A		50
0137A	D412	Tensile strength	MPa	7.1
0137A	D412	Elongation at break	%	140
0159A	D624	Tear strength - die B	kN/m	2.6
0022	D0792	Specific gravity at 23°C		1.05
		Volume coefficient of thermal expansion	1/K	9.6×10^{-4}
		Coefficient of thermal conductivity	W/(m.K)	0.17
		Electrical properties, cured 4 hours at 65°C		
0114	D149	Dielectric strength	kV/mm	21
0112	D150	Permittivity at 100Hz		2.75
0112	D150	Permittivity at 100kHz		2.75
0112	D150	Dissipation factor at 100Hz		0.001
0112	D150	Dissipation factor at 1kHz		0.001
0249	D257	Volume resistivity	Ohm.cm	5×10^{15}
		Comparative tracking index (IEC112)		600

1. Brookfield LVF, spindle #4 at 60rpm
2. Time required for catalysed viscosity to double at 23°C.

* CTM: Corporate Test Method, copies of CTMs are available on request.
ASTM: American Society for Testing and Materials.

Figure A-1: Property Datasheet for the Sylgard-184 product used PDMS preparation [CC07]

HOW TO USE

Substrate preparation

All surfaces should be cleaned and degreased with a suitable solvent prior to potting. Care should be taken to ensure that all solvent is removed.

For best adhesion, coat surfaces with DOW CORNING® 92-023 Primer or DOW CORNING® 1200 OS Primer, following the instructions and precautions given for use of these products.

Mixing

SYLGARD 184 Silicone Elastomer is supplied in lot matched kits consisting of base and curing agent in separate containers.

The two components should be thoroughly mixed using a weight or volume ratio of 10:1.

The pot life is 2 hours for catalysed SYLGARD 184 Silicone Elastomer at room temperature.

Vacuum de-airing is recommended. A residual pressure of 10-20mm mercury applied for 30 minutes will sufficiently de-air the material.

Lowering the viscosity

The viscosity of SYLGARD 184 Silicone Elastomer may be reduced by addition of up to 10% of DOW CORNING® 200 Fluid 20 cS. Added quantities of less than 5% have little or no effect on either the physical or electrical properties while larger quantities of DOW CORNING 200 Fluid 20 cS will diminish the physical strength and hardness. The addition of DOW CORNING 200 Fluid 20 cS does not alter the amount of curing agent required.

How to apply

Apply the encapsulant, being careful to avoid air entrapment. Vacuum encapsulation is recommended for complex geometries.

For information on appropriate dispensing equipment for your application, please contact Dow Corning.

Curing

SYLGARD 184 Silicone Elastomer should be cured using one of the following recommended schedules:

24 hours at 23°C, or
4 hours at 65°C, or
1 hour at 100°C, or
15 minutes at 150°C

Large components and assemblies may require longer times in order to reach the curing temperature.

At 23°C the material will have cured sufficiently in 24 hours to be handled; however full mechanical and electrical properties will only be achieved after 7 days.

Compatibility

In some cases, SYLGARD 184 Silicone Elastomer may fail to cure to optimum properties when in contact with certain plastics or rubbers. Cleaning the substrate with solvent or baking slightly above the cure temperature will normally eliminate the problem.

Certain chemicals, curing agents and plasticisers can inhibit cure. These include:

- Organo-tin compounds
- Silicone rubber containing organo-tin catalysts
- Sulphur, polysulphides, polysulphones and other sulphur containing materials
- Amines, urethanes, amides and azides.

HANDLING PRECAUTIONS

PRODUCT SAFETY INFORMATION REQUIRED FOR SAFE USE IS NOT INCLUDED. BEFORE HANDLING, READ PRODUCT AND SAFETY DATA SHEETS AND CONTAINER LABELS FOR SAFE USE, PHYSICAL AND HEALTH HAZARD INFORMATION. THE SAFETY DATA SHEET IS AVAILABLE FROM YOUR LOCAL DOW CORNING SALES REPRESENTATIVE.

USABLE LIFE AND STORAGE

When stored at or below 32°C in the original unopened containers, this product has a usable life of 24 months from the date of production.

PACKAGING

SYLGARD 184 Silicone Elastomer is available in standard industrial container sizes. For details please refer to your Dow Corning sales office.

LIMITATIONS

This product is neither tested nor represented as suitable for medical or pharmaceutical uses.

HEALTH AND ENVIRONMENTAL INFORMATION

To support customers in their product safety needs, Dow Corning has an extensive Product Stewardship organization and a team of Health, Environment and Regulatory Affairs specialists available in each area.

For further information, please consult your local Dow Corning representative.

WARRANTY INFORMATION - PLEASE READ CAREFULLY

The information contained herein is offered in good faith and is believed to be accurate. However, because conditions and methods of use of our products are beyond our control, this information should not be used in substitution for customer's tests to ensure that Dow Corning's products are safe, effective, and fully satisfactory for the intended end use. Dow Corning's sole warranty is that the product will meet the Dow Corning sales specifications in effect at the time of shipment. Your exclusive remedy for breach of such warranty is limited to refund of purchase price or replacement of any product shown to be other than as warranted. Dow Corning specifically disclaims any other express or implied warranty of fitness for a particular purpose or merchantability. Unless

Figure A-2: Guidelines for the Sylgard-184 product used in PDMS preparation [CC07]

THIS PAGE INTENTIONALLY LEFT BLANK

Appendix B

List of Vendors

1. Sylgard-184: Robert McKeown and Company,
   `http://www.robertmckeown.com`

2. Borosilicate glass disk: Technical Glass Products Inc.,
   `http://www.technicalglass.com`

3. Metal shims: Small Parts Inc.,
   `http://www.smallparts.com`

4. 3M Repositionable Spray Adhesive: Office Depot,
   `http://www.officedepot.com`

5. Polyester Sheets: Polymask Corporation (3M Industrial Tapes),
   `http://www.polymask.com`

6. Adhesive on Roller: 3M Industrial Tapes division,
   `http://www.3m.com`

7. Custom metal scaffolds: Tech Etch Inc.,
   `http://www.techetch.com`

8. Petridish, lab supplies VWR Scientific Supplies,
   http://www.vwr.com

Index

THIS PAGE INTENTIONALLY LEFT BLANK

Bibliography

[ACJ+00] J.R. Anderson, D.T. Chiu, R.J. Jackman, O. Cherniavskaya, J.C. McDonald, H. Wu, S.H. Whitesides, and G.M. Whitesides. Fabrication of topologically complex three-dimensional microfluidic systems in pdms by rapid prototyping. *Anal. Chem.*, 72(14):3158–3164, 2000.

[Ana] Personal communication with Prof. Lallit Anand, Department of Mechanical Engineering, MIT.

[Bog68] D. B. Bogy. Edge-bonded dissimilar orthogonal elastic wedges under normal and shear. loading. *ASME Journal of Applied Mechanics*, pages 460–466, 1968.

[Bol96] V. V. Bolotin. *Stability Problems in Fracture Mechanics.* Wiley, 1996.

[BWH+01] C. Bulthaup, E. Wilhelm, B. Hubert, B. Ridley, and J. Jacobson. All-additive fabrication of inorganic logic elements by liquid embossing. *Applied Physics Letters*, 79:1525–1527, 2001.

[CC07] Dow Corning and Company. Sylgard-184 product technical datasheet. URL, 2007. `http://www.dowcorning.com`.

[Cha05] M. K. Chaudhury. General adhesion: Methods of contact mechanics. *Adhesion Society Short Course*, 2005.

[Cor] Rogers Corporation. .02inch ht-6240 transparent silicone. URL. `http://www.rogerscorporation.com`.

[CW87] F. Chambon and H. H. Winter. Linear viscoelasticity at the gel point of a crosslinking pdms with imbalanced stoichiometry. *Journal of Rheology*, 31(8):683–697, 1987.

[CW91] M. K. Chaudhury and G. M. Whitesides. Direct measurement of interfacial interactions between semispherical lenses and flat sheets of poly(dimethylsiloxane) and their chemical derivatives. *Langmuir*, 7(5):1013–1025, 1991.

[CWHT02] Brian Cotterell, Gordon Williams, John Hutchinson, and Michael Thouless. Annoucement of a round robin on the analysis of the peel test. *International Journal of Fracture*, 114(3):9–13, 2002.

[Des] Personal communication with Microfluids and BioMEMS research groups at MIT.

[DSB+04] M.M.J Decre, R. Schneider, D. Burdinski, J. Schellekens, M. Saalmink, and R. Dona. Wave printing (i) : Towards large-area, multilayer microcontact printing. pages M4.9.1–M4.9.3, 2004.

[EBP58] Alfred G. Emslie, Francis T. Bonner, and Leslie G. Peck. Flow of a viscous liquid on a rotating disk. *Journal of Applied Physics*, 29(5):858–862, 1958.

[ECB03] D. T. Eddington, W. C. Crone, and D. J. Beebe. Development of process protocols to fine tune polydimethylsiloxane material properties. In *7th Intl. Conf. on Miniaturized Chemical and Biochemical Analysis Systems*, Squaw Valley, CA, 2003.

[FDHL03] A F Fercher, W Drexler, C K Hitzenberger, and T Lasser. Optical coherence tomography - principles and applications. *Reports on Progress in Physics*, 66(2):239, 2003.

[FZCS05] A. M. Forster, W. Zhang, A. J. Crosby, and C.M. Stafford. A multi-lens measurement platform for high-throughput adhesion measurements. *Measurement Science and Technology*, 16(1):81–89, 2005.

[GK03] Z.-Q. Gong and K. Komvopoulos. Effect of surface patterning on contact deformation of elastic-plastic layered media. *Journal of Tribology*, 125(1):16–24, 2003.

[GMH04] C. M. Gramlich, A. Mazouchi, and G. M. Homsy. Time-dependent free surface Stokes flow with a moving contact line. II. Flow over wedges and trenches. *Physics of Fluids*, 16:1660–1667, May 2004.

[Gri21] A. A. Griffith. The phenomena of rupture and flow in solids. *Philosophical Transactions of the Royal Society of London. Series A, Containing Papers of a Mathematical or Physical Character*, 221:163–198, 1921.

[HCF04] Chia-Hsien Hsu, Chihchen Chen, and Albert Folch. "Microcanals" for micropipette access to single cells in microfluidic environments. *Lab on a Chip*, 4(5):420–424, 2004.

[HLA04] R. Huang, S. Lele, and L. Anand. Non-linear mechanical behavior of polydimethylsiloxane (pdms): application to the manufacture of microfluidic devices. *Innovation in Manufacturing Systems and Technology report*, 2004.

[IFK96] R. Ida, M. Fujimoto, and T. Kobayashi. Apparatus for removing protective films, US Patent US005540809A, 1996.

[Isr03] J. N. Israelachvili. *Intermolecular and surface forces.* Academic Press, 2003.

[JKR71] K. L. Johnson, K. Kendall, and A. D. Roberts. Surface energy and the contact of elastic solids. *Proceedings of the Royal Society of London. Series A, Mathematical and Physical Sciences*, 324(1558):301–313, 1971.

[Joh87] K. L. Johnson. *Contact Mechanics.* Cambridge University Press, 1987.

[JW03] X. Jiang and G.M. Whitesides. Engineering microtools in polymers to study cell biology. *Engineering in Life Sciences*, 3(12):475–480, 2003.

[Kav05] F. Kavehpour. *Moving Contact Line Experiments.* PhD thesis, Massachusetts Institute of Technology, Cambridge, MA 02139, 2005.

[KBH00] Serafim Kalliadasis, Catherine Bielarz, and G. M. Homsy. Steady free-surface thin film flows over topography. *Physics of Fluids*, 12(8):1889–1898, 2000. Available from: `http://link.aip.org/link/?PHF/12/1889/1`.

[Ken04] A. Kendale. Automation of soft-lithographic micro-contact printing. Master's thesis, Massachusetts Institute of Technology, Cambridge, MA 02139, 2004.

[KLBV06] A. Khademhosseini, R. Langer, J. Borenstein, and J. P. Vacanti. Tissue engineering special feature: Microscale technologies for tissue engineering and biology. *PNAS*, 103(8):2480–2487, 2006.

[LBRS06] H. L. T. Lee, P. Boccazzi, R. J. Ram, and A. J. Sinskey. Microbioreactor arrays with integrated mixers and fluid injectors for high-throughput experimentation with ph and dissolved oxygen control. *Lab on a Chip*, 6:1229–1235, 2006.

[LS81] G. J. Lake and A. Stevenson. On the formation of waves in low angle peeling. *Journal of Adhesion*, 12:13–22, 1981.

[MB78] D. Maugis and M Barquins. Fracture mechanics and the adherence of viscoelastic bodies. *Journal of Physics D: Applied Physics*, 11(14):1989–2023, 1978.

[MFR05] A. Mata, A. J. Fleischman, and S. Roy. Characterization of polydimethylsiloxane (PDMS) properties for biomedical micro/nanosystems. *Biomedical Microdevices*, 7(4), 2005.

[MGH04] A. Mazouchi, C. M. Gramlich, and G. M. Homsy. Time-dependent free surface Stokes flow with a moving contact line. I. Flow over plane surfaces. *Physics of Fluids*, 16:1647–1659, May 2004.

[MJF89] F. Melo, J. F. Joanny, and S. Fauve. Fingering instability of spinning drops. *Physical Review Letters*, 63(18):1958–1962, 1989.

[Ohs94] S. Ohsaki. Coating film separating device and coatin film separation method using the device, US Patent 005344521A, 1994.

[SG92] W.V. Sorin and D.F. Gray. Simultaneous thickness and group index measurement using optical low-coherence reflectometry. *Photonics Technology Letters, IEEE*, 4(1):105–107, 1992.

[SHB+04] C. Stafford, C. Harrison, K. L. Beers, A. Karim, M. R. Amis, E. J. amd VanLandingham, H. C. Kim, W. Volksen, and E. E. Miller, R. D.and Simonyi. A buckling-based metrology for measuring the elastic moduli of polymeric thin films. *Nature Materials*, 3(8):545–550, 2004.

[SHP+04] Vincent Studer, Giao Hang, Anna Pandolfi, Michael Ortiz, W. French Anderson, and Stephen R. Quake. Scaling properties of a low-actuation

pressure microfluidic valve. *Journal of Applied Physics*, 95(1):393–398, 2004.

[SR04] L. W. Schwartz and R. V. Roy. Theoretical and numerical results for spin coating of viscous liquids. *Physics of Fluids*, 16(3):569–584, 2004.

[TG70] S.P. Timoshenko and J.N. Goodier. *Theory of Elasticity.* McGraw-Hill, third edition, 1970.

[TMQ02] T. Thorsen, S. J. Maerkl, and S. R. Quake. Microfluidic large-scale integration. *Science*, 298(5593):580–584, 2002.

[VFB+02] G. Vozzi, C. J. Flaim, F. Bianchi, A. Ahluwalia, and S. Bhatia. Microfabricated plga scaffolds: a comparative study for application to tissue engineering. *Material Science and Engineering*, 760, 2002.

[Voi99] O. V. Voinov. Gravity-induced spreading of a drop of a viscous fluid over a surface. *Journal of Applied Mechanics and Technical Physics*, 40(3):412–419, 1999.

[WHD00] S. K. Wilson, R. Hunt, and B. R Duffy. The rate of spreading in spin coating. *Journal of Fluid Mechanics*, 413:65–88, 2000.

[Wil52] M. L. Williams. Stress singularities resulting from various boundary conditions in angular corner of plates in extension. *Journal of Applied Mechanics*, 19:526–528, 1952.

[Wil97] J.G. Williams. Energy release rates for the peeling of flexible membranes and the analysis of blister tests. *International Journal of Fracture*, 87(3):265–288, 1997.